



Structure and Analysis of Woven Compression Bandages for Venous Leg Ulcers

Dissertation Thesis

Study programme:

P3106 Textile Engineering

Study branch:

Textile Technics and Materials Engineering

Author:

Abdelhamid Rajab Ramadan Aboalasaad, M.Eng.

Thesis Supervisor:

Ing. Brigita Kolčavová Sirková, Ph.D.

Department of technologies and structures



Declaration

I hereby certify, I, myself, have written my dissertation as an original and primary work using the literature listed below and consulting it with my thesis supervisor and my thesis counsellor.

I acknowledge that my bachelor dissertation is fully governed by Act No. 121/2000 Coll., the Copyright Act, in particular Article 60 – School Work.

I acknowledge that the Technical University of Liberec does not infringe my copyrights by using my dissertation for internal purposes of the Technical University of Liberec.

I am aware of my obligation to inform the Technical University of Liberec on having used or granted license to use the results of my dissertation; in such a case the Technical University of Liberec may require reimbursement of the costs incurred for creating the result up to their actual amount.

At the same time, I honestly declare that the text of the printed version of my dissertation is identical with the text of the electronic version uploaded into the IS/STAG.

I acknowledge that the Technical University of Liberec will make my dissertation public in accordance with paragraph 47b of Act No. 111/1998 Coll., on Higher Education Institutions and on Amendment to Other Acts (the Higher Education Act), as amended.

I am aware of the consequences which may under the Higher Education Act result from a breach of this declaration.

February 1, 2021

Abdelhamid Rajab Ramadan Aboalasaad, M.Eng.

Abstract

Woven compression bandage (WCB) is one of elastic textiles that exert pressure on muscles. With a defined tensile strength, it is possible to create the required compression on the given body parts. The proposed study aims to investigate the relationship between woven fabric deformation, porosity, and tensile stress properties of three main types of woven compression bandages. All bandage samples are applied on human leg using two and three layers bandaging techniques. The study investigated the commercial yarns available in the bandage market in addition to yarns spun at a wider range of ply twist. Moreover, the study analysed the influence of yarn material and bandaging techniques on corresponding pressure at the ankle and mid-calf positions. Results revealed that the optimum twist for plied yarn should be (1800 – 2200 turns per meter) to produce highly extensible WCB.

Another part of the dissertation was a modification of the structure and construction of a WCB made of 100% cotton, where the bandage includes an integrated tension sensor, which causes a colour change of the bandage during its deformation. The solution is sensors in the bandage in the form of threads with a colour different from the other structure of the bandage, which become visible due to deformation / stress in the bandage. Implementation is possible by applying weft threads with different colours through the weft insertion during weaving.

The measured pressure using PicoPress was compared with theoretical compression calculated by Laplace's law and Al-Khaburi's equations. The bandage porosity is calculated for all frames at different weave angles using NIS elements software. Woven bandage construction parameters which are given by the warp and weft yarns preparation, twist, count, and density along with woven fabric weave, type of weaving and finishing process are the main factors influence the bandage properties. Experimental results confirm that bandage porosity is directly proportional to the bandage extension and weave angle that ranges from 44° to 90°. The novelty of candidate study is to introduce practical remarks to the patient for optimizing the required bandage pressure by suitable extension or applied tension or weave angle for two and three layers bandaging systems.

Thermal resistance (R_{ct}) and water vapour resistance (R_{et}) are evaluated for four types of WCB, then compared with thermal foot model (TFM). Flexor Carpi (FC), Soleus (SO), and Medial Gastrocnemius (MG) muscles are selected to represent the wrist, ankle, and mid-calf muscles respectively, which are then evaluated by EMG electrical voltage test with and without

wearing WCB. Using WCB significantly decreased the muscle's activation and was associated with higher median frequency for both SO and MG muscles during the tested activities.

Keywords:

Plied warp yarns; twist level; woven bandage elasticity; short-stretch woven bandages; PicoPress compression; Laplace's equation; Thermal resistance; Muscle's activation.

Anotace

Tkané kompresní obinadla jsou jednou z možností pružných textilií, které vyvíjejí při aplikaci tlak na svaly. Při aplikaci obinadla, při definované pevnosti v tahu, je možné vytvořit požadovanou kompresi na danou část těla. Jedna z navrhovaných studií si klade za cíl zkoumat vztah mezi deformací tkaného obinadla, pórovitostí a vlastnostmi namáhání v tahu u tří hlavních typů kompresních obinadel. Všechny vzorky obinadel se aplikují na lidskou nohu pomocí dvou a třívrstvých technik bandáže. V rámci realizace disertační práce studie byla zaměřená na zkoumání mechanických vlastností komerční 100% bavlněné příze dostupné na trhu pro výrobu kompresního obinadla a experimentálně navržená sada přízí spřádaných v širším rozsahu zákrutu pro možnou výrobu kompresních 100% bavlněných obinadel. Studie navíc analyzovala vliv konstrukce příze versus bandážovací technika na odpovídající tlak v poloze kotníku a lýtka. Výsledky odhalily, že optimální zákrut pro přízi by mohl být (1800 - 2200 Z/m), aby se vytvořil WCB.

Další částí disertační práce byla modifikace struktury a konstrukce kompresního tkaného obinadla ze 100% bavlny, kde součástí obvazu je integrovaný senzor napětí, které způsobí barevnou změnu obvazu při jeho deformaci. Řešením jsou senzory v obinadle v podobě nití s barevností odlišnou od ostatní struktury obinadla, které se stanou viditelnými vlivem deformace/napětí v obinadle. Realizace je možná aplikací útkových nití s odlišnou barevností barevným házením během tkaní.

Naměřený tlak pomocí PicoPress byl porovnán s teoretickou kompresí vypočítanou Laplaceovým zákonem a Al-Khaburiho rovnicemi. Porozita obinadla se následně přepočítá ze snímaného obrazu pro všechny snímky využitím softwaru NIS elements. Hlavní parametry ovlivňující vlastnosti obinadla jsou konstrukční parametry: a) dostavou osnovních a útkových nití, zákrutem osnovních a útkových nití, materiálovým složením nití obinadla a vazbou tkaného obinadla, typem tkaní a dokončovacím procesem. Experimentální výsledky potvrzují,

že pórovitost obinadla je přímo úměrná prodloužení obvazu a úhlu deformace nití v provázání nití, který se pohybuje od 44 ° do 90 °. Modifikaci konstrukce kompresního obinadla, vložením barevných vzorů a nití v obinadle, lze použít také k jednoznačné identifikaci, zda tento obvaz je vhodný například pro vysoký či nízký stupeň komprese. Zabrání se omylům při aplikaci.

Poslední částí práce je zhodnocení chování obinadel z pohledu tepelného odporu, kde tepelný odpor (R_{ct}) a odpor vodních par (R_{et}) se hodnotí pro všechny typy WCB s následným porovnáním s modelem tepelné nohy (TFM). Pro reprezentaci svalů zápěstí, kotníku a středního lýtka jsou vybrány svaly Flexor Carpi (FC), Soleus (SO) a Medial Gastrocnemius (MG), které jsou poté hodnoceny testem elektrického napětí EMG s nebo bez nošení WCB. Použití WCB významně snížilo aktivaci svalu a bylo spojeno s vyšší střední frekvencí pro svaly SO i MG během testování.

Klíčová slova:

Dvojmo skaná příze; úroveň zákrutu; tkané obinadlo; obinadlo s krátkým tahem; PicoPress komprese; Laplacova rovnice; tepelný odpor; svalová aktivace.

List of Figures

Number	Figure description	Page
1.1	Knitted compression bandage and socks	5
1.2	Three major techniques of woven compression bandages	5
1.3	Woven bandage structure based on plain weave, without elastane	7
1.4	Woven bandage structures, based on plain weave and elastane	7
2.1	A peripheral fibre in helical model of multifilament yarn of diameter D, a) One coil of a helical fibre on yarn surface and b) Unrolled yarn surface	14
2.2	Schematic diagram of stress–strain curves of mean fibre and yarn	19
3.1	Three basic types of WCBs	20
3.2	Smart CBs with sensor	20
3.3	Presentation of the innovated cotton WCB and its structure	21
3.4	The blue marks on the three basic types of WCBs	22
3.5	A Coloured weft repeated every 1 cm during the bandage weaving	23
4.1	Load-elongation curves of the 1st and 2nd groups of yarns	28
4.2	Effect of plying twist on yarn tenacity for market yarns	29
4.3	Effect of plied yarn twist on its extension, market yarns	30
4.4	Effect of plying twist on yarn tenacity for produced yarns	30
4.5	Effect of plied yarn twist on its extension, produced yarns	31
4.6	Inhibition zone of treated yarns against: a) Escherichia Coli, b) Staphylococcus Aureus	33
4.7	Surviving bacterial colonies of: a) Escherichia Coli, b) Staphylococcus Aureus	33
4.8	Scanning electron microscopy of the un-treated and treated single yarns	34
4.9	Scanning electron microscopy of the un-treated and treated plied yarns	35
4.10	Energy dispersive X-ray mapping of the un-treated and treated single yarns	35
4.11	Energy dispersive X-ray mapping of the un-treated and treated plied yarns	36
5.1	Experimental woven compression bandages description	37
5.2	Binary area of Cotton bandage during tension	38
5.3	Binary area of Viscose/Lycra bandage during tension	38
5.4	Application of compression bandage on mannequin and real leg	39
5.5	Adjusting the bandage extension using the blue lines (coloured weft threads)	39
5.6	Testing of tensile and cyclic loading-unloading by Testometric M350-5CT	40
5.7	EMG system for Flexor Carpi, Medial Gastrocnemius and Soleus muscles	43
5.8	Woven CB samples on Thermal foot manikin	44
5.9	PERMETEST device for testing R_{ct} and R_{ct}	45
5.10	ALAMBETA testing device	45
5.11	Stretching frame at 80% extension: a) Cotton, b) CO-PA-PU bandages	45
5.12	Optimum testing procedure of measuring R_{ct} on TFM	46
5.13	Measuring R_{ct} while wearing CB over socks	47
5.14	Loading-unloading curves for Cotton, CO-PA-PU, and VI-PA bandages	48
5.15	Optimum fabric tension for Cotton, CO-PA-PU, and VI-PA bandages	49

5.16	Structure of interlacing cell in woven fabric crossing point of plain weave, warp and weft diameter (d_1 , d_2), warp and weft distance (B, A).	50
5.17	Effect of extension and warp to weft yarns angle on porosity of Cotton bandage	51
5.18	Relation between extension, warp to weft yarns angle, and porosity for CO-PA-PU bandage	52
5.19	Effect of extension and yarns angle on porosity of VI-PA bandage	52
5.20	Effect of extension level on the horizontal porosity of cotton bandage during application on real leg	54
5.21	Pressure of Cotton bandage on leg model	55
5.22	Pressure of Cotton bandage on real leg while walking	55
5.23	Pressure of CO-PA-PU bandage on real leg while walking	56
5.24	Effect of bandage extension level on the measured pressure at the ankle position for cotton bandage, statistically analysed by main effects ANOVA	56
5.25	Pressure of Viscose-Lycra bandage on real leg while walking	58
5.26	Measured bandage pressure by Picopress vs calculated by Laplace's and Al-khaburi's equations at ankle position using two layers of cotton bandage	61
5.27	Measured bandage pressure by Picopress vs calculated values at ankle position using three layers bandaging	61
5.28	Measured bandage pressure by Picopress vs calculated values at mid-calf position using two layers bandaging	62
5.29	Measured bandage pressure by Picopress vs calculated values at mid-calf position using three layers bandaging	62
5.30	Effect of cyclic loading on bandage applied tension	63
5.31	Effect of stress-relaxation on elastic recovery of long and short-stretch woven bandages	64
5.32	Effect of cyclic loading on applied load by long and short-stretch woven bandages	64
5.33	SEM of the un-treated cotton woven bandage	66
5.34	SEM of the treated cotton WCB with 1% zinc oxide nanoparticles	66
5.35	SEM of the treated cotton WCB with 2% zinc oxide nanoparticles	66
5.36	SEM of the treated cotton WCB with 3% zinc oxide nanoparticles	67
5.37	Energy dispersive X-ray map of the un-treated cotton WCB	67
5.38	EDX map of the treated cotton WCB with 1% zinc oxide nanoparticles	67
5.39	EDX map of the treated cotton WCB with 2% zinc oxide nanoparticles	68
5.40	EDX map of the treated cotton WCB with 3% zinc oxide nanoparticles	68
5.41	The skin temperature adjusting and control process of X parts of thermal manikin [36]	69
5.42	Effect of bandage extension on thermal resistance of two layers CB	70
5.43	Effect of bandage extension on thermal resistance of three layers CB	71
5.44	Effect of applied tension on thermal resistance of two layers CB	71
5.45	Effect of total thickness of layers on thermal resistance of two layers WCBs, on Alambeta and thermal foot manikin testing devices	72
5.46	Effect of total thickness of layers on thermal resistance of three layers WCBs, on Alambeta and thermal foot manikin testing devices	73
5.47	Effect of bandage extension on thermal conductivity coefficient, two layers	73
5.48	Effect of bandage extension on thermal resistance of two layers WCBs, on Alambeta and thermal foot manikin testing devices	74

5.49	Effect of bandage extension on thermal resistance of three layers WCBs, on Alambeta and thermal foot manikin testing devices	75
5.50	Experimental thermal resistance results for bandages by thermal foot manikin and Alambeta versus theoretical calculations by Maxwell-Eucken2, Schuhmeister and Militky models	79
5.51	Time dependence heat flow after contact	80
5.52	Experimental thermal resistance for bandages by ALAMBETA versus theoretical calculations by Maxwell-Eucken2, Schuhmeister and Militky models	80
5.53	Experimental thermal resistance for bandages by thermal foot manikin versus theoretical calculations by Maxwell-Eucken2, Schuhmeister and Militky models	81
5.54	Effect of bandage extension on water vapour resistance	82
5.55	Effect of bandage extension on air permeability, two layers	82
5.56	Flexor Carpi muscle voltage with and without WCB, (flexion-extension) action, 40 BPM	83
5.57	Flexor Carpi muscle voltage with and without VI-PA WCB, (squeezing a soft roll) action, 30 BPM	83
5.58	Medial Gastrocnemius muscle voltage with and without wearing CO-PA-PU bandage during (flexion-extension) action, 30 BPM	84
5.59	Medial Gastrocnemius muscle voltage with and without wearing bleached Cotton bandage while walking action, 40 BPM	84
5.60	Soleus muscle voltage with and without wearing CO-PA-PU bandage during (flexion-extension) action, 30 BPM	85
5.61	Soleus muscle voltage with and without wearing Cotton bandage while walking action, 40 BPM	85

List of Tables

Number	Table description	Page
1.1	Current sub-bandage pressure ranges (mmHg) in the British Standard (BS 7505) and recommended recalibration to match in vivo pressure measurements	6
4.1	Yarn characteristics (Group 1: plied yarns, fine count 6x2 Tex)	24
4.2	Yarn characteristics (Group 2: plied yarns, coarse counts 21x2 and 30x2 Tex)	24
4.3	Produced single yarn properties, ring-spun raw yarns	25
4.4	Produced plied yarn properties, ply of ring-spun yarns 20x2 Tex	25
4.5	Yarn properties, Group 1: plied yarns, 6x2 Tex	28
4.6	Yarn properties, Group 2: plied yarns, 21x2 and 30x2 Tex	29
4.7	Produced single yarn properties	31
4.8	Produced plied yarn properties at twist direction SS-Z	31
4.9	Produced plied yarn properties at twist direction SZ-Z	32
4.10	Produced plied yarn properties at twist direction ZZ-S	32
4.11	Inhibition zone of treated yarns according to AATCC 147	33
4.12	Inhibition zone of treated yarns according to AATCC 100	33
5.1	Samples' codes for treated cotton WCB with zinc oxide nanoparticles	41
5.2	Statistical analysis of relation between bandage extension and yarns angle	53
5.3	Statistical analysis of relation between bandage type, extension, and porosity	53
5.4	Statistical analysis of the effect of testing position and extension level on the measured pressure by PicoPress	56
5.5	Multiple regression of the relation between bandage type and extension level on the measured pressure by PicoPress at ankle position	57
5.6	Multiple regression of the relation between bandage type and extension level on the measured pressure by PicoPress at mid-calf position	57
5.7	Calculated pressure by Laplace's equation vs. measured compression at ankle position using PicoPress ($R= 4.07$ cm)	59
5.8	Multiple regression for the effect of bandage extension, number of layers, and bandage type on the measured pressure at ankle position	60
5.9	Calculated vs. measured compression values at mid-calf position ($R= 6.19$ cm)	60
5.10	Statistical analysis of measured compression at mid-calf position	61
5.11	The antibacterial activity of cotton WCB according to AATCC 147-2012	65
5.12	The antibacterial activity of cotton WCB according to AATCC 100-2019	65
5.13	Calculation of fibre filling coefficients	78
5.14	Properties of different fibres	78
5.15	EMG mean voltage of the flexor carpi muscle signals	86
5.16	EMG mean voltage for leg muscles while walking (bleached Cotton bandage)	86
5.17	EMG mean voltage for leg muscles using CO-PA-PU WCB	87
5.18	RMS values for Flexor Carpi muscle signals	87
5.19	ANOVA for Tables 5.10 & 5.13 (Flexor carpi muscle signals)	87
5.20	RMS values for MG and SO muscles' signals while walking (Cotton bandage)	88
5.21	ANOVA for Tables 5.11 & 5.15 (EMG mean voltage for leg muscles while walking)	88

Content

Table of Contents

1. Chapter 1: Overview of the Current State of the Problem	- 4 -
1.1 Compression bandages.....	- 4 -
1.2 Long and short-stretch compression bandages	- 6 -
1.3 Production methods and structures of woven compression bandages	- 6 -
1.4 Relationship between yarn parameters, weaving settings, and fabric strength.....	- 8 -
1.5 Compression therapy of venous leg ulcers.....	- 8 -
1.6 Thermal comfort properties of woven fabrics.....	- 9 -
1.6.1 Effect of pressure on heat transfer through multilayer fabrics.....	- 9 -
1.6.2 Effect of trapped air on thermal resistance of multilayer fabrics.....	- 10 -
1.7 Detection and analysis of muscles' activation	- 10 -
2. Chapter 2: The Purpose and Aim of the Thesis	- 12 -
2.1 Influence of fibre and yarn characteristics on mechanical properties of bandages.....	- 13 -
2.1.1 The mechanical behaviour of twisted short staple yarn structures.....	- 14 -
2.1.2 Effect of twist level on yarn properties.....	- 16 -
2.1.3 Evaluation of the factors affecting yarn strength.....	- 17 -
2.1.4 Stress–strain relations of fibres and yarn	- 18 -
3. Chapter 3: Structure and Behaviour of Cotton Woven Compression Bandages	- 20 -
4. Chapter 4: Analysis and Evaluation of the Warp and Weft Yarns for Cotton WCBs....	- 24 -
4.1 Methods used, studied material.....	- 24 -
4.1.1 Analysis of mechanical properties of the used warp yarns	- 24 -
4.1.2 Modification of the surface of used yarns.....	- 26 -
4.1.3 Preparing Cotton yarns treated with Silver NPs	- 26 -
4.1.4 Silver NPs activity of treated yarns.....	- 26 -
4.1.5 Testing the Nanoparticles size and its distribution	- 27 -
4.2 Summary of the achieved results	- 27 -
4.2.1 Relationship between yarn twist and tenacity.....	- 27 -
4.2.2 Silver NPs activity of treated cotton yarns.....	- 32 -
5. Chapter 5: Analysis of Individual Properties of Woven Compression Bandages.....	- 37 -
5.1 Methods used, studied material.....	- 37 -
5.1.1 Analysis of mechanical properties of WCBs	- 37 -
5.1.2 Testing of bandage pressure using Picopress.....	- 38 -

5.1.3	Relationship between the change in coloured weft spacing and compression during bandage application.....	- 39 -
5.1.4	Testing the cyclic loading-unloading during uniaxial stress.....	- 39 -
5.1.5	Treatment of the surface of cotton WCB with zinc oxide.....	- 40 -
5.1.6	Testing the muscles activation when applying WCBs.....	- 43 -
5.1.7	Analysis of thermal comfort properties of WCBs.....	- 44 -
5.2	Summary of the achieved results	- 48 -
5.2.1	Evaluation of the mechanical properties of woven compression bandages	- 48 -
5.2.2	Analysis of bandage pressure using Picopress.....	- 54 -
5.2.3	Comparison between calculated and measured compression using PicoPress	- 58 -
5.2.4	Effect of cyclic loading-unloading on bandage tension and durability.....	- 62 -
5.2.5	Verification of antibacterial activity of cotton WCB treated with Zinc Oxide NPs	- 64 -
5.2.6	Factors affecting the thermal properties testing.....	- 68 -
5.2.7	Effect of compression bandages on the muscles' activation.....	- 83 -
6.	Chapter 6: Evaluation of Results and New Findings.....	- 89 -
7.	Chapter 7: References	- 92 -
8.	List of papers published by the author	- 103 -
9.	Curriculum Vitae.....	- 105 -
9.1	Personal Data	- 105 -
9.2	Education	- 105 -
9.3	Employment Experience.....	- 105 -
9.4	Internship	- 105 -
9.5	Training.....	- 106 -
9.6	Personal Skills.....	- 106 -

List of Abbreviations and Nomenclature

CB	Compression bandage	MG	Medial Gastrocnemius
CBs	Compression bandages	SO	Soleus
WCB	Woven compression bandage	TFM	Thermal foot manikin
WCBs	Woven compression bandages	R _{ct}	Thermal resistance
CO-PA-PU	Cotton-Polyamide-Polyurethane	R _{ct}	Water vapour resistance
VI-PA	Viscose-Polyamide	R _{ct0}	Initial thermal resistance
EMG	Electromyography	MNPs	Metal Nano particles
PVP	Poly Vinyl Pyrrolidone	Sample D ₁	Immersed in Glucose for 1 min
NPs	Nano particles	Sample D ₂	Immersed in Glucose for 60 min
RMS	Root mean square	BL-CO-2	100% bleached Cotton, two layers of bandages
OE	Open end yarn	BL-CO-3	100% bleached Cotton, three layers of bandages
E.C.	Escherichia Coli	CO-PA-PU-2	Cotton-Polyamide-Polyurethane, two layers of bandages
S.A.	Staphylococcus Aureus	CO-PA-PU-3	Cotton-Polyamide-Polyurethane, three layers of bandages
CFU	Colony forming units	VI-PU-2	Viscose-Polyurethane, two layers of bandages
FC	Flexor Carpi	VI-PU-3	Viscose-Polyurethane, three layers of bandages
Std.	Standard Deviation	CO-2-TFM	100% Cotton, two layers on thermal foot manikin
VI-PU	Viscose-Polyurethane	CO-3-TFM	100% Cotton, three layers on thermal foot manikin
VI-PU-2-TFM	Viscose-Polyurethane, two layers on thermal foot manikin	CO-PA-PU-2-TFM	Cotton-Polyamide-Polyurethane, two layers, thermal foot manikin
VI-PU-3-TFM	Viscose-Polyurethane, three layers on thermal foot manikin	CO-PA-PU-3-TFM	Cotton-Polyamide-Polyurethane, three layers, thermal foot manikin
tpm	The yarn twist/meter		

1. Chapter 1: Overview of the Current State of the Problem

Compression bandage (CB) is considered one of the widespread applications of the medical textiles for leg ulcers or athletic performance. There are two main categories of these medical components, namely, knitted and woven compression bandages (WCBs). The knitted CB is usually in tubular form, but it is practically different than the compression socks (hosiery). Whereas the WCBs have vast variety of types and techniques. Compression bandaging remains a key interference in the management of venous and lymphatic diseases. This apparently simple intervention depends on the optimum selection and practical application of four complex central properties of compression bandages, namely, applied pressure, number of layers, components, and elastic properties [1].

Venous ulceration is the most common type of leg ulcers and a significant clinical problem. Chronic leg ulcers affect approximately 1% of the population and 3% of people over 65 years of age in the developed countries. The majority of leg ulcers are due to venous diseases [2-4]. Compression therapy by medical compression bandage can be achieved using short- or medium- or long-stretch techniques at maximum stretch ranges (<70%) or (70-140%) or (>140%) respectively [5, 6]. Short-stretch CB such as 100% Cotton and two-component compression system are mainly used for venous leg ulcers and oedema. With a short-stretch CB, the muscle contraction causes an intermittent narrowing of the veins, a reduction of venous reflux, and thus an improvement in the venous pump function when the patient is walking. Long-stretch CB is suitable for uncomplicated varicose veins or athletic performance, such cases require medium pressure (30-40 mmHg) [5]. In order to design effective compression bandages, researchers have attempted to describe the interface pressure applied by these bandages using mathematical models [7-10]. Few studies have been focused on the optimization and best combinations of CBs for venous leg ulcers, oedema healing, and prevention of recurrence. Most of patients depend on specialist practitioners or traditional experience.

1.1 Compression bandages

Compression bandages (CBs) consist of elastic textile that exerts pressure on muscles. It can be produced as woven or knitted CBs (tubular shape) but it is applied in folded form not simulating the compression socks, as illustrated in Figure 1.1 [11, 12]. These medical elastic structures can improve athletic performance and reduce sports injury, which exert compression and pressure on muscles to relieve muscle stiffness and fatigue during sports or other activities

[13-16]. In clinical practice, bandages are applied in the form of overlapping layers which results in multiple layers of fabric that overlay a particular point of the surface of the limb [17]. For example, CB applied with spiral 50% overlap technique will overlay the leg with two layers of bandage, CB applied with 66% overlap will result in three layers of bandage and CB applied with the figure-of-eight technique with 50% overlap will result in four layers of bandage as shown in Figure 1.2 [17], [9]. One of the most demanded applications of CBs is the compression therapy which could limit the flow of diseased surface veins, increases the flow through deeper veins, and reduces swelling. Compression might correct or at least improve the venous hypertension, mainly owing to an improvement of the venous pump and lymphatic drainage [18].

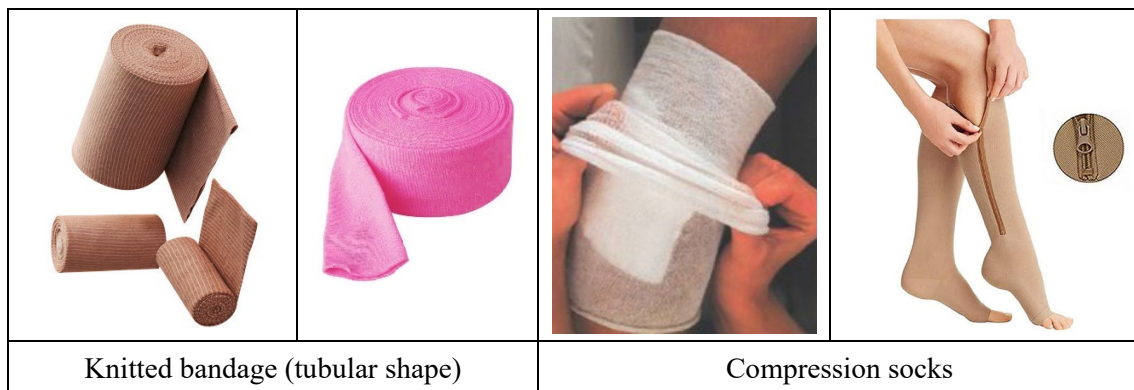


Figure 1.1. Knitted compression bandage and socks [19]

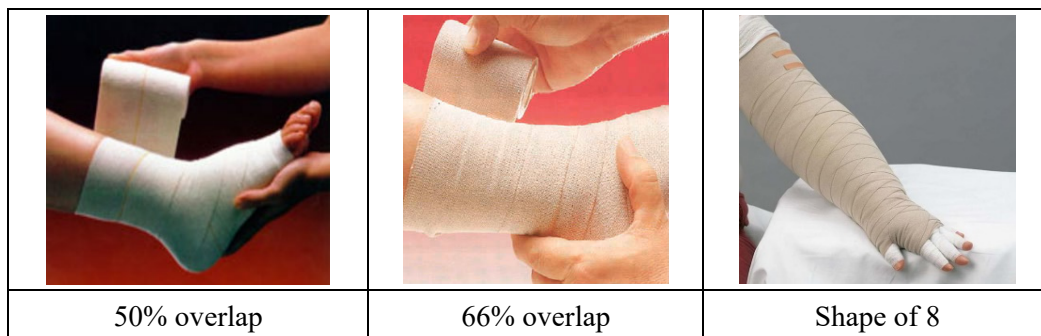


Figure 1.2. Three major techniques of woven compression bandages [20]

There was an international consensus meeting [2] recommended that the sub-bandage pressure ranges reported for bandages that are intended to apply mild, moderate, and strong compression are clearly higher than the ranges given in BS 7505, as illustrated in Table 1.1.

Table 1.1. Current sub-bandage pressure ranges (mmHg) in the British Standard (BS 7505) [21] and recommended recalibration to match in vivo pressure measurements

BS 7505, Compression Bandages	Recommendation
< 20 (light)	< 20 (mild)
21 – 30 (medium)	20 –< 40 (medium)
31 – 40 (high)	40 –< 60 (strong)
41 – 60 (extra high)	≥ 60 (very strong)

The British Standard BS7505 differentiates between three major groups of compression material (conforming stretch bandages, light support bandages, and compression bandages). It is a misconception to assign different brands of bandages to one of these three groups, because the pressure exerted by the final bandage will mainly depend on the tension during application rather than the material used. Multilayer bandages could be formed by more than two layers of a single material or, in the case of the so-called four-layer bandaging systems, by multiple layers of different bandage materials [1].

1.2 Long and short-stretch compression bandages

Long-stretch bandage (LSB) can be defined as ‘an elastic CB that contains elastic filament (rubber, Lycra, or elastane) which allows the bandage to stretch more than 120% of its original length’; it can be applied smoothly and conformed according to the contour of the human leg. According to the level of compression applied by the LSB, it might be essential to take it off at night because the resting (static) pressure when sleeping is annoying. Short-stretch (SSB) are ‘elastic CB, however, is composed of cotton yarns, but usually it’s highly twisted yarns (1200 to 2300 turns/m) [22], these yarns are interwoven to enable the bandage’s original length to be extended by almost 60 to 70% during application’. The main advantage of these short-stretch CBs is that they achieve high working pressure that is necessary for lymphatic drainage as well as venous flow [23-27].

1.3 Production methods and structures of woven compression bandages

There are three methods for producing compression bandages to achieve the optimum stretch and elasticity; first method is using highly twisted warp yarns. The optimum elastic recovery of this WCB can be achieved by adjusting the hot water treatment without tension (such as 100% cotton) [28]. The obtained bandage by this type is usually SSB, see Figure 1.3. The second method is using elastomeric filament (elastane or rubber) with Viscose or Polyamide to produce LSB, as illustrated in Figure 1.4 [29]. The third method is using two polymeric yarns which have different melting point by steaming and heat setting. The optimum

elastic recovery of WCB can be achieved by adjusting the main structural parameters of both warp yarns and fabric construction. These warp yarns' parameters are the linear density, twist level, and modulus of elasticity (E). Besides the fabric construction parameters are the yarns (warp and weft) linear density, crimp ratio (as a function of yarns' set), and packing density (as a function of weight per unit area (g/m^2) and fabric thickness).

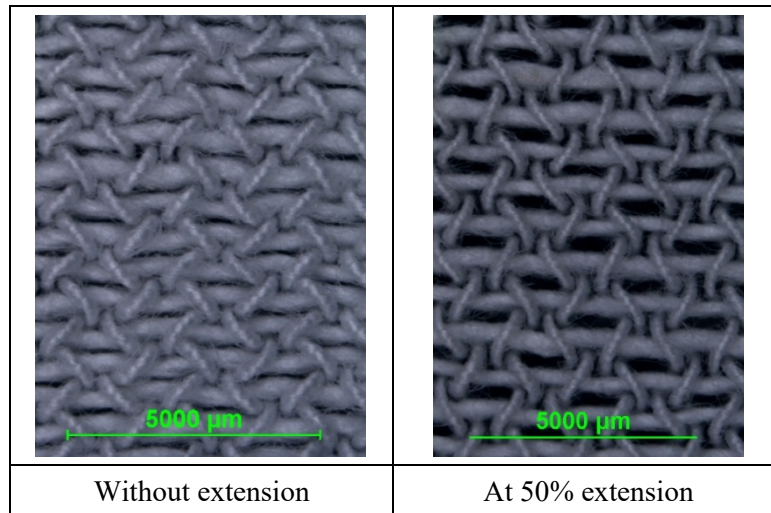


Figure 1.3. Woven bandage structure based on plain weave, without elastane

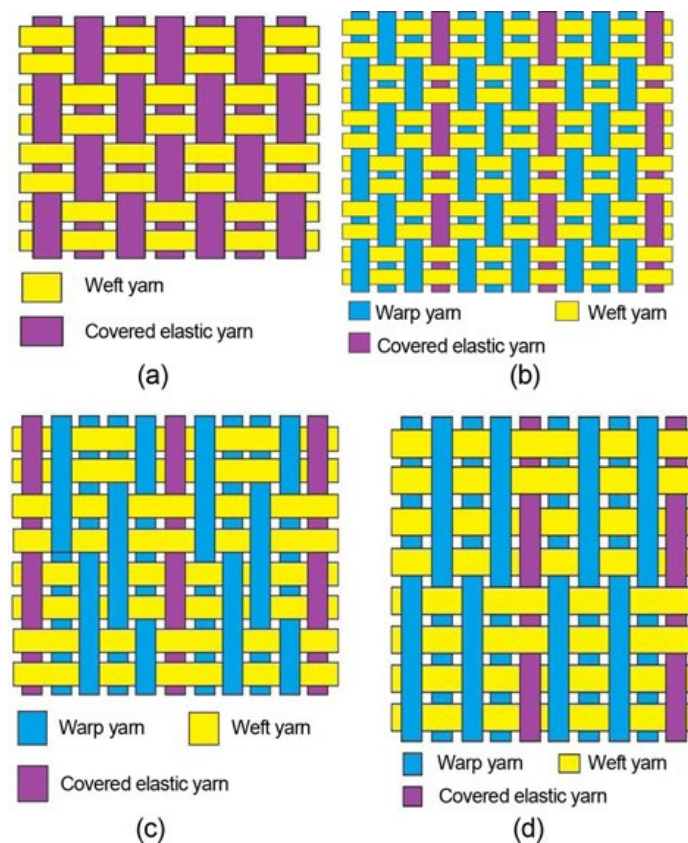


Figure 1.4. Woven bandage structures, based on plain weave and elastane [29]

The optimum elasticity of LSB is mainly dependent on the linear density of elastane filament as well as the yarns and bandage structure to achieve the required bandage tension which is responsible for the sub-bandage pressure, see [Figure 1.4](#).

1.4 Relationship between yarn parameters, weaving settings, and fabric strength

Smith concluded that yarns of lower twist had lower strength due to fibre slippage, moreover yarns of very high twist had lower strength because of increased fibre obliquity to the yarn axis. So that it necessary to adopt the optimum twist level for single and plied yarn to decrease the fibres slippage by tightening the yarn structure [\[30\]](#).

The higher yarn twist affects the fabric strength in two ways, firstly by increasing the yarn strength. Secondly it decreases the binding effect of fabric structure by increasing the yarn compactness [\[31\]](#). Similarly Essam concluded that although a higher degree of twist lead to a higher strength in the yarn for a range of twist multipliers 3 to 5, however, this is not realized in the same proportion in the fabric strength. Increasing the yarn twist beyond the twist multiplier of 4.33 does not increase the fabric strength, particularly with close woven fabrics [\[32\]](#). Likewise, Chattopadhyay concluded that higher yarn twist could increase strength up to a certain extent and beyond that it failed [\[33\]](#).

According to Taylor, the fabric strength was increased with the increase in warp and weft linear density by improving the fibre binding relative to the yarn strength [\[34\]](#). Seo et al concluded that a dense fabric showed high strength since the yarn failure was initiated at the bending point where the highest local strain occurred [\[35\]](#). Essam reported that strength of fabric increased with the increase of fabric settings (warp and weft densities) but after certain limits this increase did not yield a corresponding increase of strength [\[32\]](#).

1.5 Compression therapy of venous leg ulcers

Due to the lower blood pressure in the venous system compared to the arterial system, the walls of the veins are thinner than the companion arteries and they have larger diameters. Thin walls enable veins to have a large capacity for expansion; moreover the large diameter explains why veins store about 60% to 75% of the blood. The valves are cusps and attached by their convex edges to the venous wall. Their concave margins are directed with the flow and lie against the wall as long as the flow is towards the heart. When blood flow reverses, the valves close [\[36\]](#), [\[37\]](#). The venous network in the lower limb is divided to three systems that

work together to return blood to the heart. These systems are: the superficial veins, the deep veins and the perforator veins. There are three major deep veins below the knee: the anterior tibia vein, posterior tibia vein and peroneal vein [38]. The venous blood flow of lower extremity consists of 3 components: the superficial, communicating, and deep veins. The superficial venous system is connected to the deep venous system through smaller communicating or perforator veins. The deep veins are categorized as either intramuscular or intermuscular. These three venous systems are equipped with one-way bicuspid valves which open only toward the deep system, allowing blood to flow in a cephalad direction to prevent reflux. Blood is transferred through the leg toward the heart primarily by the pumping action of the leg muscles [39], [40].

Five types of compression therapy in venous leg ulcers (intermittent pneumatic, stockings, multi-layer, two layer short-stretch bandages, and Unna boots) were compared. The comparison included analysis of changes of the total ulcer surface area, volume, and linear dimensions inside observed groups, and ulcer healing rates. After two months the highest healing rates were in the intermittent pneumatic compression 57.14%, stocking 56.66%, and multi-layer short-stretch bandage 58.62%. Significantly much worse rate was in two layer short-stretch bandages 16.66%, and Unna boots 20% [41].

1.6 Thermal comfort properties of woven fabrics

Human thermal comfort is defined as ‘a condition of mind that expresses satisfaction with the surrounding environment’. High temperatures and humidity provide discomfort feeling and sometimes heat stress. Moreover, discomfort and heat stress reduce the productivity of labours and might lead to more serious health troubles, especially for elder people [42]. Medical CBs are designed to meet both the safety and the comfort of human beings, especially patients. The thermal resistance of fabrics is a primary determinant of body heat loss in cold environments. Generally, high thermal resistance values of the clothing are required to maintain the body under thermal equilibrium conditions. In hot environments or at high activity levels, evaporation of sweat becomes an important avenue of body heat loss and fabrics must allow water vapour to escape on time to maintain the relative humidity between the skin and the first layer of clothing about 50% [42-45].

1.6.1 Effect of pressure on heat transfer through multilayer fabrics

Compression bandages are often applied under a defined range of pressure, which is a

significant factor in determining the heat transfer properties of multilayer fabrics. O’Callaghan and Probert [56] tested the thermal resistance of one to eight layers of woven cotton, polyester, and nylon fabrics under various mechanical loads and indicated that the thermal resistance of fabric assemblies reduced with an increase in applied loading and that these losses were relatively low as compared with the changes resulting from varying the thickness. Karunamoorthy and Das [57] developed a modified version of the guarded hot plate apparatus and measured the thermal resistance and conductivity of 20 different multilayer needle-punched nonwoven fabric assemblies under three levels of compression load (700, 1400, and 2100 Pa). The test results showed that the thermal conductivity of fabric assemblies was greater at the higher compression load due to a decrease in the volume of entrapped air.

1.6.2 Effect of trapped air on thermal resistance of multilayer fabrics

When people wear multilayer clothing ensembles under cold weather conditions or in hot environments, air spaces (air layer) are present between the skin and the inner layer or between two adjacent layers. These air spaces play a vital role in determining thermal properties of clothing. The thermal resistance of multilayer fabrics with air layers increased generally as the thickness of the air spaces increased up to a critical point. When the air layer thickness increased further above this point, the rate of increase in thermal resistance was slowing down due to disturbance of convection and turbulence. This critical thickness was observed to be variable in different studies. Thus, including air spaces that are close to real life is an effective way to enhance thermal resistance of multilayer fabrics. More insulation per additional layer was obtained, when fabrics were assembled, a thin layer of air was enclosed between the layers, especially for fabrics with rough or irregular surfaces. Moreover, more insulation per additional layer could be ascribed to the fact that air spaces were between two layers, resulting in greater thermal resistance than the sum of single layers [48].

1.7 Detection and analysis of muscles’ activation

Electromyography (EMG) is ‘the subject which deals with the detection, analysis, and utilization of electrical signals emanating from skeletal muscles’. The electric signal produced during muscle activation, known as the myoelectric signal, is produced from small electrical currents generated by the exchange of ions across the muscle membranes and detected with the help of electrodes [49]. EMG aims to measure the muscle’s activation level and provide estimation for exercise intensity of selected muscles during activity. EMG signal can contribute to enhance the human body muscle’s function [50].

Compression therapy limits the flow of diseased surface veins, increases the flow through deeper veins, and reduces swelling. Patients who are compliant with compression therapy have significantly improved ulcer healing rate and decreased rate of recurrence. Compression is thought to either correct or improve venous hypertension, mainly owing to an improvement of the venous pump and lymphatic drainage. Compression also improves the blood flow velocity through deep and superficial veins [18]. Most of research related to EMG test was performed on athletics or normal volunteers, rarely work was done on real patients. Moreover some studies were using only knitted CGs or socks. Based on literature review it is essential in candidate work to analyse the effect of WCBs on selected muscles of hand and lower leg. Then discuss the muscles' behaviour of FC, SO and MG muscles while wearing WCB using surface electrodes by e-Motion electromyography wireless tester.

2. Chapter 2: The Purpose and Aim of the Thesis

The purpose of this thesis is to study the structure and behaviour of short-stretch cotton woven compression bandages (WCBs). The aims of this thesis are focused on three main parts: definition of the structure of WCBs, modification of the construction of WCBs as well as analysis of properties, and behaviour of WCBs. Based on the definition of structure as well as the behaviour of WCBs, it is possible to create better conditions during the application of a bandage by a patient, nurse, and athletic user. Based on the modification of the construction of WCBs, we are able to find a connection between structure and applied tension of a bandage during static and dynamic applications. Moreover, the motivation of this research is to investigate the optimum conditions for compression therapy using long- and short-stretch WCBs. The methodology is based on evaluating the elastic recovery of both types of bandages during uniaxial stress and cyclic loading-unloading to simulate the real activities of a patient or athletic performance during resting and walking actions. The main topics of this thesis are:

- 1) Analysis of input staple twisted cotton yarn for producing 100% cotton bandages
 - 1.1. Staple twisted (plied) cotton yarn versus mechanical properties.
 - 1.2. Modified surface of input threads to produce multifunctional WCBs.
- 2) Analysis and modification of cotton woven bandage structure

To achieve the required goals of the thesis, it was necessary to:

- 2.1. Evaluate the structure of three basic types of WCBs showing the material, production as well as deformation viewpoint during the uniaxial stress.
- 2.2. Study and modify the construction as well as the structure of woven cotton bandage: The bandage includes an integrated tension sensor, which causes a change in the spacing of coloured threads during its deformation. The solution is sensors in the bandage in the form of a different colour pick from the other structure of the bandage. Different colour picks with regular distance become visible due to deformation / stress in the bandage. The production of this bandage is possible by applying weft threads with different colours by a fancy picking mechanism of a weaving machine. The colour patterns and threads in the bandage can also be used to uniquely identify whether the bandage is suitable, for example, for a high or low degree of compression. Thanks to this sensor, it

is possible to accurately quantify the tensile force in the bandage, during its application and during the ongoing compression of living tissue. It is therefore both a matter of facilitating the application of the bandage and of checking the condition of the bandage after its application. Appropriate adjustment of the tensile force in the bandage will be beneficial for accelerating the healing processes.

- 2.3. Introduce a new method to predict the corresponding bandage tension by measuring the bandage extension and porosity using digital camera attached to the tensile testing device.
- 2.4. Compare the practical pressure measured by Picopress with theoretical compression forces calculated by a modified Laplace's law equation.
- 2.5. Evaluate the elastic recovery of WCBs during cyclic loading-unloading on the tensile testing device then compare these results with the bandage application on mannequin and human leg at different positions and activities.

3) Evaluation of other individual properties of woven bandages

- 3.1. Study the effect of compression bandages on lower leg muscles' performance using eMotion wireless EMG system.
- 3.2. Discuss the factors affecting thermal comfort properties of WCBs, using the ALAMBETA and PERMETEST at different extension levels. Moreover compare the obtained results with the thermal foot manikin as a virtual simulation of the real bandaging system.
- 3.3. Validate the experimental results of thermal resistance on ALAMBETA and thermal foot manikin with three mathematical models.

2.1 Influence of fibre and yarn characteristics on mechanical properties of bandages

There is a strong positive correlation between the cotton warp yarns ply twist and the required cotton bandage elasticity. This bandage elasticity can be defined as 'the elastic recovery after extension or compression when it is subjected to repeated stresses and activities'. Moreover the yarn strength is a function of the fibres characteristics (mainly the fibre fineness,

cross-section, and tenacity) as well as the yarn parameters (i.e. twist coefficient, number of fibres in cross-section, and yarn evenness).

2.1.1 The mechanical behaviour of twisted short staple yarn structures

The geometric arrangement of filaments (fibrils) in the structure of twisted fibre bundles can be described by a model of concentric helices, the so-called ideally helical model, as illustrated in Figure 2.1 [51], [52]. This model assumes the following:

- The axes of all fibres have the shape of a helix with the same direction of rotation.
- Helices of all fibres have one common axis, which is a multifilament yarn axis.
- The height of one coil of each helix is the same.
- The packing density is the same at all places inside the multifilament yarn.

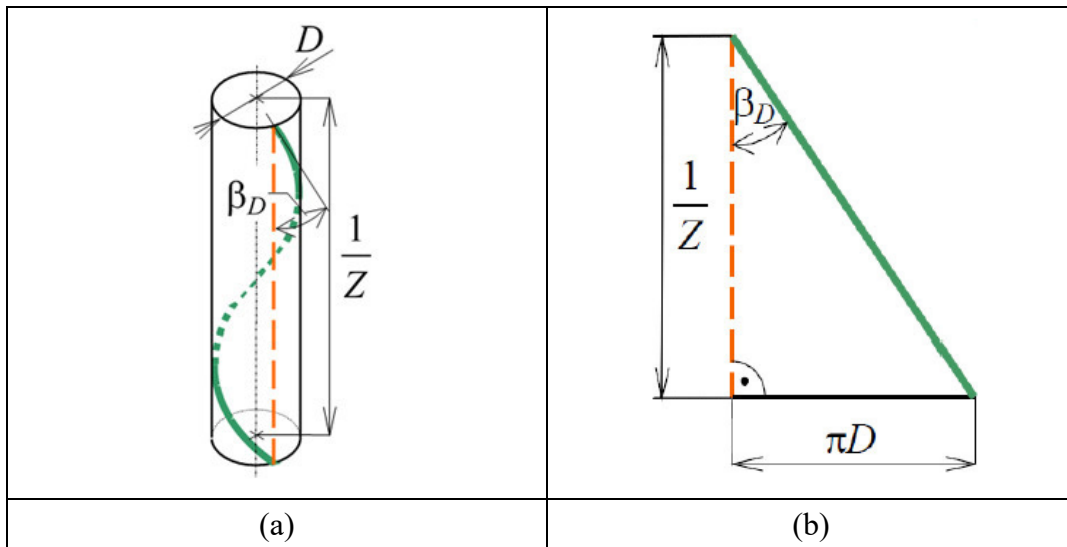


Figure 2.1. A peripheral fibre in helical model of multifilament yarn of diameter D [53],
a) One coil of a helical fibre on yarn surface and **b)** Unrolled yarn surface

Mertová, et al. [33] considered that peripheral fibres have the shape of a helix with an angle of fibre slope to the multifilament yarn axis β_D and the height of one fibre coil is $1/Z$. The surface of multifilament yarn forms a triangle. According to Figure 1.5 they obtained equation (1.1):

$$\tan \beta_D = \pi D Z = \frac{2\sqrt{\pi\alpha}}{\sqrt{\mu\rho}} \quad (1.1)$$

Where β_D denotes the slope angle of peripheral fibre to the linear axis of the twisted fibre bundle (the angle of peripheral fibre), D is the diameter of cylindrical helix of peripheral fibres axis, Z is the number of twists per unit length of the twisted fibre bundle, α is Koechlin's

twist coefficient, ρ is the fibre density, and μ is the packing density of fibre bundle. The relationship between twist (Z) and fineness (T) of the twisted fibre bundle was derived by Koechlin, see equation (1.2):

$$Z = \frac{\rho}{\sqrt{T}} \quad (1.2)$$

They confirmed that increasing the twist level has increased the angle of peripheral fibres (β_D) and the angle between the axis of fibre on the surface and the line parallel to the yarn axis (β') increased as well. There was shortening (twist take-up) of the multifilament yarn because of twisting. It was associated with an increase in yarn count value which was expressed by the substance cross-sectional area of multifilament yarn [54].

Despite wide application of short staple yarns, the twist reinforcing or strength generating mechanism as a fundamental structure assembling means for the materials has not been clearly understood. There is no general theory that can be used to explain the mechanics of such structures. The problems in understanding the structural mechanics of staple yarns are primarily caused by two factors as indicated, for example, by Goswami [55], that is, the discontinuities in fibre length and the slippage of fibres during yarn extension. Factors such as twist and fibre migration (i.e., variation in radial position in a yarn) in staple yarns acquire different dimensions, since they are the only reasons why a bundle of short fibres is held together in a linear assembly. Moreover, in staple fibre yarns, the fibre volume fraction is not only low, but also variable, which results in no clearly defined surface of the structure. Besides, because of the structural changes of short-fibre yarn at different twist levels, it is essential to consider the yarn fibre-volume fraction, and consequently all the mechanical properties of the yarn, to be variables of yarn twist. This makes the analysis extremely difficult [56].

Pan tried to develop a general constitutive theory governing the mechanical behaviour of twisted short fibre structures. He started with a high twist case, so that the effect of fibre slippage during yarn extension could be ignored. He established a relationship between the mean fibre volume fraction and the twist level of the yarn. He concluded that the tensile and shear moduli are proportional to the fibre tensile modulus, with the proportionality constants consisting of three parts, one being the fibre volume fraction, the second was the length efficiency factor in which the fibre dimensions are included, and the third reflecting the effect of fibre obliquity or fibre orientation distribution in the yarn. Twist affects the values of the yarn moduli through these factors [56].

2.1.2 *Effect of twist level on yarn properties*

One of the important factors which influence the yarn properties is ‘the slope angle of the fibre to the yarn axis’, which called the ‘twist angle’. This angle changes with the level of single or multifilament yarn twist. When the twist per meter increased, the yarn diameter decreased, the individual fibrils came closer, whereas the yarn elongation increased. Increasing the twist level of staple yarn improved their tenacity whereas the higher twist of multifilament yarns reduced their strength which is an important factor in terms of their end-use, especially for technical applications [57].

Abbasi and others produced three counts (30, 40 and 50 Tex) of 70/30 Cotton/Polyester blends at various twist levels (170, 190, 210 and 230 turns/m) to investigate the effect of twist on physical and mechanical properties of low twist yarn. They concluded that the yarn manufactured with 230 turns/m and 50 Tex showed better yarn strength as compared to other twist levels and yarn counts. Increasing the twist level decreased the coefficient of variation in 30, 40 and 50 Tex; this may be due to higher amount of fibres present in yarn cross-section. The irregularity index and yarn hairiness of low twist yarn decreased with the increase of count, moreover it decreased with the increase of twist per meter for the same count [58].

Sreenivasan produced 32 Ne ring spun yarn at three tension levels using travellers of counts 4/0, 6/0, and 8/0. Five different twist multipliers (3.5, 4, 5, 6, and 7) were used for each traveller. He concluded that the yarn unevenness (U %) as measured on the USTER Evenness Tester increases from 17 to 20% with the increase in twist for all three travellers. He analysed why the percent unevenness increased while the C.V. of diameter decreased for higher twist multipliers. It is possibly because in the case of the diameter, at the initial stages of twisting, twist tended to flow into the thinner places leading to a greater compression of these places, and consequently the C.V. of diameter increased. But as the twist increased and the thin places became saturated with twist, it flowed into the thicker places and a greater uniformity in twist as well as in diameter resulted [59].

Kotb investigated the dependence of yarn quality (strength, evenness and imperfections) on the yarn material, twist factor, plying, linear density and cotton ratio of the manufactured yarn, through linear regression equations. 3 types of cotton fibres and six staple polyester types produced by 6 different companies in different countries were used to produce one hundred and six yarns on a ring spinning machines (cotton and blended yarns of cotton/polyester 50/50). The yarn linear density varied from 16 to 40 (Ne), the twist multiplier

for single yarns varied from 3.45 - 4.6, and the twist multiplier for two plied yarns from 2.7 - 4.2 [60]. She noticed that increasing the twist factor, within the working range, increased the yarn strength by average percent 29%. Moreover, the yarn strength slightly increased from yarn count 16 to 20 Ne then it was significantly decreased at 40 Ne. The average yarns irregularity (CV %) decreased from 25 to 21% when changing the twist factor from 3.8 to 4.6 α_c [60].

Altas, S., et al. produced three yarns were spun using linear densities of 29.5, 19.6, and 14.7 Tex and analysed. For each yarn count, three twist coefficients (103, 115, and 127 α_{tex}). Yarn evenness, faults, hairiness and diameter properties were tested using a USTER® Tester 5. In carded yarns, an increase of twist coefficient increases the evenness, tenacity and elongation values and decreases USTER hairiness and diameter values significantly. In combed yarns, the increase in twist coefficient increases tenacity and elongation and decreases the number of thick places, neps, hairiness, and diameter values significantly [61].

2.1.3 Evaluation of the factors affecting yarn strength

The spun-yarn tenacity is mainly affected by the fibre characteristics, spinning process parameters, and yarn structure. Moreover, the fibre fineness, fibre orientation, yarn linear density, and twist level are the most significant factors which control the cohesion forces of spun-yarn strength. Many researchers tried to establish fundamental theories for the staple-fibre yarn strength, such as those provided by Hearle [52], Zurek [62], and Eldeeb [63] applying different approaches based on force deformation analysis. The limitations of using mathematical models for staple-fibres structure decreased the ability of a specific model to simulate and predict the practical yarn performance. There was also a study that analysed the short fibre yarns by using the energy approach, but this method couldn't deal with the fibre slippage effect due to the energy dissipation involved. A finite element method was used to simulate the yarn structure [64], which provided a numerical solution.

Gegauff [65] was the first to theoretically analyse the yarn strength in terms of yarn structure. He derived a simple mathematical relationship between twist angle and yarn strength. Gurney [66] extended that relationship by taking into account the length and frictional properties of fibres in addition to the twist in yarns. He demonstrated that the staple yarn under tension was affected by two types of forces (forces that press the fibres normally and forces that tend to cause slippage). He suggested that if the ratio of the forces tending to cause the slippage to the normal forces exceeded a certain critical value, (which corresponds to the coefficient of friction), then the slipping might occur [67].

2.1.4 Stress–strain relations of fibres and yarn

All theoretical equations described in this subtitle follow the published article of Neckář [68]. Let us consider that an axial force F_Y is acting on a yarn of fineness T , then the engineering tensile stress σ_{EY} can be expressed as:

$$\sigma_{EY} = \frac{F_Y}{S} \quad (1.3)$$

$$\text{Where} \quad S = \frac{T}{\rho} \quad (1.4)$$

The variable S represents the substance cross-sectional area of yarn by Johannsen [69] and ρ indicates the density of the fibres constituting the yarn. The substance cross-sectional area of yarn is defined as ‘the summation of sectional areas of the fibres present in yarn cross-section’. Then, the engineering specific tensile stress of the yarn Y can be expressed as follows:

$$\sigma_Y = \frac{F_Y}{T} = \frac{F_Y}{S \rho} = \frac{\sigma_{EY}}{\rho} \quad (1.5)$$

Similarly, if the axial force F_f is acting on a fibre of fineness t , then the tensile stress of this fibre is $\sigma_f = F_f/s$, where s denotes the cross-sectional area of the fibre. Then, the specific stress of the fibre σ_f is

$$\sigma_f = \frac{F_f}{t} = \frac{F_f}{s \rho} = \frac{\sigma_{Ef}}{\rho} \quad (1.6)$$

Where $(t = s \rho)$ indicates the fineness of the fibre. The force F_Y applied on the yarn causes an axial deformation by increasing initial length L_o to the extended length L_Y . The difference $\Delta L = L_Y - L_o$ is called yarn elongation and the relative strain is known as yarn axial strain and can be written as

$$\varepsilon_Y = \frac{L_Y - L_o}{L_Y} \quad (1.7)$$

Similarly, the initial length L_o of a fibre increases to a longer length L_f , so that the fibre axial strain can be

$$\varepsilon_f = \frac{L_f - L_o}{L_f} \quad (1.8)$$

Figure 2.2 schematically illustrates the specific stress-strain curve of twisted staple yarn and a similar average curve of corresponding fibre. When dealing with yarns and fibres, the specific stresses are functions of strains. Let us suppose that each such function starts from the

origin as an increasing function. The maximum points of specific stress on stress-strain curves determine the breaking specific stress of the fibre σ_f^* (fibre tenacity) and the breaking specific stress of the yarn σ_Y^* (yarn tenacity). The corresponding strains a_f and a_Y are known as breaking strains.

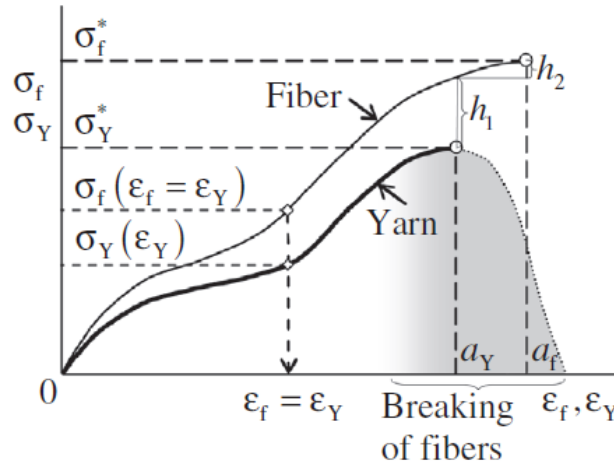


Figure 2.2. Schematic diagram of stress–strain curves of mean fibre and yarn

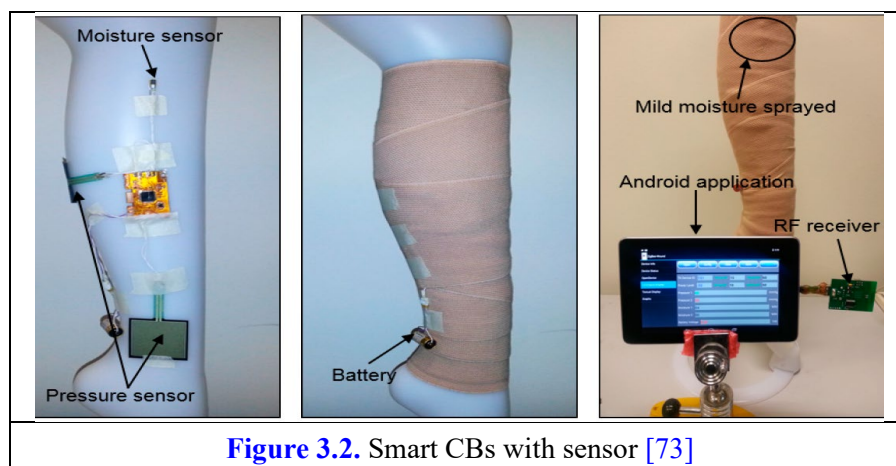
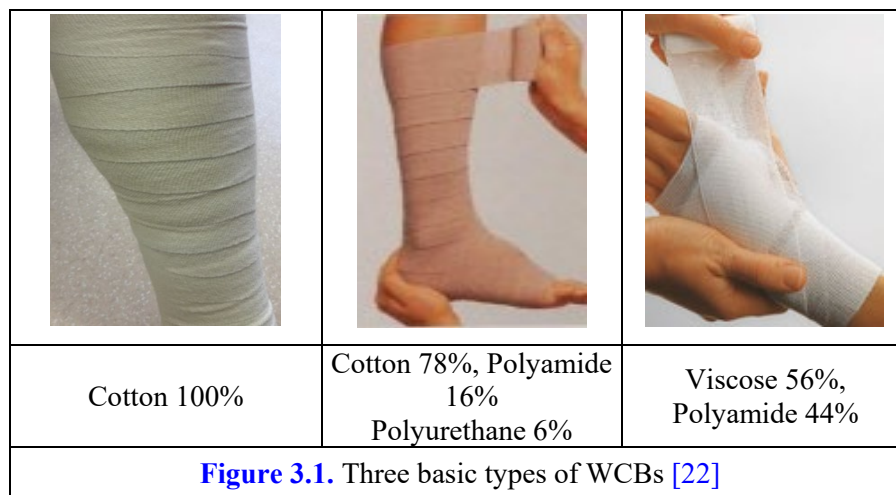
Let us consider that a yarn is prepared from one type of fibre material. ‘The ratio of yarn tenacity and mean fibre tenacity’ is called the coefficient of fibre strength utilization in yarn φ_σ^* , which is smaller than one in all practical cases, it can be described as follows,

$$\varphi_\sigma^* = \sigma_Y^* / \sigma_f^* \quad (1.9)$$

Most of the research based on staple yarns is focused on the prediction of the yarn modulus and the maximum strength. Some researchers investigated the failure response and whole stress-strain curve for the yarns. Also, little attention has been paid to the yarn behaviour under tensile loading. Most of the theoretical work such as Platt [70] and Hearle [71] including other empirical research summarized a fact that understanding tensile behaviour of twisted yarns needs knowledge of constituent fibre properties, the structure of yarns, and testing parameters. The twist level, fibre properties, and fibres’ orientation are the main parameters that may influence the coefficient of fibre stress utilization of staple spun yarns. Zubair et al. proposed a mathematical model, based on the assumptions of small deformation, constant packing density, and contraction ratio. He used numerical integration considering real fibre stress-strain relationship and fibre orientation before the process of yarn break when all fibres are mechanically stressed [72]. Neckář et al. attempted to validate the theoretical models compared with the experimental results [68].

3. Chapter 3: Structure and Behaviour of Cotton Woven Compression Bandages (WCBs)

There are two categories of bandages in the market (normal and smart bandages): The simple or normal bandages, their price is cheap, their structure is simple and based on the plain weave, as shown in [Figure 3.1 \[22\]](#). The second category is smart CBs which have sensors to give the user direct reading of the exerted pressure on the part of the body during any activity, but it's so much costly compared to the first category, see [Figure 3.2 \[73\]](#).



The compression of living tissue using textile bandages is only estimated based on the personal experience of the bandage applicator. The main aim of this thesis is focused on modification of construction of short-stretch cotton WCBs. The bandage includes an integrated tension sensor (fancy picking of different picks), which causes a change in the spacing of coloured threads during its deformation. Based on the study and evaluation of this deformation we are able at the end to give the patient, nurse, or any other user an accurate remarks to adjust the applied compression to the body part, see [Figure 3.3](#). It is possible to convert the simple

bandage to smart bandage by modifying the bandage structure such as adding the blue marks (rectangles of 2cm x 1cm to be squares of 2x2 cm² at 100% extension) or adjusted according to the required bandage tension, as illustrated in Figure 3.4. This modification could control the bandage tension as a function of the applied extension that ranges from 50 to 100% depending on the bandage construction and the number of layers [22].

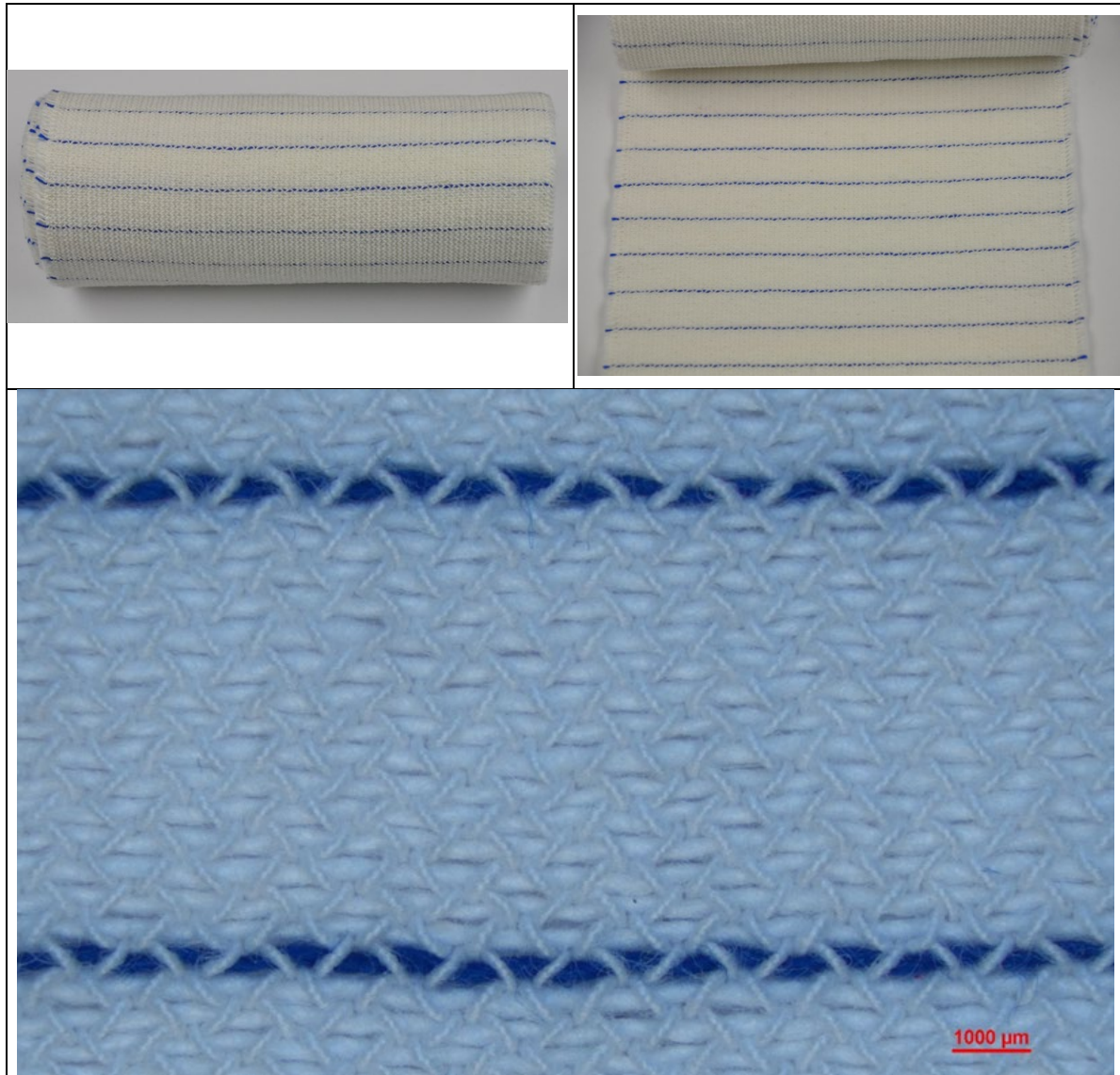


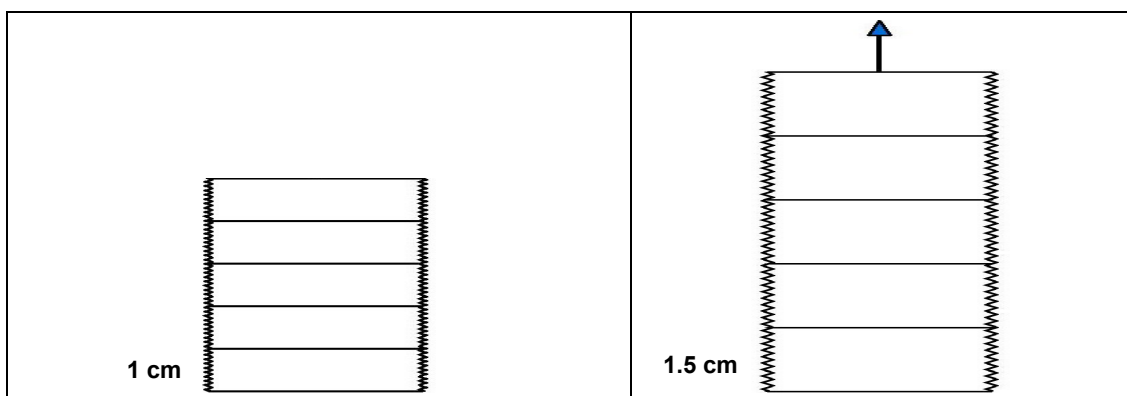
Figure 3.3. Presentation of the innovated cotton WCB and its structure



Figure 3.4. The blue marks on the three basic types of WCBs

Secondly, the total production cost could be reduced by using different coloured weft repeated every 1 cm during the weaving process as illustrated in [Figure 3.5](#), instead of printing or adding the coloured marks after bandage production. Moreover, multifunctional antimicrobial double weft WCB can be produced using highly twisted warp yarns (ply twist 1800 to 2300 twists/m) and only the surface weft yarns in contact with the patient skin will be treated with Zinc or Titanium Nano-particles [28]. As a result, the bandage cost would significantly be reduced and the final product would achieve the smart performance which might gain higher marketing prices and benefits.

There is scarce information relating to the effect of high ply twist on the warp yarns elasticity that are being used in woven bandages [74]. Therefore, this study initially investigates the commercial yarns available in the bandage market in addition to yarns spun at a broader range of ply twist. Moreover, the study reveals the influence of bandage material, structure, and the bandaging techniques on its mechanical and thermal comfort properties as well as durability since there is a few sources about this point [36].



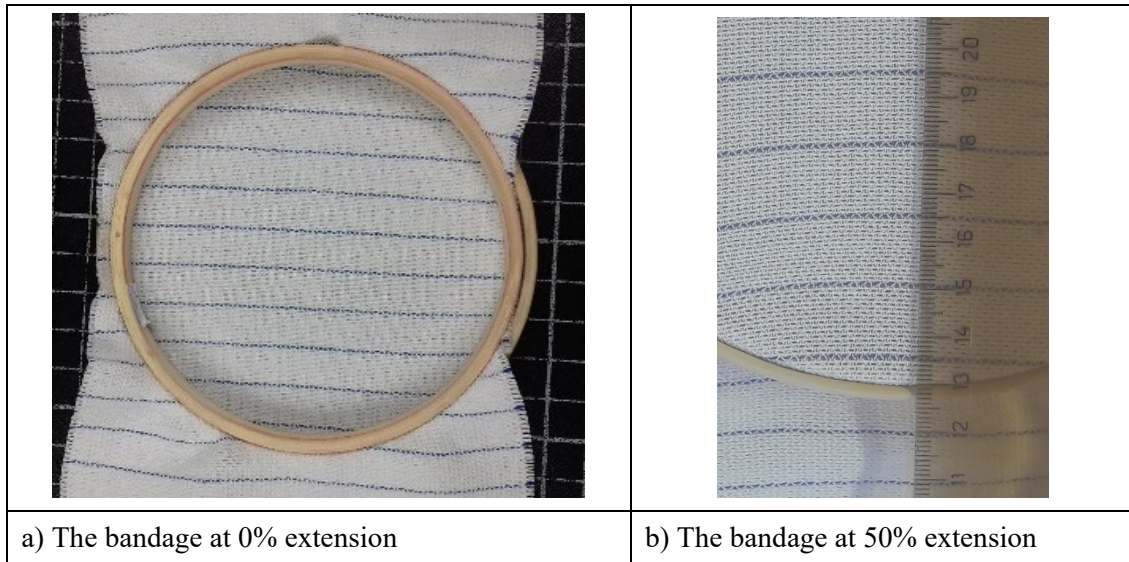


Figure 3.5. A Coloured weft repeated every 1 cm during the bandage weaving

The evaluation of the recalculation of the change in the spacing of coloured wefts (deformation) of the cotton bandage and the resulting compression during the bandage application is described in the following chapters, (more details in parts 5.2.1.3. and 5.2.3.). Based on these fancy weft threads or the blue rectangles, it is necessary to demonstrate the three levels of bandage tension (low: 50% extension and 50% overlap, medium: 100% extension and 50% overlap, and high: 100% extension and 66% overlap) applied on the 1st position (ankle at average radius 3.9 cm), 2nd (mid-calf at average radius 6.2 cm), and 3rd (below the knee at average radius 4.9 cm). The main conclusion is that the optimum applied tension is directly proportional with bandage extension and its porosity for all bandage types. As a short-stretch WCB, 100% Cotton bandage needs 60% extension to achieve the required bandage tension 10N that achieve a corresponding compression of approximately 30 mmHg for average leg radius of 5 cm and bandage width 10 cm using two layers bandaging technique.

4. Chapter 4: Analysis and Evaluation of the Warp and Weft Yarns for Cotton WCBs

4.1 Methods used, studied material

The experimental work of the Ph.D. thesis was carried out on two main parts, the first was analysis and evaluation of the twisted warp yarns as well as the treated weft yarns with antibacterial nanoparticles. The second was evaluation of the structural, mechanical, thermal, muscle activation properties of the three basic types of WCBs then produce a new modified structure of WCB to simulate the smart bandages with low cost.

4.1.1 Analysis of mechanical properties of the used warp yarns

The methodology plan was divided to two steps, the 1st was to evaluate the mechanical properties of the used plied warp yarns for producing WCB in market. Moreover as a result, the 2nd step was to produce a special range of warp yarns at ply twist 600 to 2200 twists/m to achieve the required high extensibility and elasticity of the WCB. The main factors influencing the cotton WCB tensile properties are the warp yarns twist, linear density, and tenacity. The required bandage tension can be adjusted by optimum bandage extension as a function of warp yarns twist and other properties. Two groups of warp yarns were kept in a conditioning room for 24 hours at standard temperature (20 ± 2 °C) and relative humidity (65%) before testing. The tested warp yarns characteristics can be summarized in [tables 4.1 & 4.2](#):

Table 4.1: Yarn characteristics (Group 1: plied yarns, fine count 6x2 Tex)

Yarn Twist (twist/m)	Actual Yarn Count (Tex)
300	11.78
600	12.16
900	12.87
1200	13.24
1500	13.71
1800	13.96

Table 4.2: Yarn characteristics (Group 2: plied yarns, coarse counts 21x2 and 30x2 Tex)

Yarn Twist (twist/m)	Nominal Yarn Count (Tex)	Actual Yarn Count (Tex)
1850	21x2	49.37
2100		51.15
2200	30x2	74.72
2300		80.27

The load-elongation curve of the warp yarns was measured according to the standard test method ASTM D2256 [75]. Instron 4411 tensile testing machine was used to measure the tension developed in the yarn while keeping gauge speed of 180 mm/min. The device gauge length was set to 500 mm. Twist per meter was measured on TWIST LAB-2531C twist testing machine according to standard procedure CSN 80 0701. The yarn linear density was measured from a lea of one hundred meters according to the standard test method CSN 80 0050. Five samples for each type of yarn were prepared on lea making machine and each sample was weighed in grams on weighing balance and yarn count was determined from the mean of five yarn samples.

To produce the new proposed double weft WCBs, single ring-spun yarns were produced from Egyptian cotton fibres - Giza 86, according to the following spinning parameters by using Rieter G37 ring spinning and their properties are listed in Table 4.3.

Table 4.3: Produced single yarn properties, ring-spun raw yarns

Nominal yarn count (Tex)		15	15	20	20	25	25	30	30
Twist direction		S	Z	Z	S	S	Z	Z	S
Actual yarn count (Tex)	Average	14.7	15	19.7	19.8	24.6	24.7	29.5	29.8
	C.V. (%)	1.6	1.7	1.6	1.3	1.2	1.11	1.1	1.04
	Std. (Tex)	0.24	0.26	0.32	0.26	0.30	0.27	0.32	0.31
Twist/m		1031	1062	910	925	803	799	751	748

The linear density of the weft yarns was kept 60 Tex for all bandage samples. As far as the warp yarns are concerned, among all above single yarns, the 20 Tex yarns in S and Z-direction were chosen to be plied on DirecTwist twister on two plies at a nominal twist level ranges from 600 to 2200 twist/m and at different twist direction as demonstrated in Table 4.4.

Table 4.4: Produced plied yarn properties, ply of ring-spun yarns 20x2 Tex

Twist direction, SS-Z		SZ-Z		ZZ-S	
Ply twist, twists/m	Actual yarn count, Tex	Ply twist, twists/m	Actual yarn count, Tex	Ply twist, twists/m	Actual yarn count, Tex
606	40.03	597	40.87	602	39.63
1181	41.88	1216	42.18	1204	41.29
1761	45.78	1793	46.68	1773	48.40
2185	52.26	2168	55.45	2172	54.42

4.1.2 Modification of the surface of used yarns

Most of the available WCBs are designed to achieve the gradual compression for leg ulcer healing or athletic performance. Current study aims to introduce multifunctional performance by compression therapy, antimicrobial, and wound care for the normal user or patients. So it is necessary to treat the warp and weft yarns which in contact with the human body with effective antimicrobial agent such as Silver Nanoparticles (NPs) or Zinc Oxide or Titanium Dioxide.

4.1.3 Preparing Cotton yarns treated with Silver NPs

Colloidal form of Silver NPs was prepared using Glucose as reducing agent. Uniform Ag-NPs were obtained by reduction of Silver nitrate at 70°C under atmospheric pressure. Poly Vinyl Pyrrolidone (PVP) was used as stabilizer. Glucose Ag-NPs were synthesized by dissolving AgNO₃ (157 mg) and PVP (5 g) in 100 ml of 40% (w/w) of Glucose syrup. 5 ml of sodium chloride were added to the samples for complete reaction and to convert all the ionic Silver to NPs [76]. Ten samples, 200-300 m of bleached Cotton yarns were wound on perforated Polypropylene bobbins, their thickness ranges from 5-10 mm. Five samples were immersed in Glucose Ag-NPs solution for 1 min (D₁) and the other samples for 60 min (D₂).

4.1.4 Silver NPs activity of treated yarns

For the tests, pathogenic bacterial strains were used for the qualitative test method (AATCC 147) and quantitative test method (AATCC 100). Escherichia Coli (E.C.) - CCM 2024 (ATCC 9637), gram-negative rod-shaped bacteria and Staphylococcus Aureus (S.A.) - CCM 2260 (ATCC 1260), gram-positive rod-shaped bacteria were purchased from Czech Collection of Microorganisms, Masaryk University in Brno.

A) Method AATCC 147: 1 ml of the bacterial inoculums (E.C. and S.A.) at a concentration of 10⁸ CFU/ml was individually inoculated onto Petri blood agar plate, the test sample was inserted into the middle of the plate. The prepared samples were cultivated in thermostat 24 hours / 37 °C [77].

B) Method AATCC 100: 10 ml of E.C. and S.A. at a concentration of 10⁸ CFU/ml were applied on the sample. The sample was placed in a sterile container and cultured 24 hours / 37 °C. After 24 hours, 10 ml of physiological solution was added and the sample was shaken. 1 ml of solution was removed and plated onto Petri blood agar plate. The samples were cultured for 24 hours / 37 °C. The antibacterial activity of AgNPs treated cotton fabrics was

quantitatively determined before and after washing using bacterial percentage reduction test (AATCC 100-2004) according to the American Association of Textile Chemists and Colorists Technical Manual (2010) [78].

4.1.5 Testing the Nanoparticles size and its distribution

Some samples of single and plied warp yarns were treated with silver nanoparticles. Moreover two types of the new produced bandage samples were treated with three concentrations of zinc oxide nanoparticles in powder form with 15 g/L binder. The nanoparticles size and its distribution were evaluated using the scanning electron microscopy (SEM) and the energy dispersive X-ray (EDX) for the treated and un-treated single and plied yarn samples as well as the two types of WCBs.

4.2 Summary of the achieved results

4.2.1 Relationship between yarn twist and tenacity

A Matlab code was created to calculate the average load-elongation curves for each yarn (using raw data of 50 samples for each yarn sample). For comparison between yarns, the program interpolates the elongation data using equal step (0.05 mm) before the breaking point and gives the corresponding load values.

Figure 4.1 and Table 5.17 illustrate that increasing the plied yarn twist, in group 1, from 300 to 600 twist/m increases the yarn tenacity and breaking elongation by 5.16 and 8.21% respectively. After that, the yarns breaking load gradually decreases by increasing the yarn twist from 900 up to 1800 twist/m, on the contrary, the yarns extension significantly increases by 27.48%. Whereas the plied yarn, group 2, at twist 2100 twist/m is giving fewer tenacity values than 1850 twist/m by 20.86%, moreover the tenacity decreased by a percent 15.73% at 2300 twist/m. These lower values of tenacity may be due to the increase in twist angle near to the perpendicular level (wrapping angle $\approx 87^\circ$) at the highest levels of ply twist, as a result the horizontal component of the forces contributing in yarn strength is decreasing.

The obtained results in Figures 4.1 - 4.3 contribute to selecting the optimum yarn twist, but it's not conclusive because the twist range and the yarns count are different. At least (1500-1800 twist/m) are required for producing high extension Cotton compression bandages, whereas to achieve 100% elastic Cotton compression bandage (2200 – 2300 twist/m) would be used. The optimum extension level and applied load entirely depend on the final end-use of the compression bandage either for venous leg ulcers or athletic performance.

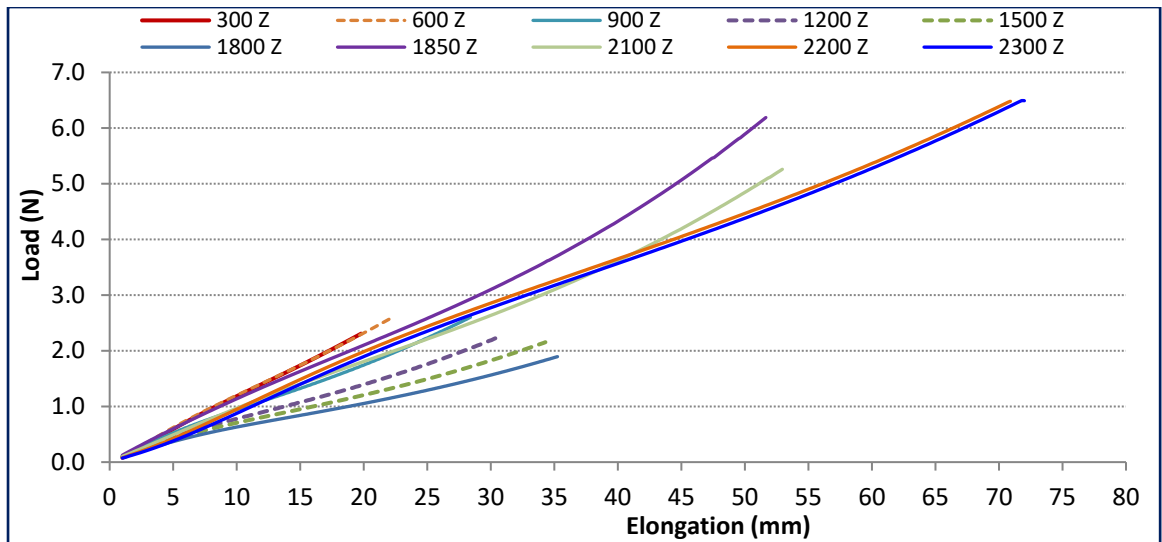


Figure 4.1. Load-elongation curves of the 1st and 2nd groups of yarns

Tables 4.2 and 4.3 summarize the mechanical properties of the plied yarns that commonly used in producing the WCB in market. Increasing the ply twist of fine count 6x2 Tex, from 300 to 1800 twist/m, increases the actual plied yarn linear density by 18.51% for fine count 6x2 Tex. As for coarse counts in group 2, the actual yarn count increases by 27.88 and 33.78% for nominal counts 21x2 and 30x2 at twist level 2100 and 2300 twist/m respectively.

Taking into consideration the yarn properties; the comparison would be using the tenacity (cN/Tex) and extension (%) of the yarns as illustrated in equations (5.1) to (5.3).

$$\text{Tenacity} = \text{Breaking load (N)} * 100 / \text{Yarn count (Tex)} \quad (5.1)$$

$$\text{Strain} = \Delta L / L_1 \quad \text{or} \quad \text{Extension (\%)} = \Delta L * 100 / L_1 \quad (5.2)$$

$$\Delta L = L_2 - L_1 \quad (5.3)$$

Where:

L_1 is the initial (gauge) length; L_2 is the extended length of yarn.

Table 4.5: Yarn properties, Group 1: plied yarns, 6x2 Tex

Yarn twist (twist/m)	Actual yarn count (Tex)	Tenacity		Extension	
		Average (cN/Tex)	Standard deviation Std. (cN/Tex)	Average (%)	Std. (%)
300	11.78	23.64	1.4275	4.75	0.6118
600	12.16	24.86	1.5201	5.14	0.6515

900	12.87	23.51	1.9156	6.44	0.8210
1200	13.24	20	1.7504	6.98	0.7502
1500	13.71	18.09	1.4808	7.67	0.6346
1800	13.96	16.49	1.5827	8.21	0.6783

Table 4.6: Yarn properties, Group 2: plied yarns, 21x2 and 30x2 Tex

Yarn twist (twist/m)	Nominal yarn Count (Tex)	Actual yarn count (Tex)	Tenacity		Extension	
			Average (cN/Tex)	Std. (cN/Tex)	Extension (%)	Std. (%)
1850	21x2	49.37	15.53	1.2982	12.01	0.6491
2100		51.15	12.85	1.2596	12.19	0.6298
2200	30x2	74.72	9.86	1.4965	15.78	0.7483
2300		80.27	8.52	1.2289	15.77	0.6144

These yarn parameters can be displayed as shown in Figures 4.2 & 4.3 to give accurate comparison and best selection of the optimum (critical) yarn twist. The candidate results of yarn tenacity and breaking elongation wouldn't be reached when producing the elastic WCBs because these bandages are only produced using the elastic region of the warp yarns. The 1st group of plied yarns achieves higher tenacity values than the 2nd group but lower extension. So the best selection of the yarn twist and count depends on the end use of the compression bandage.

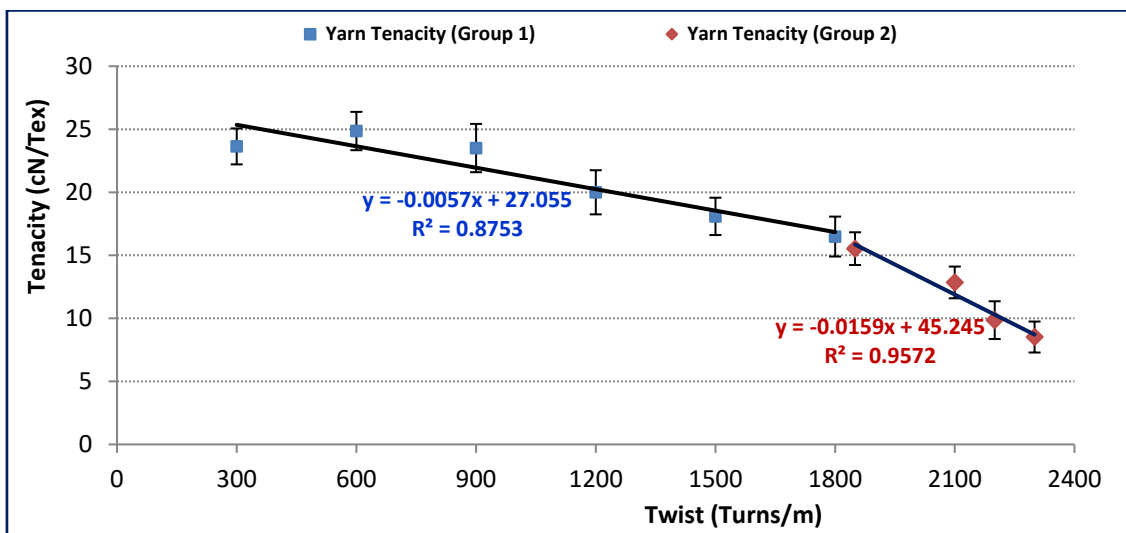


Figure 4.2. Effect of plying twist on yarn tenacity for market yarns

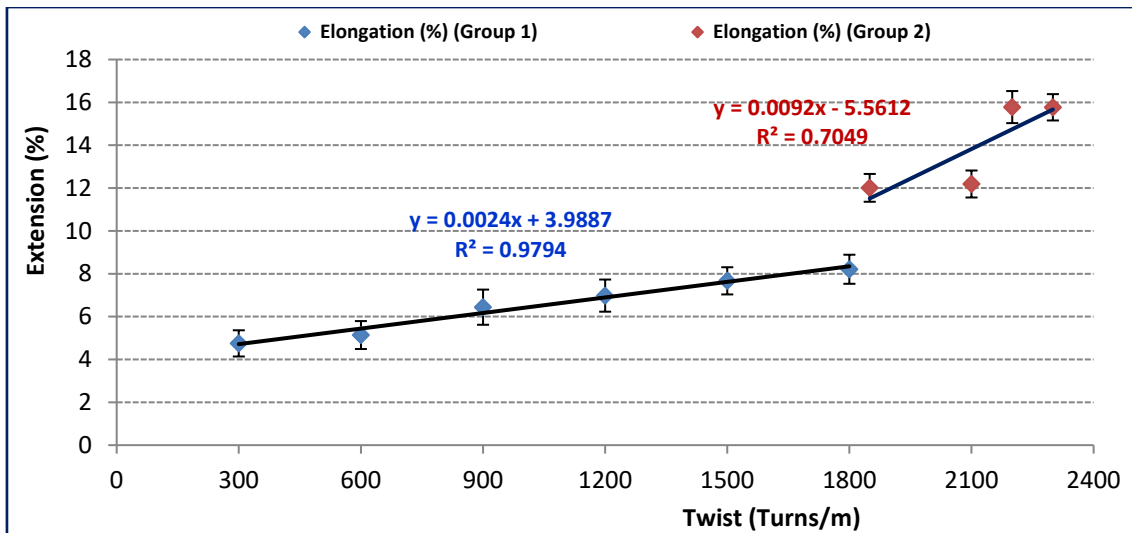


Figure 4.3. Effect of plied yarn twist on its extension, market yarns

The evaluation of the used plied warp yarns in market for producing the WCB and the new produced yarns concluded that the warp yarn tenacity should be greater than 16 cN/Tex and its extension should be at least 12% to produce the highly stretched 100% Cotton WCB, as displayed in Figures 4.2 – 4.5 and listed in Tables 4.7 - 4.10. The twist range (1500 - 1800 twist/m) is required – at least – for producing high extension Cotton compression bandages, whereas to achieve 100% elastic Cotton compression bandage (2200 – 2300 twist/m) would be used. The optimum extension level and applied load totally depends on the final end-use of the WCB either for venous leg ulcers or athletic performance.

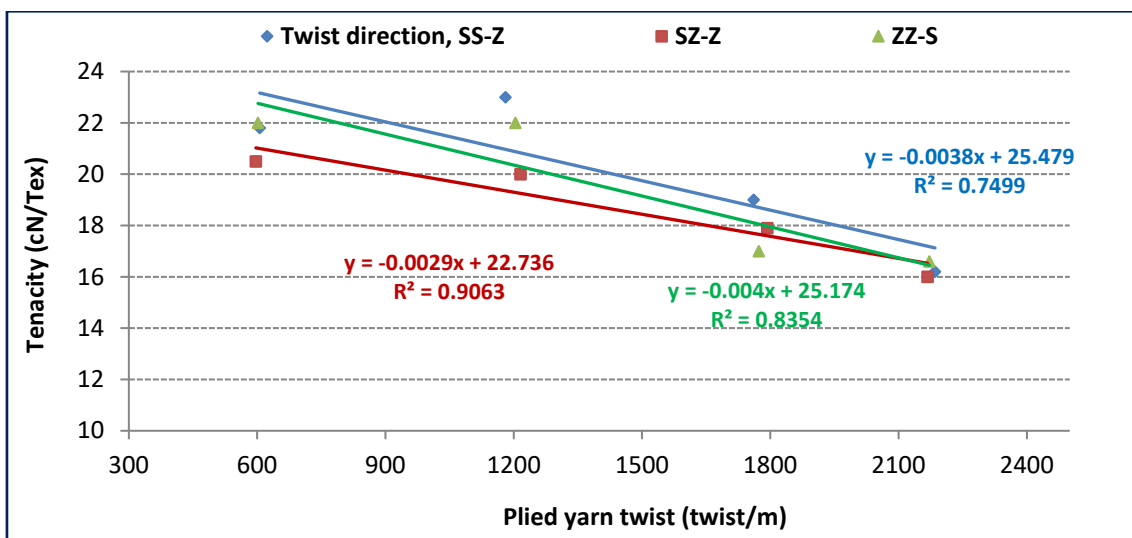


Figure 4.4. Effect of plying twist on yarn tenacity for produced yarns

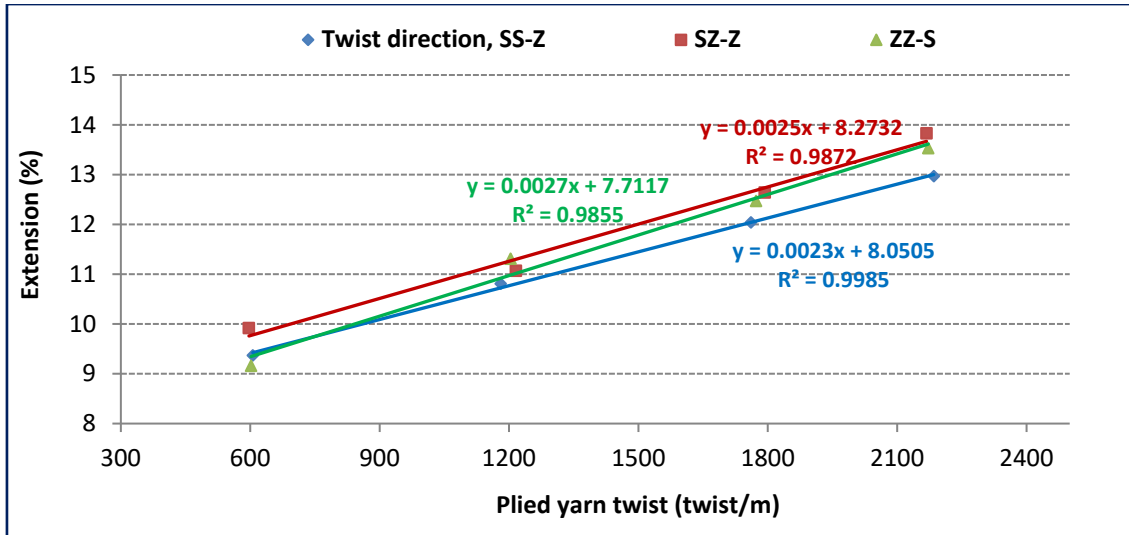


Figure 4.5. Effect of plyed yarn twist on its extension, produced yarns

Table 4.7: Produced single yarn properties

Nominal yarn count (Tex)		15	15	20	20	25	25	30	30
Twist direction		S	Z	Z	S	S	Z	Z	S
Actual yarn count (Tex)	Average	14.7	15	19.7	19.8	24.6	24.7	29.5	29.8
	C.V. (%)	1.6	1.7	1.6	1.3	1.2	1.11	1.1	1.04
	Std. (Tex)	0.24	0.26	0.32	0.26	0.30	0.27	0.32	0.31
Twist/m		1031	1062	910	925	803	799	751	748
Twist factor (α _m)	Average	127.3	127.3	127.3	127.3	127.3	127.3	127.3	127.3
	C.V. (%)	3.3	3.1	3	2.7	2.33	2.5	2.3	2.4
	Std. (α _m)	4.20	3.95	3.82	3.44	2.97	3.18	2.93	3.06
Tenacity (cN/Tex)	Average	19	19.5	20.3	20.5	22.2	22	21	21.9
	C.V. (%)	6.6	6.15	5.8	6	5.6	5.5	4.4	4.3
	Std. (cN/Tex)	1.254	1.199	1.177	1.23	1.243	1.21	0.924	0.942

Table 4.8: Produced plyed yarn properties at twist direction SS-Z

Twist direction, SS-Z				
Actual yarn count, Tex	Ply twist, twists/m	Tenacity	Std.	Extension
		(cN/Tex)		(%)
40.03	606	21.8	1.09	9.37
41.88	1181	23	0.92	10.81
45.78	1761	19	0.912	12.04
52.26	2185	16.2	0.648	12.97

Table 4.9: Produced plied yarn properties at twist direction SZ-Z

Twist direction, SZ-Z				
Actual yarn count, Tex	Ply twist, twists/m	Tenacity	Std.	Extension
		(cN/Tex)		(%)
40.87	597	20.5	1.0455	9.92
42.18	1216	20	0.86	11.07
46.68	1793	17.9	0.895	12.64
55.45	2168	16	0.48	13.83

Table 4.10: Produced plied yarn properties at twist direction ZZ-S

Twist direction, ZZ-S				
Actual yarn count, Tex	Ply twist, twists/m	Tenacity	Std.	Extension
		(cN/Tex)		(%)
39.63	602	22	0.99	9.16
41.29	1204	22	1.32	11.31
48.40	1773	17	0.884	12.47
54.42	2172	16.6	0.664	13.53

4.2.2 Silver NPs activity of treated cotton yarns

Metal Nano particles (MNPs), such as Silver [79-84], Gold and Copper have achieved special attraction because of their catalytic [85], electronic [86] and unique optical properties [87] making them very attractive in the fields of particularly sensing, bio-conjugation, and surface enhancement Raman spectroscopy [88], [89]. One of the widespread approaches to the synthesis of MNPs involves the reduction reaction of metal ions in a polymeric solution [90-92].

- **Method AATCC 147**

Treated test samples (D₁ and D₂) show comparable antibacterial activities on both tested strains (E.C. and S.A.). The antimicrobial activity of D₁ and D₂ is significantly appeared through clear inhibition zone compared to the standard sample (D₀) that does not show any inhibition of bacteria strains (as illustrated in Table 4.11 and Figure 4.6).

- **Method AATCC 100**

The number of surviving bacterial colonies are considered and counted in this test method, see Table 4.12. Compact incidence means that the number of surviving bacterial

colonies is not countable, as shown in Figure 4.7.

Table 4.11: Inhibition zone of treated yarns according to AATCC 147

Method ATCC147	Sample D ₀ standard	Sample D ₁	Sample D ₂
<i>Escherichia Coli</i>	No effect	Inhibition zone Ø 1,44 mm	Inhibition zone Ø 1,58 mm
<i>Staphylococcus Aureus</i>	No effect	Inhibition zone Ø 2,06 mm	Inhibition zone Ø 2,01mm

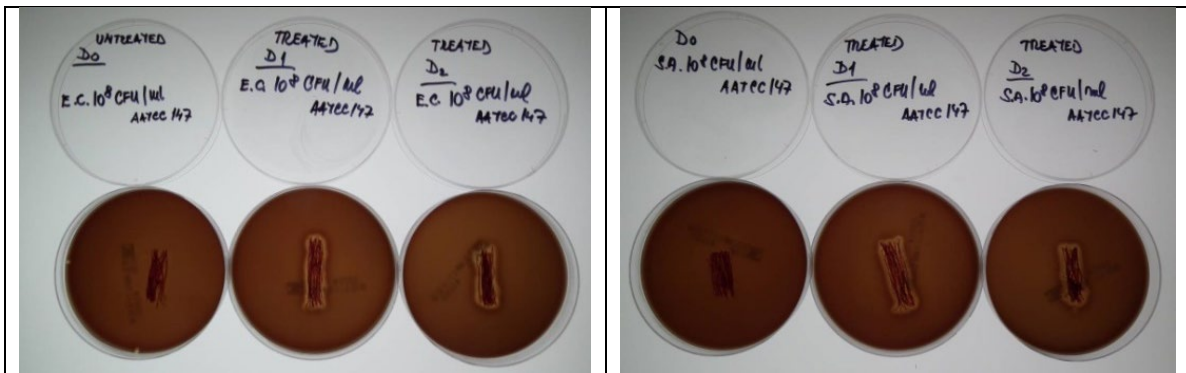


Figure 4.6. Inhibition zone of treated yarns against: a) *Escherichia Coli*

b) *Staphylococcus Aureus*

Table 4.12: Antibacterial assessment by quantitative test according to AATCC 100

Method ATCC100	D ₀ standard	Sample D ₁	Sample D ₂
<i>Escherichia Coli</i>	Compact incidence	0	0
<i>Staphylococcus Aureus</i>	Compact incidence	1	0

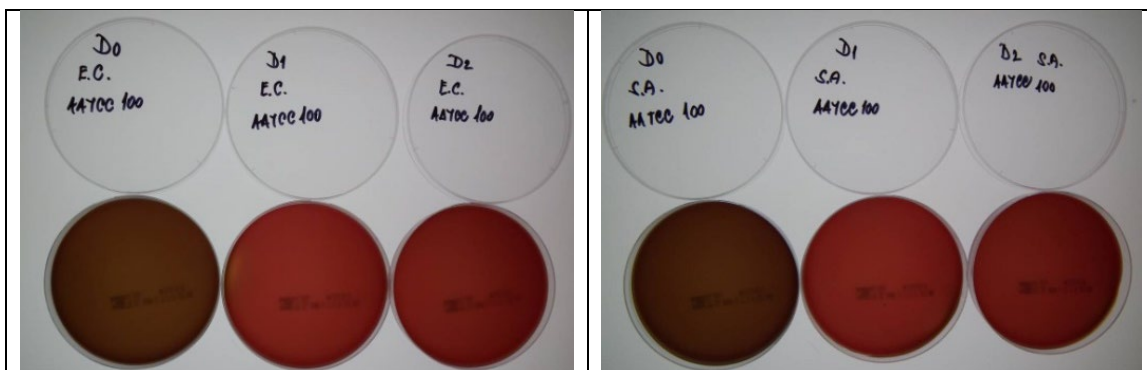


Figure 4.7. Surviving bacterial colonies of: a) *Escherichia Coli*

b) *Staphylococcus Aureus*

4.2.2.1 Scanning electron microscopy and energy dispersive X-ray of the yarns

The scanning electron microscopy of the treated and un-treated single and plied cotton

yarn samples are illustrated in [Figures 4.8 and 4.9 respectively](#). The silver NPs size and distribution are totally clear for the treated yarn samples. Moreover the energy dispersive X-ray mapping for the yarn samples confirmed the NPs percent in the total composition of yarn EDX mapping, see [Figures 4.10 & 4.11](#).

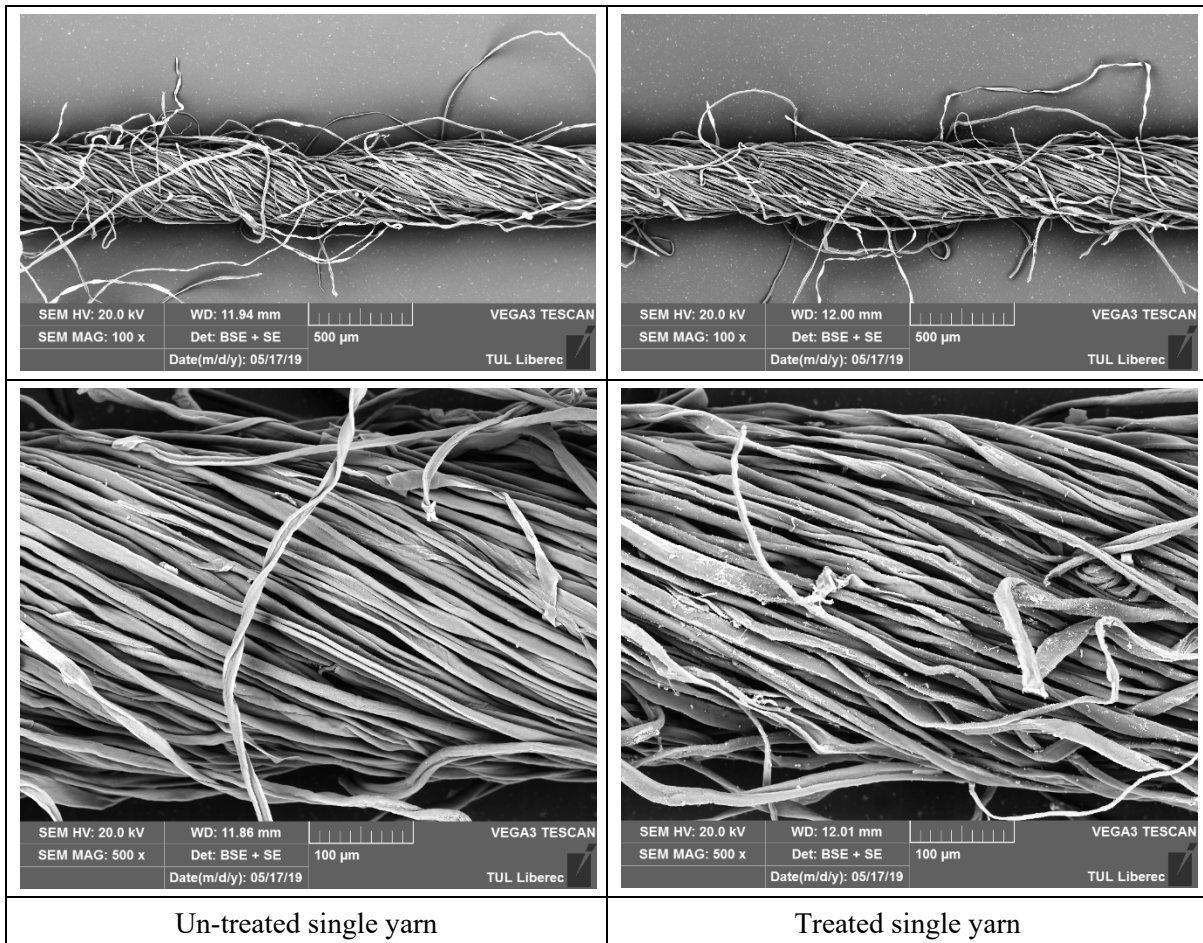
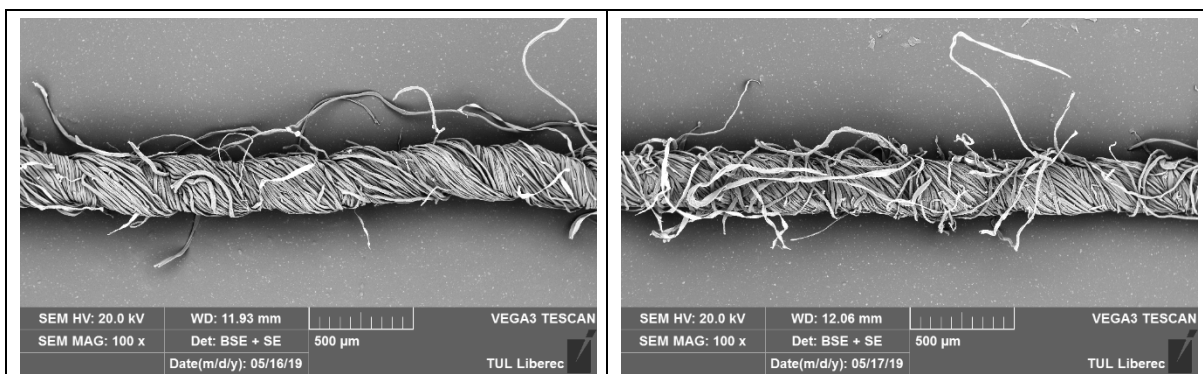


Figure 4.8. Scanning electron microscopy of the un-treated and treated single yarns



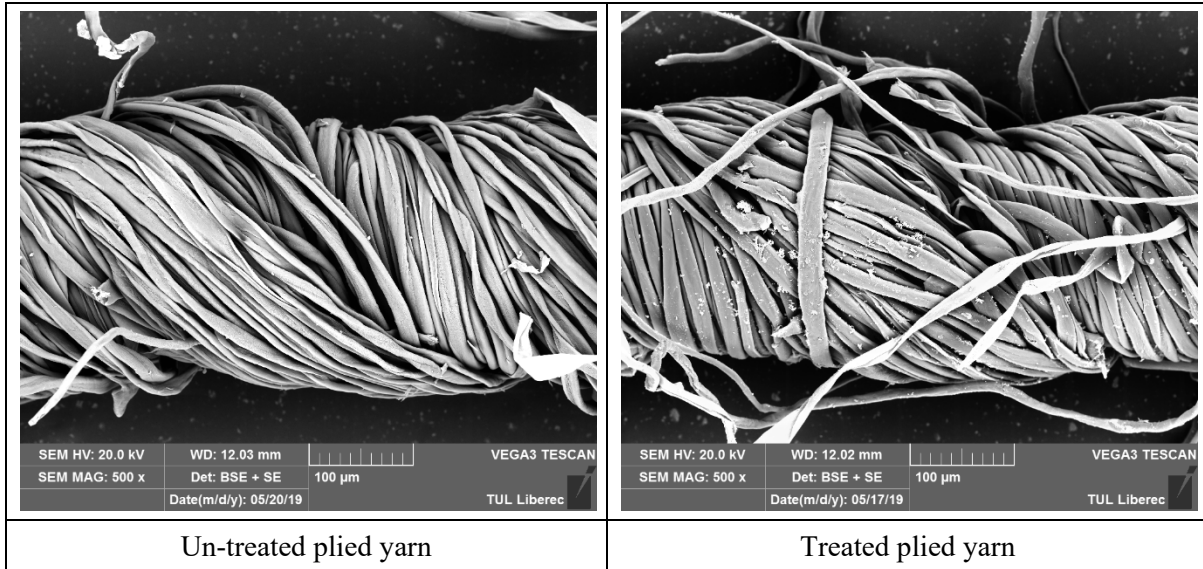


Figure 4.9. Scanning electron microscopy of the un-treated and treated plied yarns

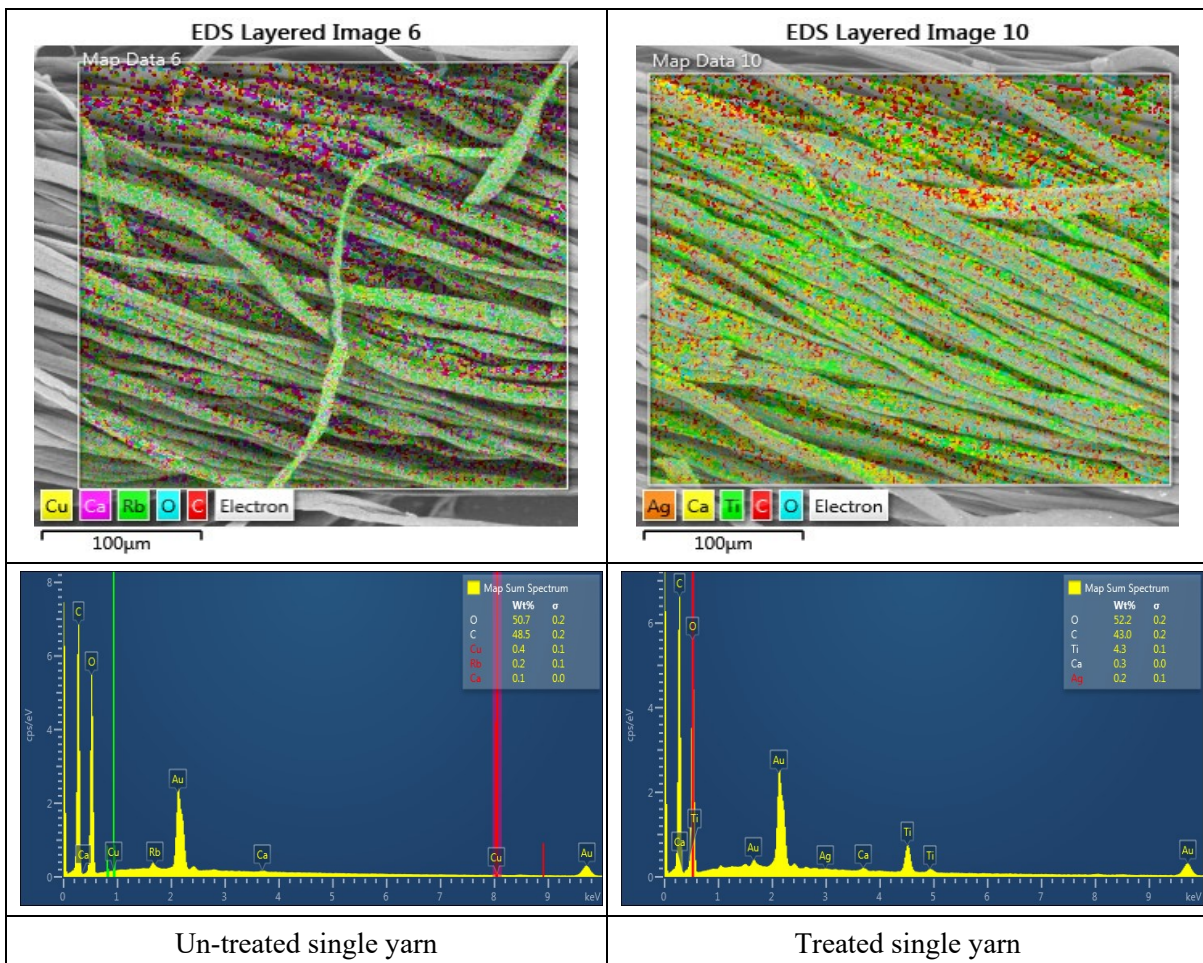


Figure 4.10. Energy dispersive X-ray mapping of the un-treated and treated single yarns

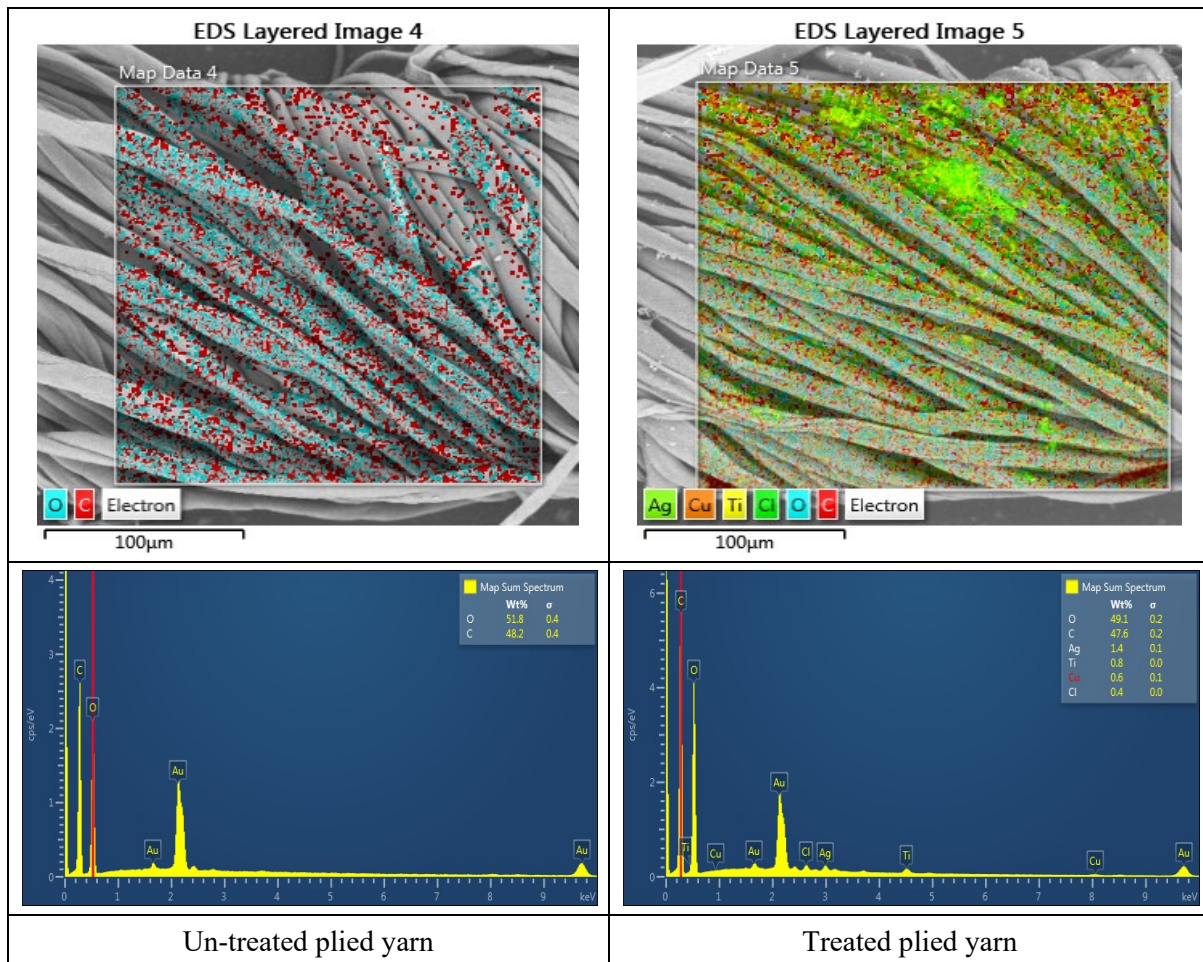


Figure 4.11. Energy dispersive X-ray mapping of the un-treated and treated plied yarns

5. Chapter 5: Analysis of Individual Properties of Woven Compression Bandages

5.1 Methods used, studied material

5.1.1 Analysis of mechanical properties of WCBs

A) Three types of WCB were used for testing as shown in Figure 5.1. These bandages' structures are plain weave. Yarn counts and densities are different depends on the construction and technology of the final product.

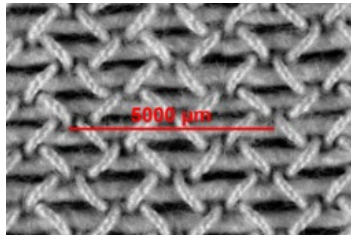
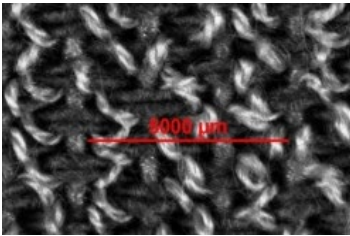
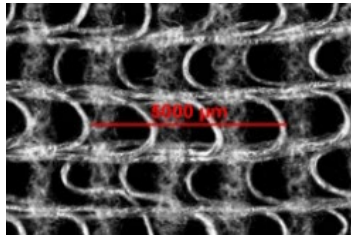
		
<p>a) 100% Bleached Cotton Warp set: 8 ends/cm Weft set: 15 picks/cm Warp count: Cotton, 20x2 Tex, 2x1200 twist/m, SS/Z, ZZ/S Weft count: Cotton, 75 Tex, OE. Fabric weight: 210.25 g/m² Fabric thickness: 1.06 mm</p>	<p>b) CO-PA-PU bandage Warp set: 11 ends/cm Weft set: 18 picks/cm Warp count: Cotton, 10x2 Tex - Polyamide, 7.8 Tex - Polyurethane, 42.5 Tex Weft count: Cotton, 36.9 Tex Weight: 236.48 g/m² Thickness: 1.09 mm</p>	<p>c) VI-PA bandage Warp set: 12 ends/cm Weft set: 14 picks/cm Warp count: Viscose, 16.5 Tex, open end (OE), Polyamide – 7.8 Tex Weft count: Viscose, 16.5 Tex. Weight: 83.34 g/m² Thickness: 0.91 mm</p>

Figure 5.1. Experimental woven compression bandages description

B) Compression bandages tension is evaluated according to the standard test method ISO 13934-1:1999(E) [93]. Testometric M350-5CT was used to measure the tension developed in the bandage while extension at a constant speed of 100 mm/min. The device gauge length was set to 100 mm.

C) Bandage porosity is calculated by measuring the binary area fraction using high resolution camera. While subjecting the bandage samples to a constant extension, the resultant images were recorded using digital camera. There are 120 frames (images) for each sample; these images were analysed by NIS-Elements software to measure binary area fraction using Threshold technique as shown in Figures 5.2 & 5.3.

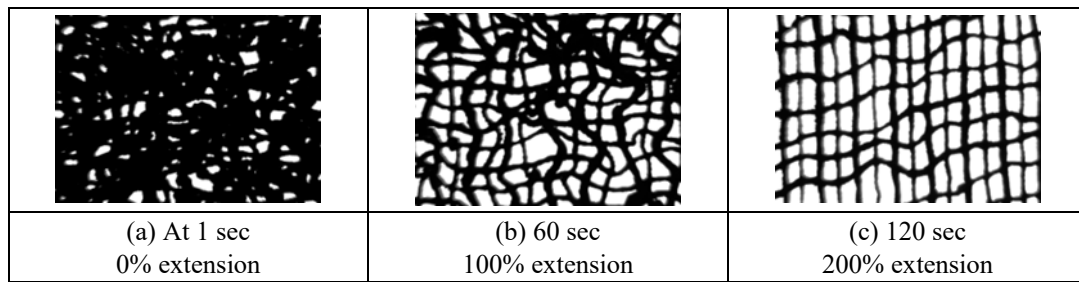


Figure 5.2. Binary area of Cotton bandage during tension

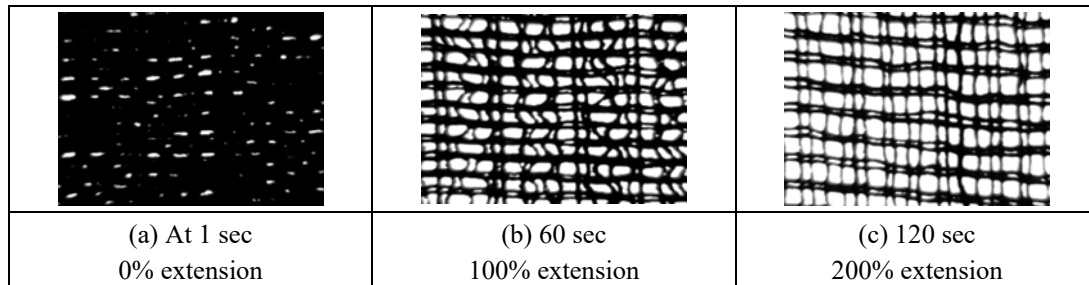


Figure 5.3. Binary area of Viscose/Lycra bandage during tension

5.1.2 Testing of bandage pressure using Picopress

The same three types of bandages were worn on both mannequin model and real leg to test and analyse the effect of WCB extension and porosity on bandage pressure at ankle and mid-calf position in both static and walking conditions. Recalculations of tensile force based on a specified extension range during bandage application are performed in [part 5.9](#). Practical bandage pressure is measured using Microlab Picopress instrument M-700 tester, which gives both digital readings and graphical charts as well. The ankle and calf positions were adjusted to leg circumferences of 21.4 and 32.4 cm respectively for mannequin model, 25.6 and 38.9 cm respectively for real leg, as illustrated in [Figure 5.4](#) [94]. The obtained results are both digital numbers and graph forms. There are three levels of bandage tension (low: 50% extension and 50% overlap, medium: 100% extension and 50% overlap, and high: 100% extension and 66% overlap) applied on 1st position (ankle at radius 4.07 cm), 2nd (mid-calf at radius 6.19 cm), and 3rd (below the knee at radius 4.9 cm) [22].

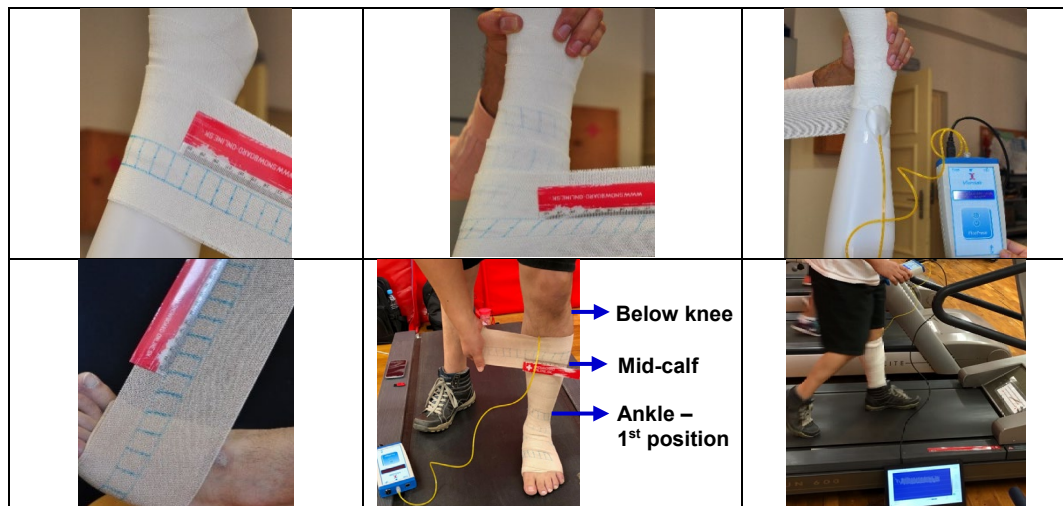
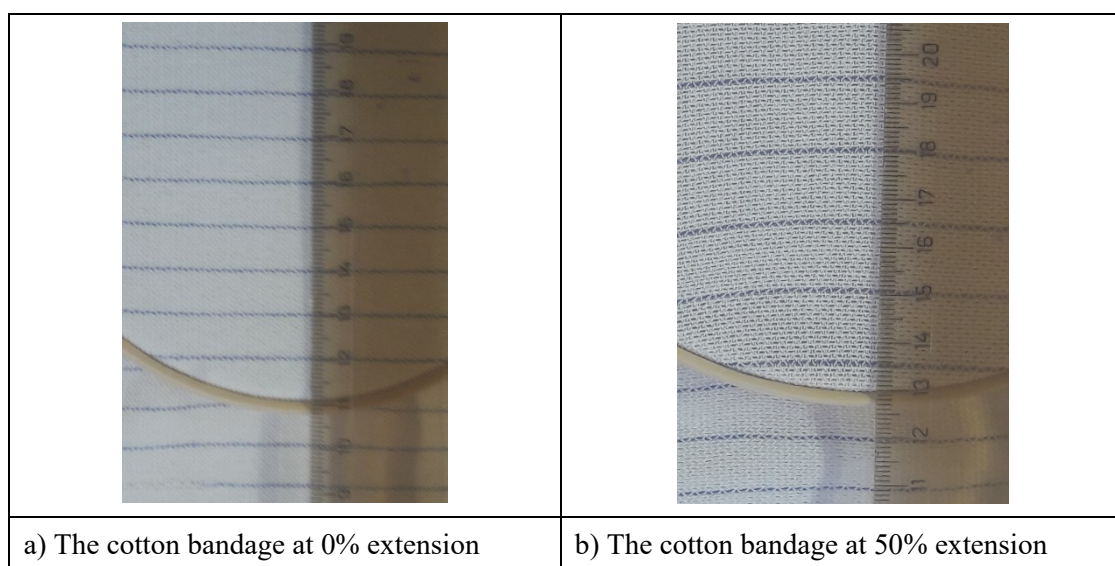


Figure 5.4. Application of compression bandage on mannequin and real leg

5.1.3 Relationship between the change in coloured weft spacing and compression during bandage application

Candidate study added the blue coloured weft during the weaving process of the 100% cotton WCB, as previously illustrated in [Figure 3.4](#) as well as [Figure 5.2](#). These blue marks (repeated lines every 1 cm) enables for accurate adjustment and evaluation of the applied bandage extension (100% extension at blue line spacing 2 cm). The activity of the new WCB could be evaluated using the same previous procedure to achieve the associated optimum pressure by the compression bandage on any part of the body, see [Figures 5.4 and 5.5](#).



a) The cotton bandage at 0% extension

b) The cotton bandage at 50% extension

Figure 5.5. Adjusting the bandage extension using the blue lines (coloured weft threads)

5.1.4 Testing the cyclic loading-unloading during uniaxial stress

Moreover the cyclic loading-unloading tests during the uniaxial stress were evaluated

for both the 100% bleached cotton and CO-PA-PU WCBs to confirm the durability and effectiveness of bandages for different applications, as illustrated in [Figure 5.6](#).







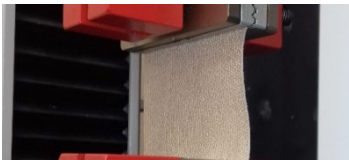

Action of bandage test	CO-PA-PU WCB	Bleached Cotton WCB
Sample size 10x10 cm ² , original gauge length 5 cm		
Elongation by 3 cm; extension by 60%, then relaxation 1 cm that extension becomes 40%, then again extension 60% for 6 cycles		
After 6 cycles of loading- unloading		
After 5 days of cyclic loading-unloading		

Figure 5.6. Testing of tensile and cyclic loading-unloading by Testometric M350-5CT

5.1.5 Treatment of the surface of cotton WCB with zinc oxide

Two types of WCB (fabric) samples has been treated with three concentrations of ZnO nanoparticles as follows, 1%, 2%, and 3% in powder form with 15 g/L binder. The samples' coding for un-treated and treated cotton WCB with zinc oxide nanoparticles is described in [Table 5.1](#) and the antibacterial tests were performed according to the following standards:

1. AATCC 147 Test Method: 147-2012 - Assessment of Antibacterial Activity of Textile materials: Parallel Streak Method.
2. AATCC 100 Test Method: 100-2019 - Assessment of Antibacterial Finishes on Textile Materials.

Table 5.1: Samples' codes for treated cotton WCB with zinc oxide nanoparticles

State	Sample code	Sample code
Untreated, standard	1- with blue colour every 1 cm	2- without colours
Treated, 1% ZnO NPs	[1-1]	[2-1]
Treated, 2% ZnO NPs	[1-2]	[2-2]
Treated, 3% ZnO NPs	[1-3]	[2-3]

The used culture media was a physiological saline solution and the agar media was blood agar (Columbia) - purchased from Bio-Rad spol. s.r.o. The tested bacterial strains were purchased from the Czech Collection of Microorganisms, Masaryk University Brno.

- Escherichia coli (E.C.) - CCM 2024 (ATCC 9637), is a gram-negative rod-shaped bacterium.
- Staphylococcus aureus (S.A.) - CCM 2260 (ATCC 1260), a gram-positive cocci bacterium.

5.1.5.1 *AATCC Test Method: 147-2012 - Assessment of Antibacterial Activity on Textile materials: Parallel Streak Method.*

It is a qualitative, indicative method and should precede the AATCC 100 method. The antibacterial treated WCB sample is placed on agar, on which bacteria are inoculated in several lanes. After 24 hours of incubation, the growth of bacteria under the test sample and the inhibition zone are evaluated. A modification of this method is to inoculate bacteria in the whole area (it is possible to start from a suitable dilution of bacteria). The same is evaluated - the growth of bacteria under the sample and the halo zone.

Note: This method can therefore be used to verify whether the active substance is released from the sample into the environment (i.e. halo zones of different sizes appear) or whether the active substance is bound in the sample and the effect is manifested only below the sample.

The methodology of this method can be summarized in the following steps:

- A square of WCB (fabric) measuring 18x18 mm (according to the standard) was cut out.

- Samples were placed in sterile vials, covered with foil (vial lids were also covered with foil) and sterilized in an autoclave for 15 minutes at 121 °C.
- 1 ml of bacterial inoculum with a concentration of 10⁸ CFU / ml was inoculated (spread with a microbiological stick) individually on a Petri dish with blood agar.
- The test sample was placed in the centre of the dish and pressed firmly against the agar.
- Incubation of bacteria took place in a thermostat at 37 °C for 24 hours whereas incubation of yeast took place in a thermostat at 25 °C for 24 hours.
- Subsequently, the halo zone (its size) and the inhibition of bacteria under the sample (sample bottom) were evaluated.

5.1.5.2 *AATCC Test Method: 100-2019 - Assessment of Antibacterial Finishes on Textile Materials*

It is a quantitative method in which the reduction factor is evaluated, which indicates the percentage by which the inoculated bacterial concentration was reduced. The result is the number of surviving bacterial colonies (CFU) and R (reduction, %) is calculated. The result is always compared with the untreated sample (standard).

Moreover the methodology is illustrated in the following steps:

- A small WCB sample measuring 18x18 mm was placed in a sterile container.
- 100 µl of the appropriate bacterial strain of concentration was applied to the sample 10⁵ CFU / ml (the whole sample must be wetted with a bacterial inoculum).
- Incubate the samples in a thermostat at 37 °C for 24 hours.
- After incubation, 10 ml of saline was added and vortexed.
- After vortexing, 1 ml was pipetted off and inoculated on a blood agar petri dish (triplets inoculated from each sample) and the number of CFUs were calculated, which was compared with standard.

5.1.6 Testing the muscles activation when applying WCBs

Viscose-Polyamide and two types of Cotton compression bandages were used for hand and lower leg muscles testing respectively [95], [96]. VI-PA bandage was used to test the Flexor Carpi (FC) muscle voltage during different wrist actions (flexion-extension, squeezing a soft roll) with and without wearing CB, as shown in Figure 5.6. The applied compression by VI-PA bandage is adjusted and standardized to medium compression ranges 22 ± 2 mmHg (through 70% bandage extension and 50% overlap). Bleached Cotton and CO-PA-PU bandages were used to test Medial Gastrocnemius (MG) and Soleus (SO) muscles behaviour during the standardized protocol actions (flexion-extension and while walking). The lower leg bandage pressure was adjusted to compression ranges 30 ± 2 mmHg (by 100% bandage extension and 50% overlap) [97].

There are two methods of using EMG in measuring muscle activity; needle EMG uses needle sensors that penetrate the skin and subcutaneous adipose tissue or surface EMG using skin-mounted electrodes. The advantage of needle EMG is that the test administrator does not have to consider the effects of cross-talk between muscles or the superficial fat layer between the muscle and skin which can cause signal impedance. However, this method is invasive to the participant and is not practical during isotonic muscle actions, making surface EMG the most common method of measuring muscle activity. The advantages of surface EMG are that it is safe, easy, non-invasive, and has the ability to objectively quantify energy of muscle [98].

All these tests were carried out on 6 healthy men (age ranges 28-38 years) using 'eMotion' wireless EMG system at different metronome beats 20, 30, and 40 beats/min (BPM). Surface electrodes were mounted on the mentioned muscles of the human skin as shown in Figure 5.7 [99]. In order to investigate the change of muscles activity, root mean square (RMS) is processed by exporting the filtered signals to MATLAB software using band-pass filtering between 20–500 Hz.



Figure 5.7. EMG system for Flexor Carpi, Medial Gastrocnemius and Soleus muscles [99]

5.1.7 Analysis of thermal comfort properties of WCBs

The main three types and Viscose-Polyurethane (VI-PU) WCBs were wrapped on thermal foot manikin (TFM) at range of extension (10 to 80%) using both 50 and 66% overlap (i.e. two and three layers bandaging respectively). Thermal resistance (R_{ct}) was measured using TFM for all types of CBs as shown in Figure 5.8 [100]. Relative water vapour permeability (%) and water vapour resistance (R_{et}) were measured using the PERMETEST instrument [101] (Sensora, Czech Republic) according to ISO 11092 standard, at laboratory conditions (T: 22 ± 2 °C, RH: $50 \pm 2\%$), as shown in Figure 5.9 [102]. The obtained results of R_{ct} were compared to ALAMBETA [103] testing device results as shown in Figure 5.10 [104].

All bandage samples were measured using ALAMBETA at initial porosity (0% extension) and (20 to 100%) using special tensioning frame as shown in Figure 5.11. The ALAMBETA testing corresponded well to the use of socks inside a shoe (boundary conditions of first order). It can be used for bandages as well assuming that the athletic or patient could wear the bandage while daily activities.

Air permeability test was carried out using FX3300 air permeability tester according to ASTM D737 at working pressure of 100 Pa and 20 cm² test area [105], [106].

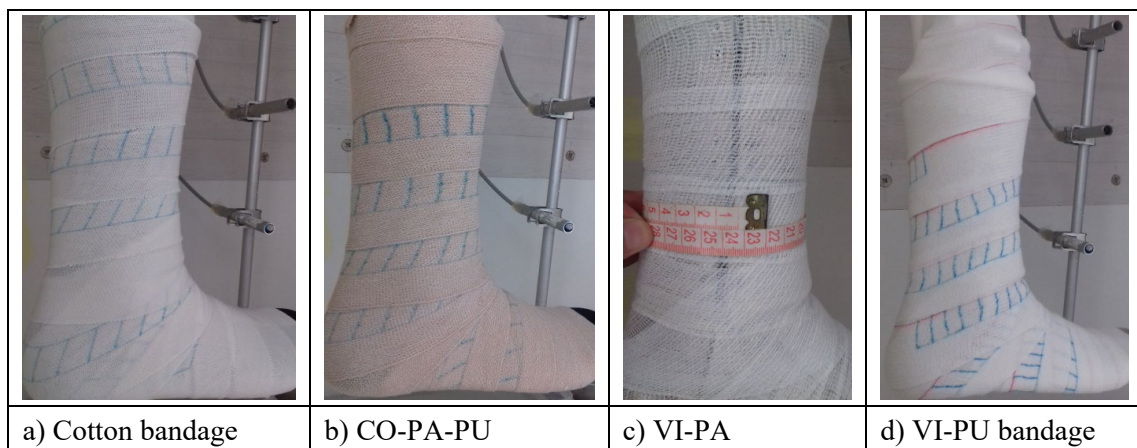


Figure 5.8. Woven CB samples on thermal foot manikin

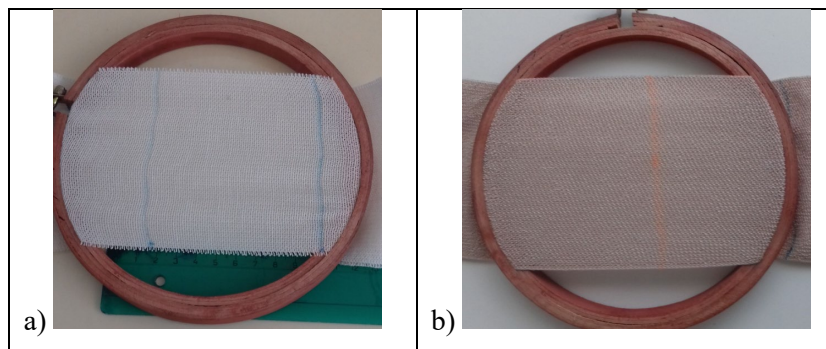
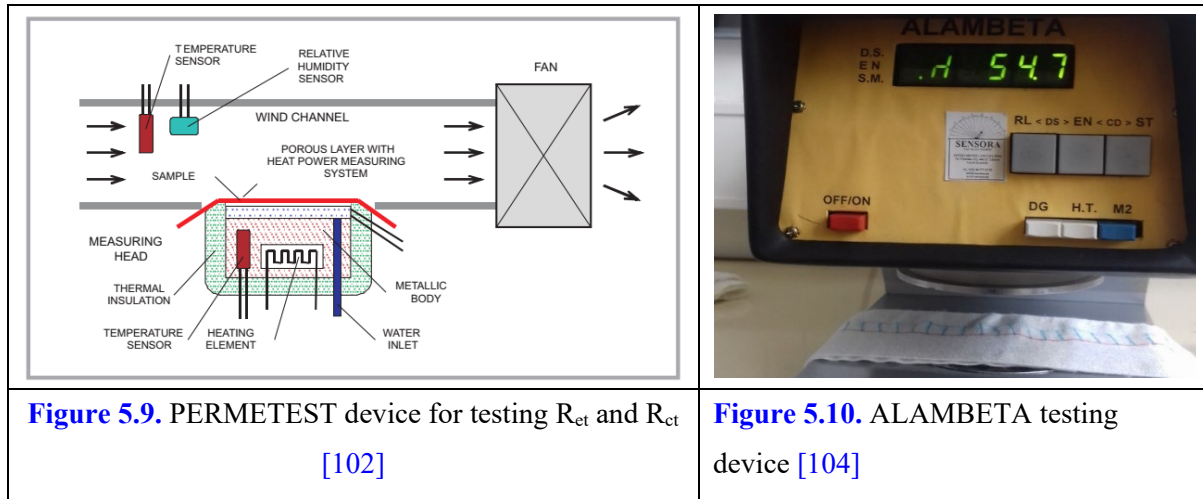


Figure 5.11. Stretching frame at 80% extension: a) Cotton, b) CO-PA-PU bandages

5.1.7.1 Adjusting the thermal resistance measurement on Thermal Foot Model

The following steps are practical example to show how to adjust and stabilize the optimum conditions of TFM to test R_{ct} of CB, see [Figure 5.12](#). Segments 1, 3 are kept OFF because WCB effect usually starts after these segments, device door is opened. There are two types of testing (i.e. nude and clothed manikin) [107]. For accurate comparison, mercerized Cotton socks are used to cover TFM as underwear for all measured samples to ensure more stabilization and steady conditions.

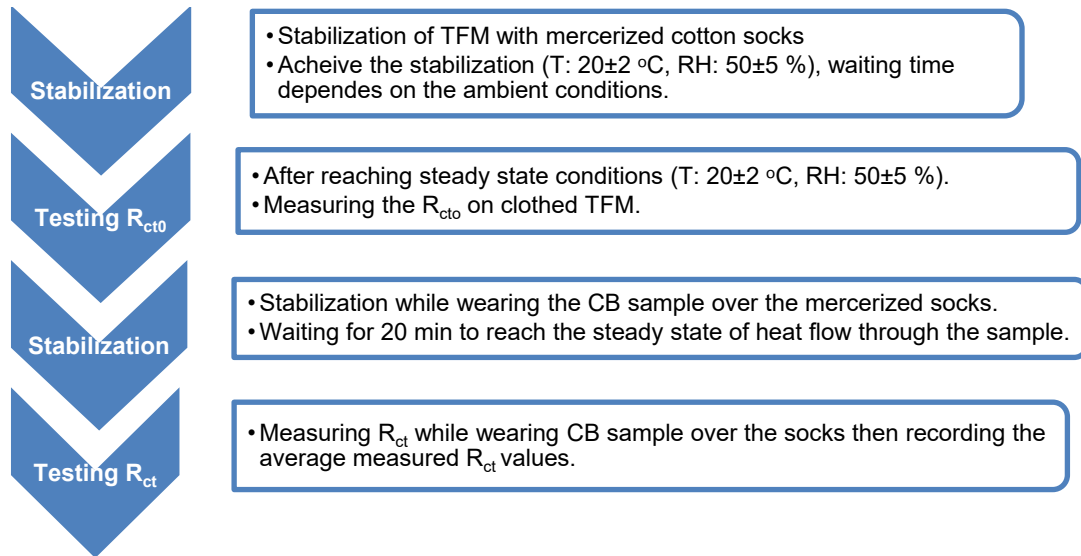


Figure 5.12. Optimum testing procedure of measuring R_{ct} on TFM

The stabilization process continues till the device reads the standard ambient conditions ($T: 20 \pm 2 \text{ }^\circ\text{C}$, $\text{RH}: 50 \pm 5\%$), after that measurement of the initial thermal resistance (R_{ct0}), then stabilization (waiting for 20 min) while wearing WCB sample over socks. Finally R_{ct} values can be measured using the measured R_{ct0} as a reference value, see [Figure 5.13](#) and Equation (1) [108].

$$R_{ct} = \frac{A \cdot (T_s - T_a)}{H} - R_{ct0} \quad (1)$$

$$R_{et} = \frac{A \cdot (p_s - p_a)}{H} \quad (2)$$

Where: R_{ct} is the dry resistance of sample only ($\text{m}^2 \cdot ^\circ\text{C}/\text{W}$),

T_s is the hot plate surface temperature ($^\circ\text{C}$),

T_a is the ambient temperature ($^\circ\text{C}$),

H/A is the zone heat flux (W/m^2),

R_{ct0} is the clothed TFM dry resistance ($\text{m}^2 \cdot ^\circ\text{C}/\text{W}$),

R_{et} is the evaporative resistance of sample only ($\text{m}^2 \cdot \text{Pa}/\text{W}$),

p_s is the saturation vapour pressure at hotplate surface (Pa),

p_a is the ambient partial vapour pressure (Pa).

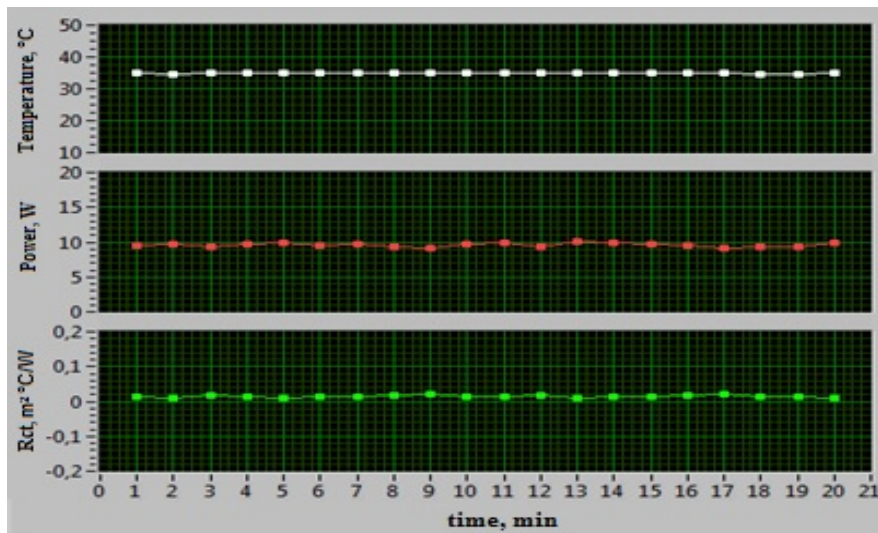


Figure 5.13. Measuring R_{ct} while wearing CB over socks

5.2 Summary of the achieved results

5.2.1 Evaluation of the mechanical properties of woven compression bandages

5.2.1.1 Loading-unloading uniaxial test for WCBs

When the three bandage types were subjected to uniaxial stress at full extension (i.e. closer to endpoint of elasticity); CO-PA-PU bandage achieved approximately 300N at 200% extension, whereas VI-PA and Cotton bandages at 150% extension had 280 and 750N respectively. These results confirm the highest elasticity of the CO-PA-PU bandage compared to 100% Cotton bandage. Figure 5.14 illustrates that all bandage samples recovered its original length after relaxation.

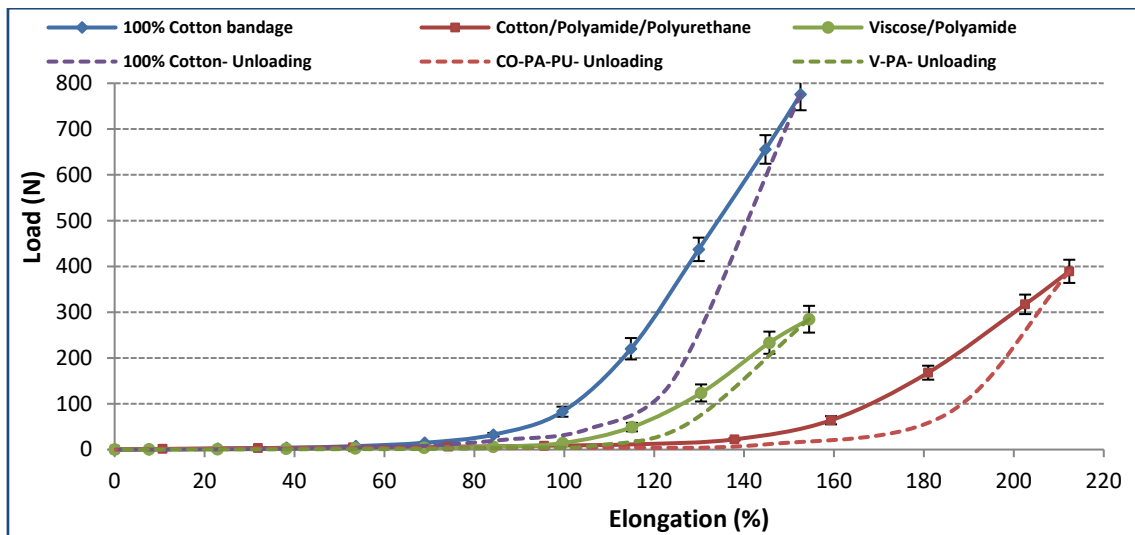


Figure 5.14. Loading-unloading curves for Cotton, CO-PA-PU, and VI-PA bandages

This elastic recovery is due to the optimum extensibility of bandages in elasticity zone, moreover there is no dwell time while stretching the CB samples. But when these bandages are worn or wrapped on human body there will be a bit residual deformation due to higher applied bandage tension and longer treatment time.

5.2.1.2 Optimum fabric tension for woven compression bandages

As the optimum required bandage tension is approximately 10N, that value is achieving the average bandage pressure (4000 Pa or 30 mmHg) according to Laplace's equation (9) for two layers bandaging at leg radius 5 cm and bandage width 10 cm. Figure 5.15 confirms that CO-PA-PU and VI-PA bandages require 110% and 92% extension respectively while Cotton bandage requires only 60% extension to achieve the required bandage tension 10N, see Table 5.7. The Cotton bandage extension depends on the highly twisted plied yarns (1200 twist/m)

that enable to achieve the required bandage stretch, but these bandages have lower extension (short-stretch) compared to CO-PA-PU that contains 6% of elastomeric filament (Polyurethane) which gives higher extensibility (long-stretch bandage). Whereas the VI-PA bandage consists of two types of yarns having different thermal and melting points, in which case the stretch is given by steaming then heat setting at the required percent of shrinkage.

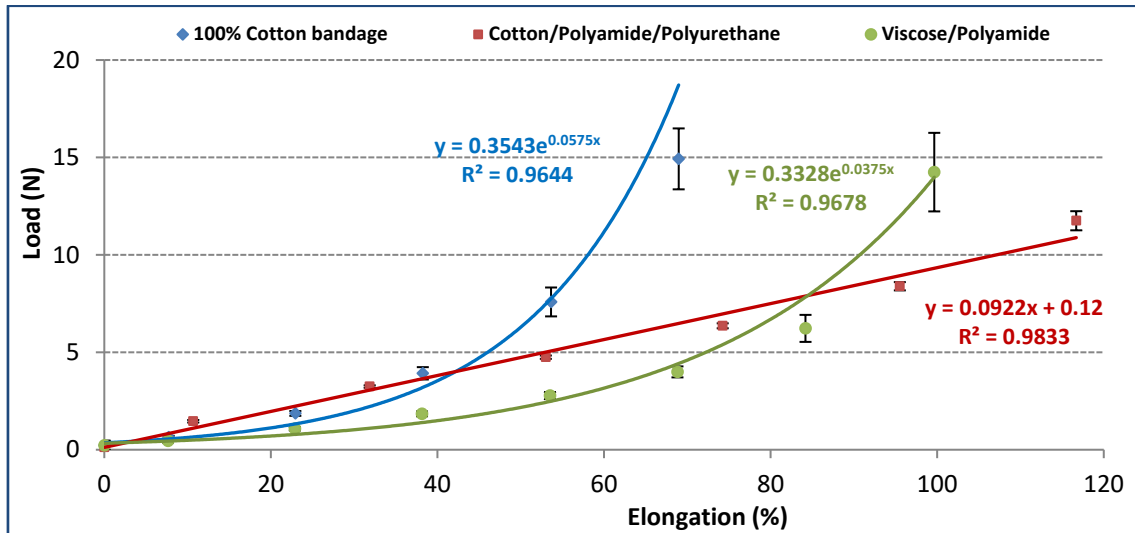


Figure 5.15. Optimum fabric tension for Cotton, CO-PA-PU, and VI-PA bandages

5.2.1.3 *Effect of bandage structure, extension, and yarns angle on bandage porosity*

The factors affecting bandage porosity such as (warp and weft yarns count, density, twist, cover factor, and fabric structure) are changing during the bandage extension. One of the main variables during bandage application is the applied tension to achieve the required compression. A lot of models were presented for the description of porosity in woven fabrics, some of them described the porosity between yarns in the fabric (the inter-yarn porosity), and the others described the porosity between fibres inside the yarn (the intra-yarn porosity). According to theory of a 2-D model, the horizontal porosity (ϵ_h) is defined as ‘a complement to the woven fabric cover factor (CF)’, see [Figure 5.16](#).

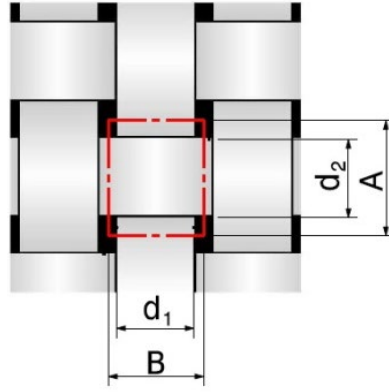


Figure 5.16. Structure of interlacing cell in woven fabric crossing point of plain weave, warp and weft diameter (d_1 , d_2), warp and weft distance (B , A).

Woven fabric cover factor is given on the basis of illustrated structure of woven fabric in Figure 5.16 by equation (5.4) as followed:

$$\left\{ CF = \frac{\text{visible area covered by yarns}}{\text{total area of cell}} = \frac{d_1 A + d_2 B - d_1 d_2}{AB} = CF_{\text{warp}} + CF_{\text{weft}} - CF_{\text{warp}} CF_{\text{weft}} \right\} \quad (5.4)$$

Based on known parameters of warp and weft density (D_1 and D_2), we can write equation (5.5):

$$A = \frac{1}{D_2} \quad \text{and} \quad B = \frac{1}{D_1} \quad (5.5)$$

The horizontal porosity (ϵ_h) can be calculated by image analysis as ‘the area of pores in a perpendicular projection of woven fabric’ [109]. Real values can be measured as illustrated in equation (5.6):

$$\epsilon_h = 1 - CF = 1 - (d_1 D_1 + d_2 D_2 - d_1 d_1 D_2 D_2) \quad (5.6)$$

While dealing with two dimensional fabrics, porosity is defined as ‘the ratio of the projected geometrical area of the opening across the material to the total area of the material’ [110], [111]. A classical 2-D model of porosity seems insufficient for a tightly woven fabric. Neighbouring yarns are very close and the projected area of inter-yarn pores approaches to zero. As air flows through the woven fabric, it flows around the yarns and it does not flow only in the perpendicular direction [112], [113]. Gee introduced the well-known ‘ends plus intersection theory’, which he modified, and called the ‘curvature theory’ [114]. Until then a ‘maximum theory’ had been the subject of several research. Some researchers [115-119] have used a more theoretical approach, whereas others [120] used more experimental means. Kienbaum has successfully joined theoretical and experimental investigations, and presented

his own theory which can be applied to all weaves and different yarn structures [109].

The overall volume porosity (ϵ) can be defined theoretically as ‘the fraction of void space in a porous medium’, see equation (5.8).

$$\text{Overall porosity } (\epsilon) = 1 - \text{Fabric packing density} \quad (5.7)$$

$$\epsilon = 1 - \frac{\rho_F}{\rho_f} = 1 - \frac{w}{t \cdot \rho_f} \quad (5.8)$$

Where ρ_F is the fabric density and ρ_f is the fibre density (g/cm^3), w is the fabric weight (g/m^2), and t is the fabric thickness (mm) [121].

Figure 5.17 confirms that the horizontal porosity of cotton bandage is significantly improving by increasing the bandage extension and the angle between warp and weft. The statistical analysis of the obtained results is summarized in Tables 5.2 & 5.3. The bandage extension and type have significant effects on weave angle and porosity (significance level, $P = 0 < 0.05$) using both one and multiple variable linear regression. The same trend has been analysed for CO-PA-PU and VI-PA bandages during the uniaxial stress on the Testometric M350-5CT as illustrated in Figures 5.18 and 5.19.

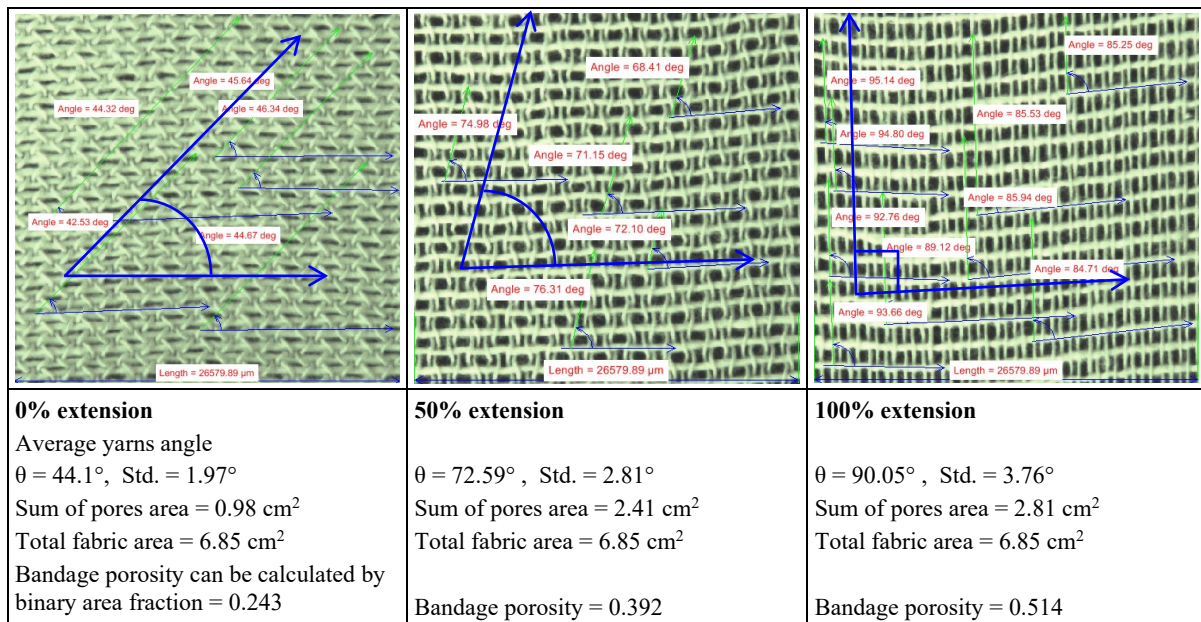


Figure 5.17. Effect of extension and warp to weft yarns angle on porosity of Cotton bandage

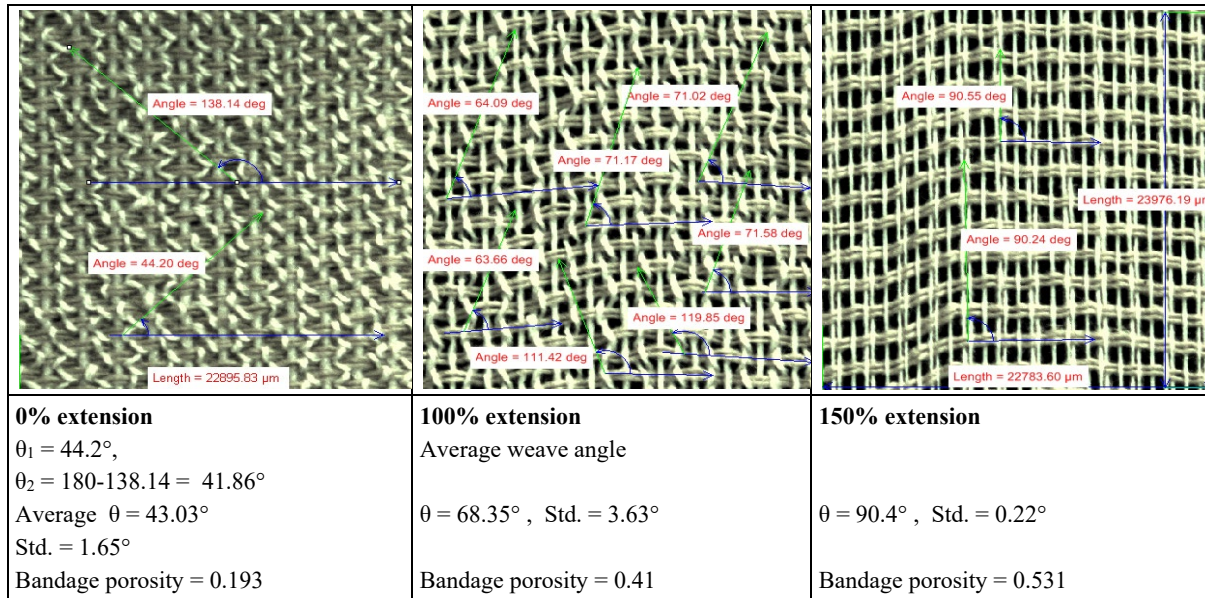


Figure 5.18. Effect of extension and yarns angle on porosity of CO-PA-PU bandage

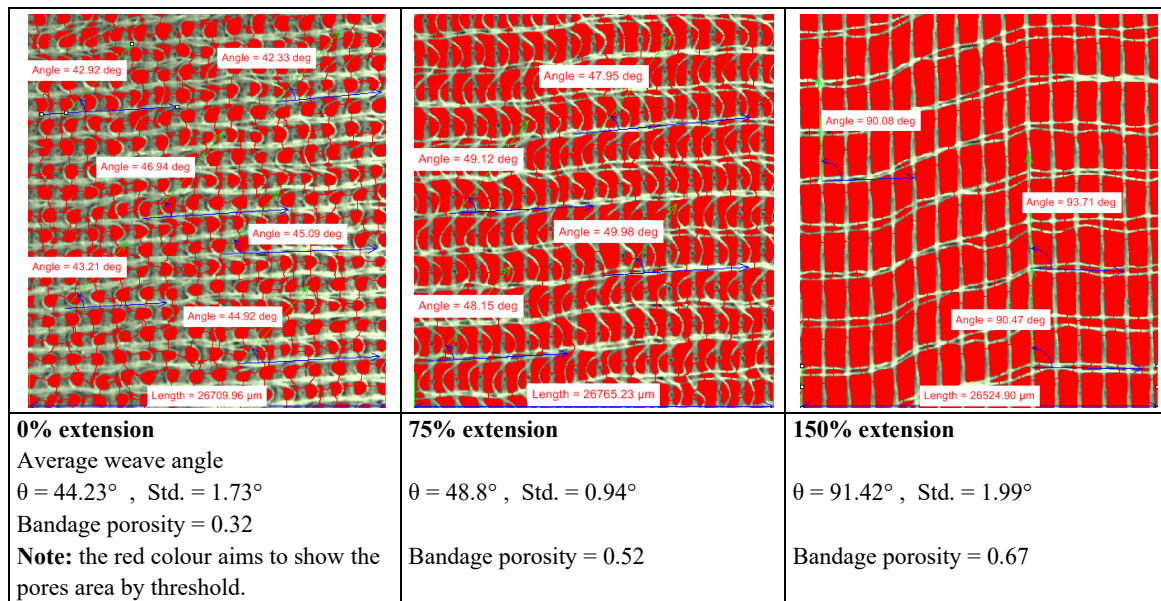


Figure 5.19. Effect of extension and yarns angle on porosity of VI-PA bandage

Table 5.2. Statistical analysis of relation between bandage extension and yarns angle

ANOVA ^c

Model		Sum of Squares	df	Mean Square	F	Sig.
1	Regression	16175.052	1	16175.052	343.050	.000 ^a
	Residual	2027.478	43	47.151		
	Total	18202.530	44			
2	Regression	16574.873	2	8287.437	213.849	.000 ^b
	Residual	1627.657	42	38.754		
	Total	18202.530	44			

a. Predictors: (Constant), Extension

b. Predictors: (Constant), Extension, Bandage Type

c. Dependent Variable: Angle between warp and weft

Table 5.3. Statistical analysis of relation between bandage type, extension, and porosity

ANOVA ^c

Model		Sum of Squares	df	Mean Square	F	Sig.
1	Regression	.702	1	.702	89.393	.000 ^a
	Residual	.338	43	.008		
	Total	1.040	44			
2	Regression	.987	2	.493	391.993	.000 ^b
	Residual	.053	42	.001		
	Total	1.040	44			

a. Predictors: (Constant), Extension

b. Predictors: (Constant), Extension, Bandage Type

c. Dependent Variable: Porosity

As for the application of 100% cotton bandage on real leg, the bandage horizontal porosity has been analysed as a function of the bandage extension level and the angle between warp and weft threads as displayed in [Figure 5.20](#).

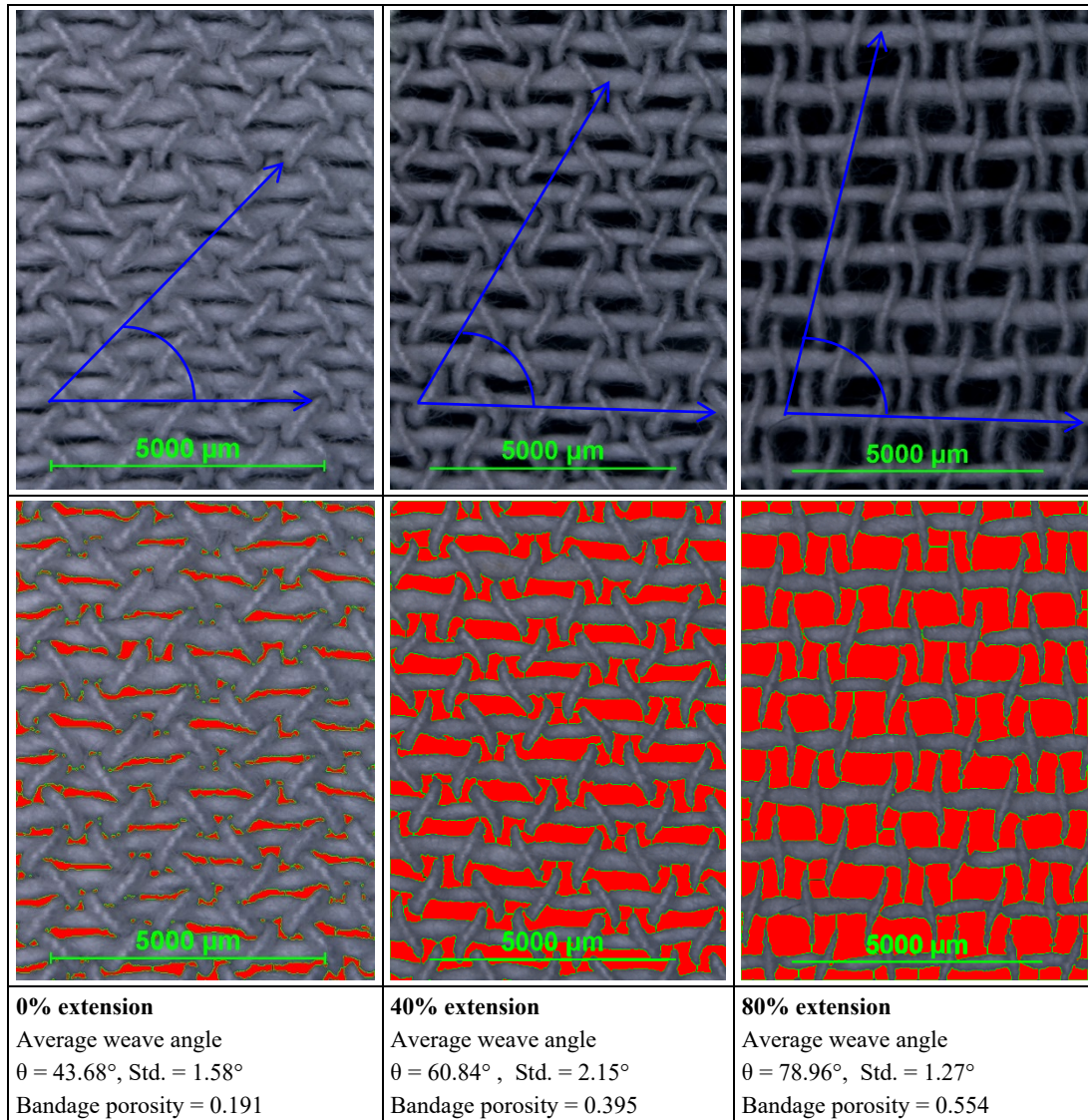


Figure 5.20. Effect of extension level on the horizontal porosity of cotton bandage during application on real leg

5.2.2 Analysis of bandage pressure using Picopress

Experimental pressure of WCBs (100% Cotton and VI-PU) is measured using Picopress on mannequin leg, as shown in Figure 5.21. The same compression test is carried out for all types of bandages on real leg at the 1st, 2nd, and 3rd positions, as previously illustrated in Figure 5.4. The first type of bandages is 100% Cotton using highly twisted plied Cotton yarns. Average compression values at 1st position for the three tension levels (low, medium, high) were about (24, 37, 59 mmHg) respectively. The obtained results at 1st position are decreasing by average percent 12% after three hours, whereas compression values for 2nd position were (16, 29, 50 mmHg) decreasing by average percent 11%, as shown in Figures 5.22 - 5.25. These losses may be due to the bandage slippage or less fixation on leg model.

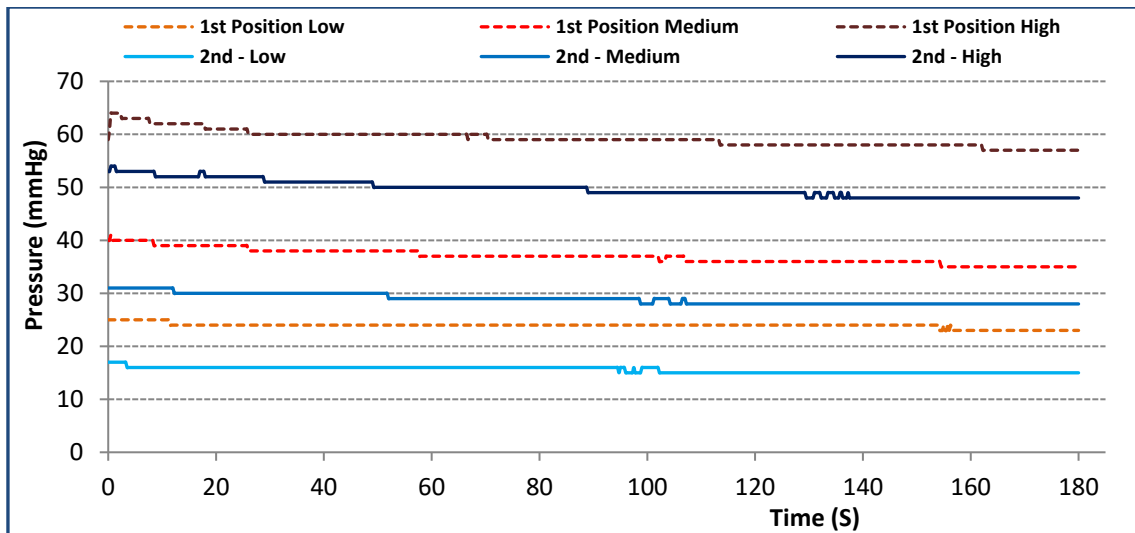


Figure 5.21. Pressure of Cotton bandage on leg model

As for applying compression bandages on a real leg; all compression tests were applied on the same group of 4 men, their age ranges 28 to 37 years old. [Figure 5.22](#) emphasizes the significant change of compression during walking, which is oscillating between (18-33, 27-43, and 36-61 mmHg) for 1st position, (8-16, 18-27, and 35-51) for 2nd position, see [Table 5.4](#). These oscillations during walking and running should be considered while wearing the compression bandages for long time to achieve effective healing rates. [Figure 5.23](#) shows the pressure of CO-PA-PU compression bandage while walking; that is ranging (10-19, 20-35, and 34-50 mmHg) for 1st position, (17-23, 22-26, and 27-37 mmHg) for 2nd position, and (12-15, 13-18, and 13-19 mmHg) for 3rd position. Oscillating ranges of CO-PA-PU bandage are lower than the 100% Cotton bandage because of more extensibility.

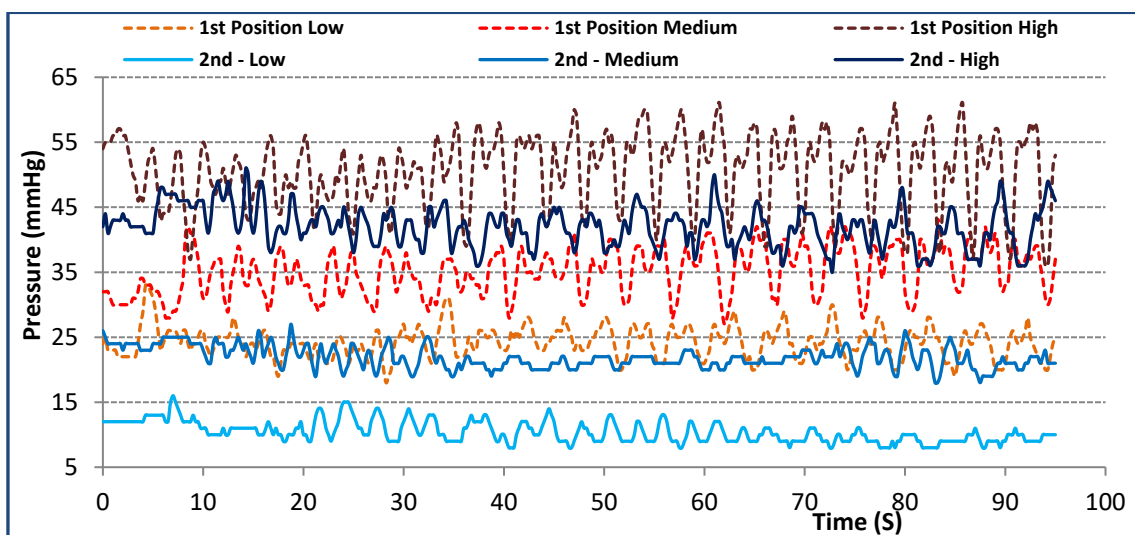


Figure 5.22. Pressure of Cotton bandage on real leg while walking.

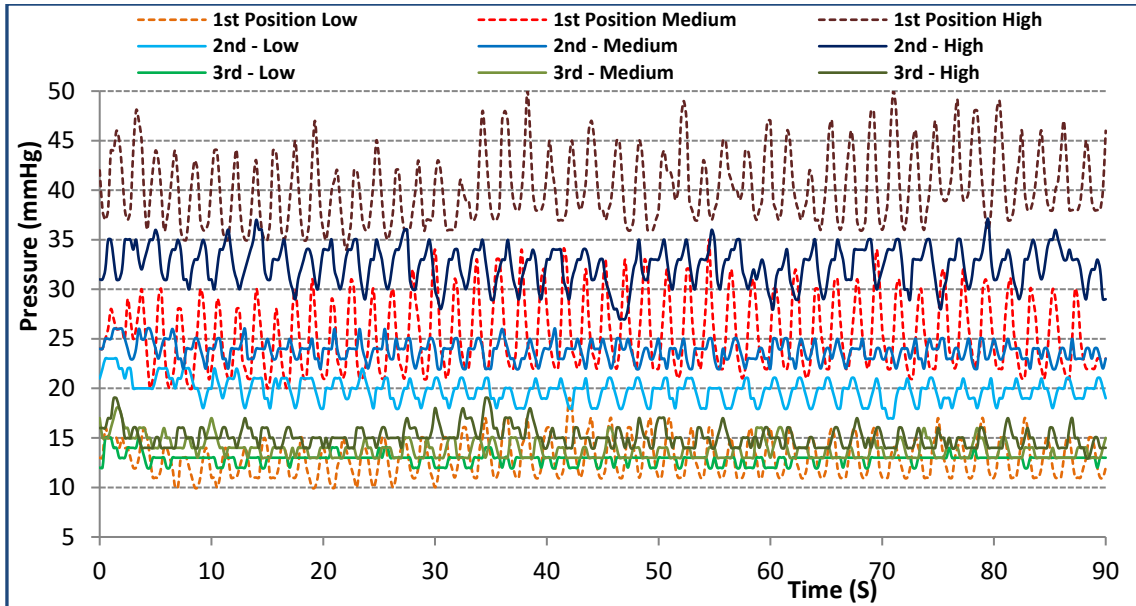


Figure 5.23. Pressure of CO-PA-PU bandage on real leg while walking.

Table 5.4. Statistical analysis of the effect of testing position and extension level on the measured pressure by Picopress

Regression Summary for Dependent Variable: Pressure (Picopress pressure-Full results)						
R= .96026393 R ² = .92210681 Adjusted R ² = .92203839 F(2,2277)=13478. p<0.0000 Std. Error of estimate: 3.8462						
N=2280	b*	Std. Error of b*	b	Std. Error of b	t(2277)	p-value
Intercept			19.4759	0.322196	60.4472	0.00
Testing position	-0.429365	0.005849	-11.8263	0.161098	-73.4106	0.00
Extension Level	0.858925	0.005849	14.4875	0.098652	146.8544	0.00

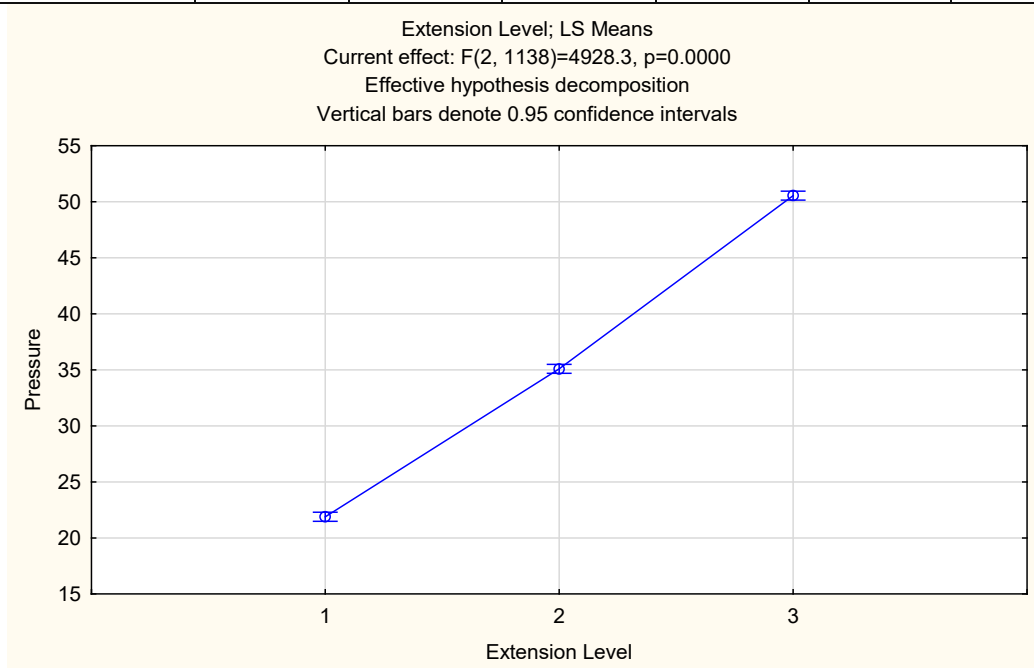


Figure 5.24. Effect of bandage extension level on the measured pressure at the ankle position for cotton bandage, statistically analysed by main effects ANOVA

Table 5.5. Multiple regression of the relation between bandage type and extension level on the measured pressure by Picopress at ankle position

N=3330	Regression Summary for Dependent Variable: Pressure (Picopress pressure-Full results-Ankle-Bandage type) R= .91682084 R ² = .84056045 Adjusted R ² = .84046460 F(2,3327)=8769.9 p<0.0000 Std. Error of estimate: 5.3412					
	b*	Std. Error of b*	b	Std. Error of b	t(3327)	p-value
Intercept			7.09069	0.332057	21.3539	0.00
bandage type	-0.157535	0.006923	-2.56436	0.112687	-22.7565	0.00
Extension Level	0.903185	0.006923	14.79009	0.113362	130.4683	0.00

Table 5.6. Multiple regression of the relation between bandage type and extension level on the measured pressure by Picopress at mid-calf position

N=3330	Regression Summary for Dependent Variable: Pressure (Picopress pressure-Full results-Mid-calf-Bandage type) R= .91080126 R ² = .82955894 Adjusted R ² = .82945648 F(2,3327)=8096.5 p<0.0000 Std. Error of estimate: 4.3094					
	b*	Std. Err. of b*	b	Std. Err. of b	t(3327)	p-value
Intercept			2.89335	0.267907	10.7998	0.000000
bandage type	-0.067807	0.007157	-0.86130	0.090917	-9.4735	0.000000
Extension Level	0.908274	0.007157	11.60631	0.091461	126.8984	0.000000

While Viscose-Polyurethane CB introduced lowest oscillating pressure range i.e. (14 - 19, 26 - 30, and 46 - 56 mmHg) for 1st position and (12 - 16, 17 - 22, and 32 - 45) for 2nd position, as illustrated in [Figure 5.25](#). This low range of pressure is due to Lycra extensibility. Moreover the Viscose-Polyamide bandage is giving the lowest compression pressure values compared to other types; this may be due to yarns characteristics and type of heat setting to give the stretch and extensibility of the bandages, this type of bandage is more suitable for hand muscles.

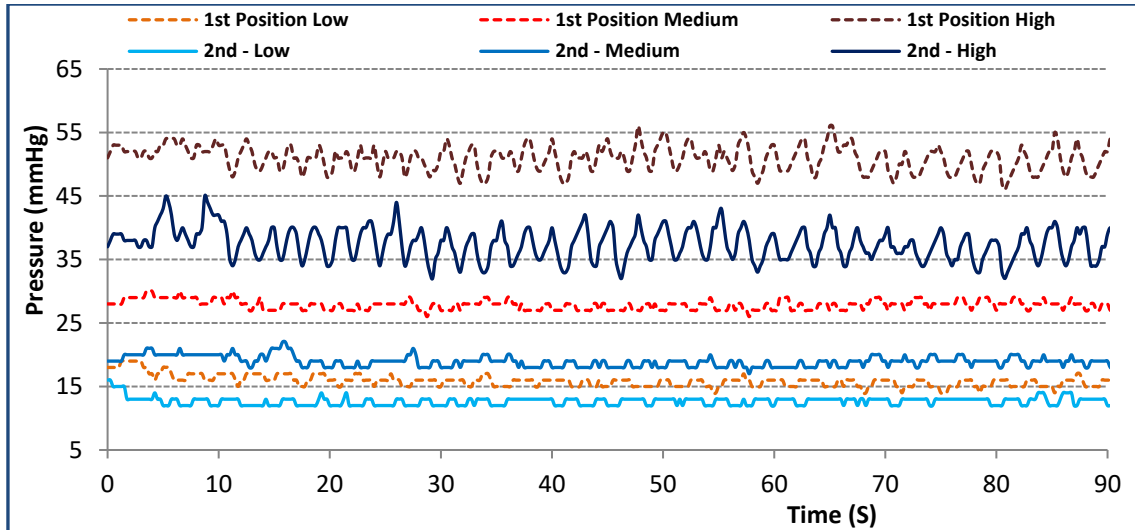


Figure 5.25. Pressure of Viscose-Polyurethane bandage on real leg while walking.

5.2.3 Comparison between calculated and measured compression using PicoPress

100% Cotton, CO-PA-PU, and VI-PU bandages were worn one by one on real leg to test the real compression pressure at ankle and mid-calf position in both static and walking conditions at different extension levels. Ankle and calf positions were adjusted at leg circumference of 25.6 and 38.9 cm respectively. Deviation percent was calculated as the difference between measured compression using Picopress and calculated pressure by Laplace's equation (5.10) [8, 9, 122, and 123], as illustrated in Tables 5.7 & 5.8.

$$\text{Pressure (Pascal)} = \frac{\text{Tension (N)} * \text{No. of Layers}}{\text{Radius (m)} * \text{Bandage width (m)}} \quad (5.9)$$

$$\text{Pressure (mmHg)} = \frac{T (N) * n}{R (m) * W (m)} * 0.0075 \quad (5.10)$$

The level of pressure exerted on a medical device matches with the Laplace's equation stating that the pressure (P expressed in Pa) of a compression applied to the skin surface is directly proportional to the tension (T in N) of the compression material and number of layers, and inversely proportional to the radius of curvature (R in m) of limb surface to which it is applied and the bandage width (W in m) [124].

$$\text{Deviation percent (\%)} = \frac{P_{\text{Calculated}} - P_{\text{Picopress}}}{P_{\text{Calculated}}} * 100 \quad (5.11)$$

Table 5.7. Calculated pressure by Laplace's equation vs. measured values at ankle position using Picopress ($R= 4.07$ cm)

Bandage type	No of layers	Extension (%)	Applied Tension (N)	Std. of tension	Measured compression Picopress (mmHg)	Calculated pressure values (mmHg)			
						Laplace's equation	Deviation percent (%)	Al Khaburi's equation	Deviation percent (%)
100% Cotton bandage	2	20	1.75	0.19	7.02	6.45	-8.84	6.29	-11.52
		30	2.81	0.07	10.84	10.36	-4.67	10.11	-7.24
		40	3.94	0.12	14.62	14.52	-0.68	14.17	-3.16
		50	6.06	0.31	21.71	22.33	2.79	21.80	0.41
		60	9.79	0.82	35.19	36.08	2.47	35.22	0.07
		70	13.37	1.41	45.71	49.28	7.24	48.09	4.96
		80	17.26	1.92	56.83	63.61	10.66	62.09	8.47
	3	20	1.8	0.22	10.58	9.95	-6.32	9.60	-10.22
		30	2.92	0.11	16.39	16.14	-1.53	15.57	-5.25
		40	4.05	0.17	21.83	22.39	2.50	21.60	-1.07
		50	6.24	0.39	32.67	34.50	5.29	33.28	1.83
		60	10.12	0.94	51.61	55.95	7.75	53.97	4.37
		70	13.85	1.55	68.38	76.57	10.69	73.86	7.42
		80	17.93	2.13	83.62	99.12	15.64	95.62	12.55
CO-PA-PU bandage	2	20	1.41	0.19	5.57	5.20	-7.19	5.07	-9.82
		40	3.58	0.13	13.81	13.19	-4.67	12.88	-7.24
		60	5.25	0.21	20.13	19.35	-4.04	18.88	-6.59
		80	8.64	0.49	32.15	31.84	-0.96	31.08	-3.45
		100	10.73	0.73	41.62	39.55	-5.25	38.60	-7.83
		120	13.97	1.65	47.93	51.49	6.91	50.25	4.62
	3	20	1.43	0.18	8.35	7.91	-5.62	7.63	-9.49
		40	3.64	0.15	21.06	20.12	-4.66	19.41	-8.49
		60	5.37	0.19	30.49	29.69	-2.71	28.64	-6.47
		80	8.91	0.53	46.43	49.26	5.74	47.52	2.29
		100	10.94	0.97	56.39	60.48	6.76	58.34	3.35
		120	14.23	2.19	71.69	78.67	8.87	75.89	5.53

The obtained results in Tables 5.7 & 5.8 and Figures 5.26 – 5.29 confirm that there are significant deviations when applying Laplace's equation for two and three layers bandaging ranging ± 0.68 to $\pm 15.64\%$. The highest deviation values were clearly significant at high extension levels 60-80%, this might be due to the compactness and high compression especially at ankle position. Moreover Jawad Al Khaburi developed this equation (5.12) to include the increase in limb circumference due to multilayer bandaging; this equation has decreased the deviation range to be ± 0.07 : $\pm 12.55\%$ as illustrated in the following equations [17, 125]:

$$P = \sum_{i=1}^n \frac{T_i (D_i + t_i)}{0.5 * W_i * D_i^2 + W_i * t_i (D_i + t_i)} * 0.0075 \quad (5.12)$$

$$\text{Where } D_i = D + \sum_{i=1}^n 2 t_{i-1} \quad (5.13)$$

Table 5.8. Multiple regression for the effect of bandage extension, number of layers, and bandage type on the measured pressure at ankle position

Regression Summary for Dependent Variable: Measured pressure, Picopress (Ankle position) R= .92307130 R ² = .85206063 Adjusted R ² = .83188708 F(3,22)=42.237 p-value = 0.000000002671713						
N=26	b*	Std. Error of b*	b	Std. Error of b	t(22)	p-value
Intercept			-17.3050	10.53323	-1.64290	0.114621
Bandage Type	-0.342728	0.087243	-14.7613	3.75753	-3.92845	0.000718
No of layers	0.298003	0.082003	12.7969	3.52141	3.63404	0.001466
Extension	0.929065	0.087243	0.6829	0.06413	10.64922	0.000000

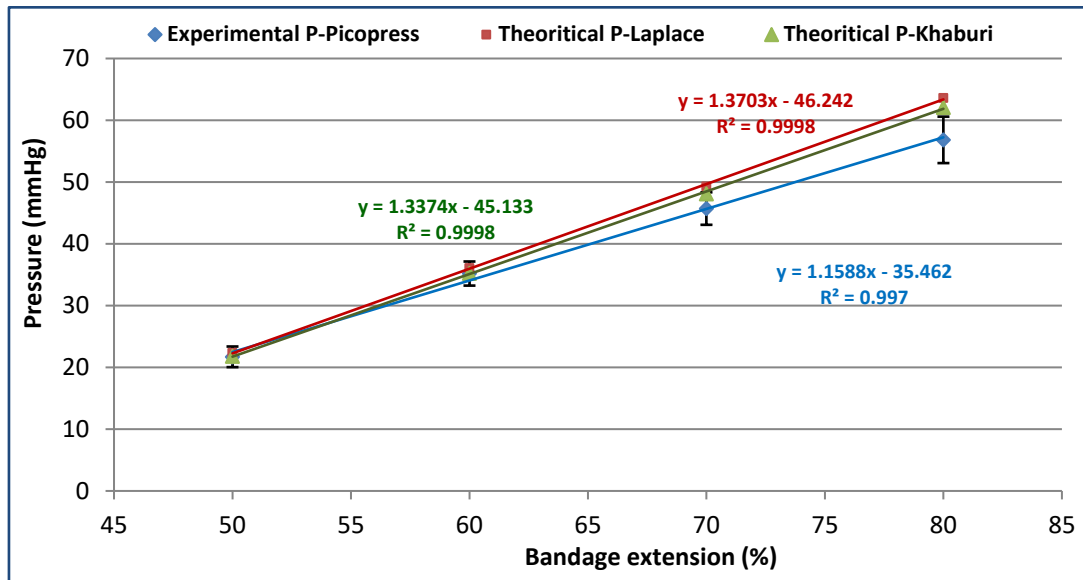
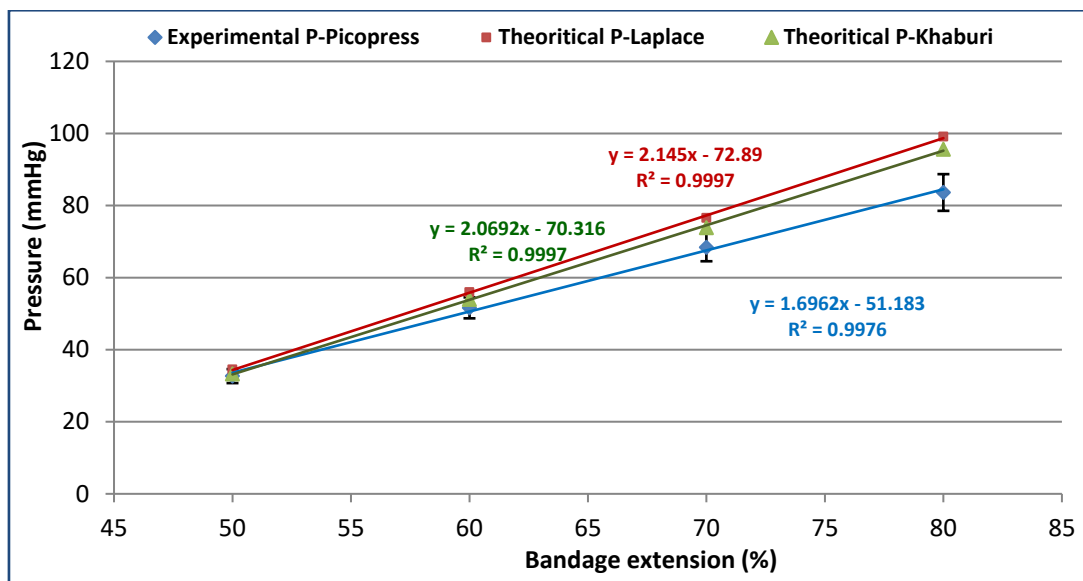
Results of [Table 5.9](#) conclude that the deviation when applying Laplace's equation for mid-calf position is ranging ± 0.27 to $\pm 13.14\%$, while the deviation range of Al Khaburi's equation is ± 0.14 to $\pm 11.04\%$.

Table 5.9. Calculated vs. measured pressure values at mid-calf position (R= 6.19 cm)

Bandage type	No of layers	Extension (%)	Applied Tension (N)	Std. of tension	Measured compression Picopress (mmHg)	Calculated pressure values (mmHg)			
						Laplace's equation	Deviation percent (%)	Al Khaburi's equation	Deviation percent (%)
100% Cotton bandage	2	20	1.71	0.19	4.61	4.14	-11.25	4.08	-13.05
		30	2.74	0.07	7.13	6.64	-7.38	6.53	-9.12
		40	3.82	0.12	9.5	9.26	-2.63	9.11	-4.28
		50	5.89	0.31	14.21	14.27	0.44	14.05	-1.17
		60	9.55	0.82	23.08	23.14	0.27	22.77	-1.34
		70	13.15	1.41	30.85	31.87	3.19	31.36	1.62
		80	16.86	1.92	37.75	40.86	7.60	40.21	6.11
	3	20	1.76	0.22	7.08	6.40	-10.67	6.25	-13.34
		30	2.83	0.11	10.73	10.29	-4.31	10.04	-6.83
		40	3.97	0.17	14.11	14.43	2.22	14.09	-0.14
		50	6.11	0.39	20.92	22.21	5.80	21.69	3.53
		60	9.85	0.94	33.47	35.80	6.52	34.96	4.26
		70	13.46	1.55	44.21	48.93	9.64	47.77	7.46
		80	17.41	2.13	54.97	63.28	13.14	61.79	11.04
CO-PA-PU bandage	2	20	1.39	0.19	3.75	3.37	-11.33	3.31	-13.13
		40	3.54	0.13	9.33	8.58	-8.76	8.44	-10.52
		60	5.19	0.21	13.28	12.58	-5.59	12.38	-7.30
		80	8.54	0.49	21.65	20.69	-4.62	20.37	-6.31
		100	10.56	1.11	26.94	25.59	-5.28	25.18	-6.98
		120	13.61	1.90	33.15	32.98	-0.51	32.46	-2.14
		3	20	1.42	0.18	5.71	5.16	-10.63	5.04
	40		3.61	0.15	14.41	13.12	-9.82	12.81	-12.47
	60		5.29	0.19	20.63	19.23	-7.29	18.78	-9.88
	80		8.71	0.53	32.89	31.66	-3.89	30.91	-6.39
	100		10.83	1.24	38.37	39.37	2.53	38.44	0.18
	120		14.11	2.38	45.94	51.29	10.43	50.08	8.27

Table 5.10. Statistical analysis of measured pressure at mid-calf position

N=26	Regression Summary for Dependent Variable: Measured pressure, Picopress (Mid-calf position) R= .92422059 R ² = .85418370 Adjusted R ² = .83429966 F(3,22)=42.958 p-value = 0.00000000228151764 Std. Error of estimate: 5.8675					
	b*	Std. Error of b*	b	Std. Error of b	t(22)	p-value
Intercept			-11.8498	6.884002	-1.72136	0.099220
Bandage Type	-0.323736	0.086614	-9.1788	2.455738	-3.73768	0.001141
No of layers	0.294456	0.081413	8.3238	2.301418	3.61683	0.001528
Extension	0.932014	0.086614	0.4510	0.041911	10.76051	0.000000

**Figure 5.26.** Measured bandage pressure by Picopress vs calculated by Laplace's and Al-khaburi's equations at ankle position using two layers of cotton bandage**Figure 5.27.** Measured bandage pressure by Picopress vs calculated values at ankle position using three layers bandaging

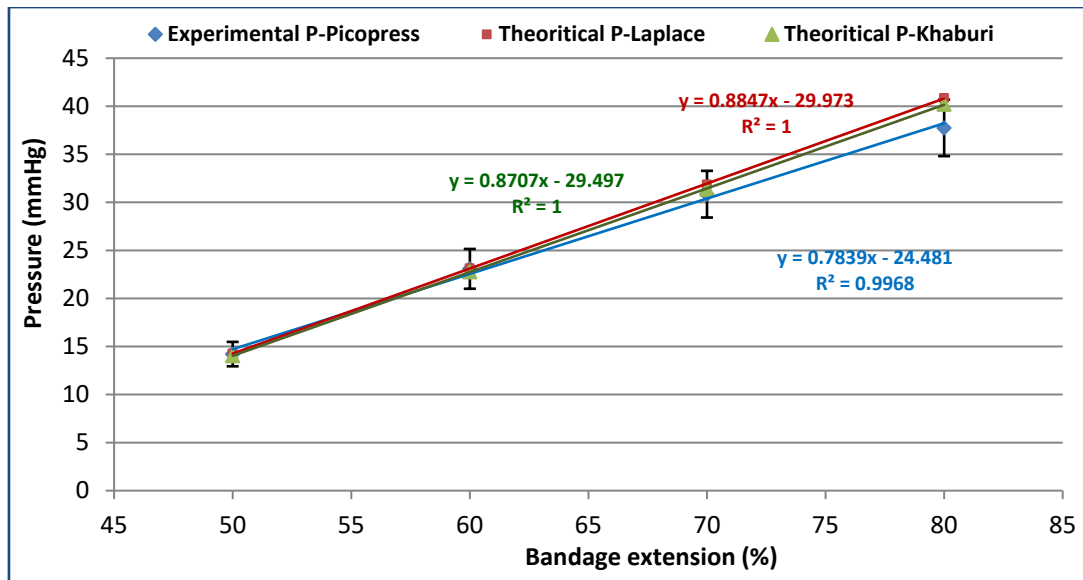


Figure 5.28. Measured bandage pressure by Picopress vs calculated values at mid-calf position using two layers bandaging

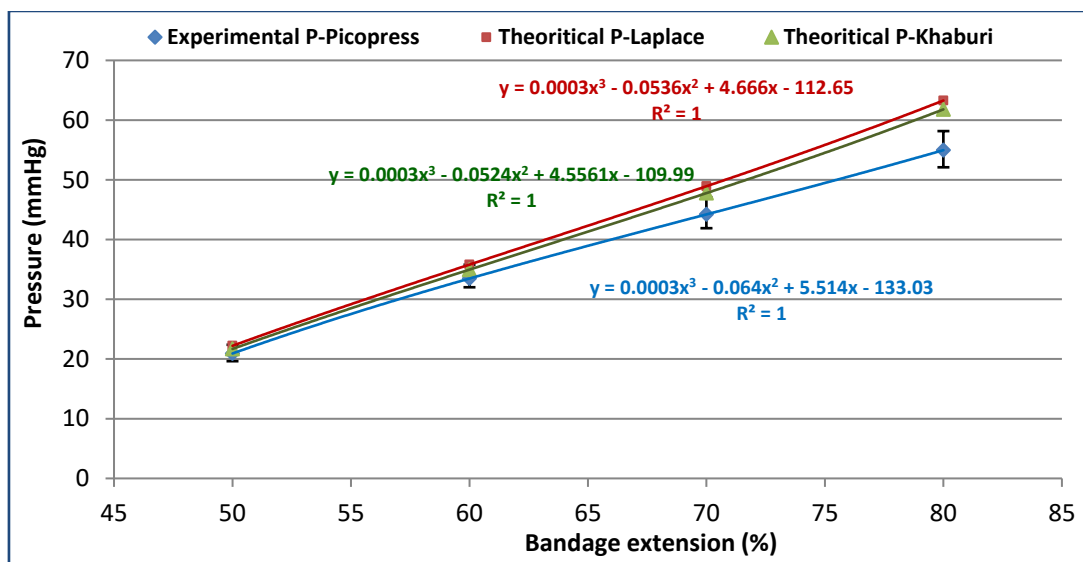


Figure 5.29. Measured bandage pressure by Picopress vs calculated values at mid-calf position using three layers bandaging

5.2.4 Effect of cyclic loading-unloading on bandage tension and durability

Two types of WCBs (100% Cotton short-stretch and CO-PA-PU long-stretch) were selected to investigate the relation between cyclic loading and the applied bandage tension at 60% and 120% extension. Elongation by 3 cm results in extension by 60% and dwell time for 2 seconds, then unloading 1 cm reduces extension to be 40% and dwell time for 2 seconds, then repeating whole cycle for 5 or 6 repeats then relaxation. Cyclic loading-unloading could simulate the walking action when wearing WCB, but the main obstacle is that the testing time

is limited compared to the bandage application time. The uniaxial load of Cotton short-stretch WCB decreased by 11.82% after 6 cycles of loading-unloading, whereas CO-PA-PU long-stretch WCB lost only 4.81% of its applied load at 60% extension. Moreover CO-PA-PU lost 18.11% at 120% extension, see [Figure 5.30](#). So that it is essential to include and compensate these reductions of bandage tension during its selection and application.

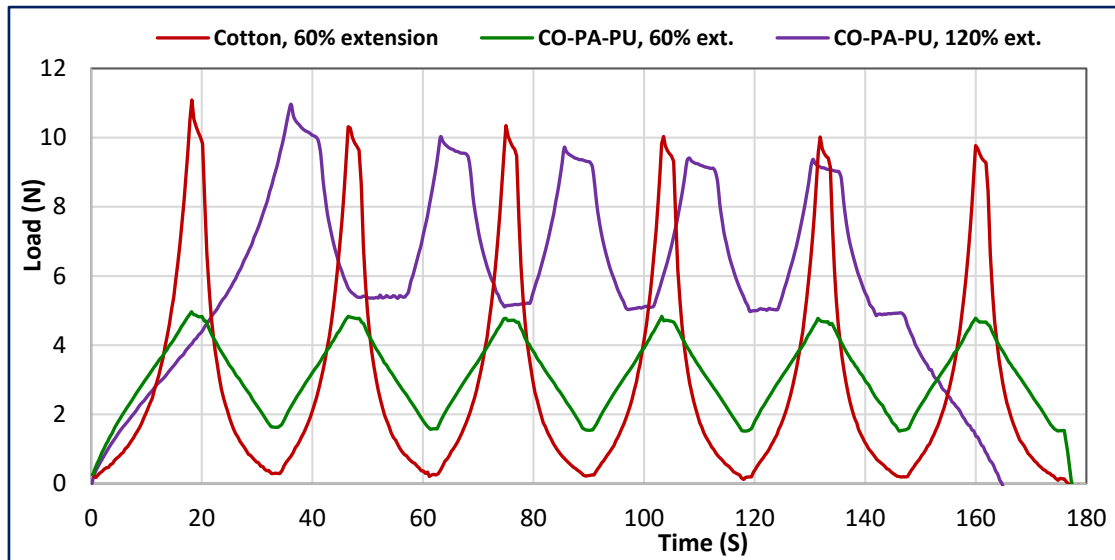


Figure 5.30. Effect of cyclic loading on bandage applied tension

5.2.4.1 *Stress-relaxation test for long and short-stretch WCBs*

[Figures 5.31 & 5.32](#) illustrates that CO-PA-PU LSB recovered approximately 99% of its original length after stress-relaxation; this elastic recovery gives beneficial options through the optimum elasticity when applying the LSB. While Cotton SSB recovered only 93% of its gauge length after 5 days of cyclic load-relaxation. Even when this bandage was wrapped on human leg for five days (12 hr/day), there is a very little residual deformation after longer treatment time. On the contrary when Cotton WCBs used for the same time; there was a significant residual deformation, see [Figure 5.31](#). Moreover it lost approximately 28.6% of its activity, as confirmed by the cyclic loading-unloading tests, see [Figure 5.32](#).

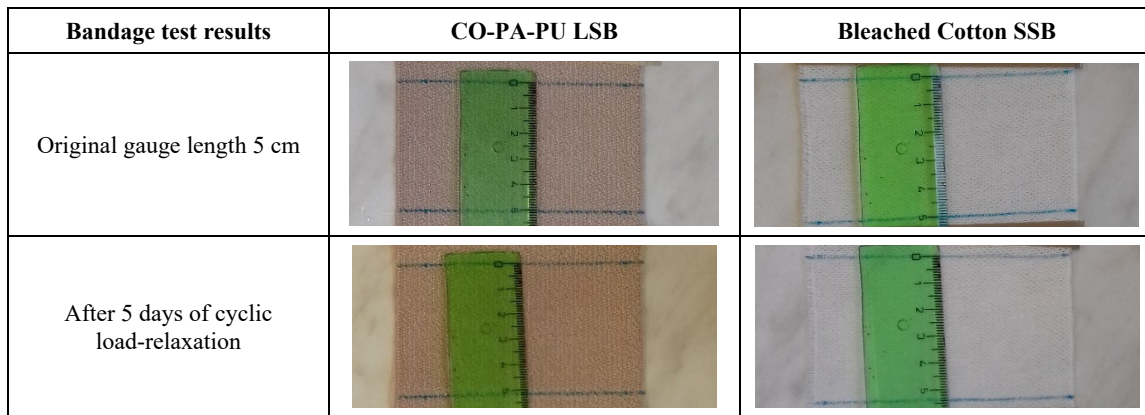


Figure 5.31. Effect of stress-relaxation on elastic recovery of long and short-stretch woven bandages

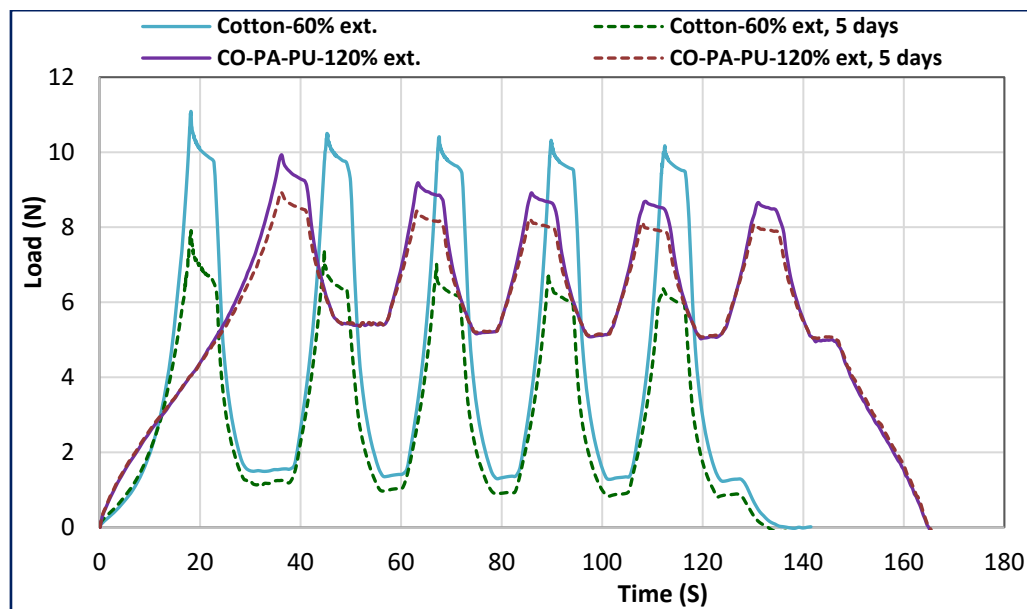


Figure 5.32. Effect of cyclic loading on applied load by long and short-stretch woven bandages

5.2.5 Verification of antibacterial activity of cotton WCB treated with Zinc Oxide NPs

The treated samples with three concentrations: 1%, 2%, and 3% ZnO Nanoparticles in powder form with 15 g/L binder showed a positive results of antibacterial activity for both gram-positive and gram-negative bacteria strains as listed in [Table 5.11](#).

Halo zones did not appear in any of the tested samples as listed in [Table 5.12](#). In samples 1-2, 1-3 and 2-3, 100% inhibition was found under the sample in both tested bacterial strains, i.e. the treatment did not allow the growth of bacteria under the WCB sample. This enhancement is very positive for the bandages' applications.

Table 5.11: The antibacterial activity of cotton WCB according to AATCC 147-2012

Sample number	<i>Escherichia coli</i> inhibition zone size - mm / % inhibition below sample	<i>Staphylococcus aureus</i> inhibition zone size - mm / % inhibition below sample
Standard 1	0 mm, 0%	0 mm, 0%
[1-1]	0 mm, 0%	0 mm, 0%
[1-2]	0 mm, 100%	0 mm, 100%
[1-3]	0 mm, 100%	0 mm, 100%
Standard 2	0 mm, 0%	0 mm, 0%
[2-1]	0 mm, 0%	0 mm, 0%
[2-2]	0 mm, 0%	0 mm, 0%
[2-3]	0 mm, 100%	0 mm, 100%

The quantitative method showed 95% inhibition in all tested WCB samples on both tested bacterial strains, which is 95% compared to the standard. Moreover the higher concentrations of ZnO Nanoparticles did not increase the antibacterial activity.

Table 5.12: The antibacterial activity of cotton WCB according to AATCC 100-2019

Sample number	<i>Escherichia coli</i> % inhibition	<i>Staphylococcus aureus</i> % inhibition
Standard 1	---	---
[1-1]	95%	95%
[1-2]	95%	95%
[1-3]	95%	95%
Standard 2	---	---
[2-1]	95%	95%
[2-2]	95%	95%
[2-3]	95%	95%

5.2.5.1 *Scanning electron microscopy and energy dispersive X-ray of the bandage samples*

The SEM of the un-treated and treated cotton WCB samples are displayed in [Figures 5.33 and 5.34 to 5.36](#) respectively. The zinc oxide nanoparticles' size and its distribution are investigated for the treated bandage samples and the EDX mapping confirmed the percent of ZnO nanoparticles' in the total composition of bandage samples as illustrated in [Figures 5.37 to 5.40](#).

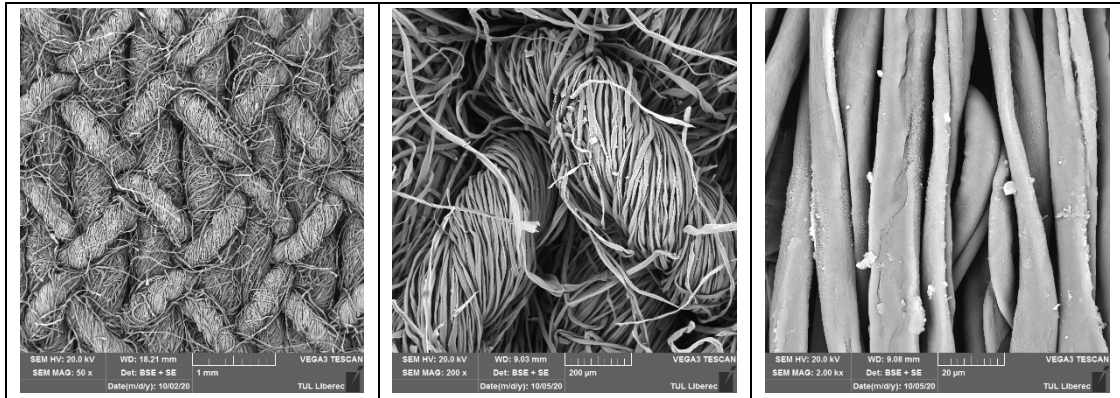


Figure 5.33. SEM of the un-treated cotton woven bandage

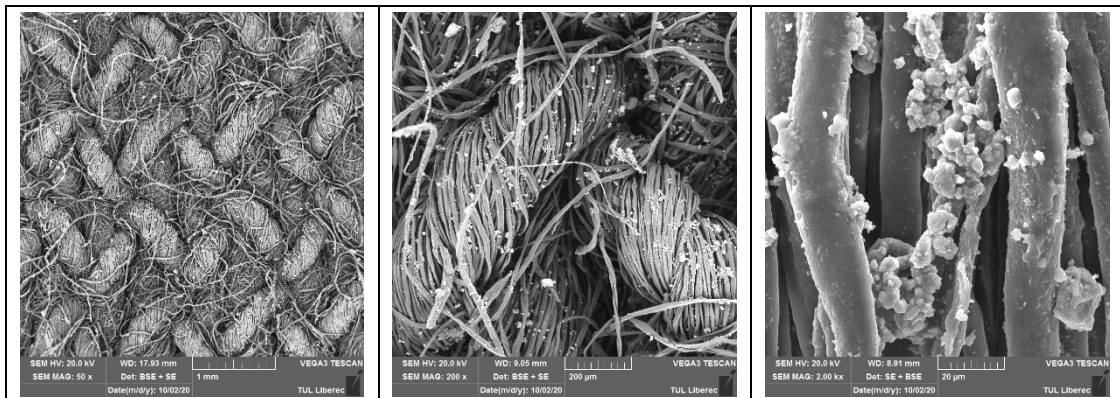


Figure 5.34. SEM of the treated cotton WCB with 1% zinc oxide nanoparticles

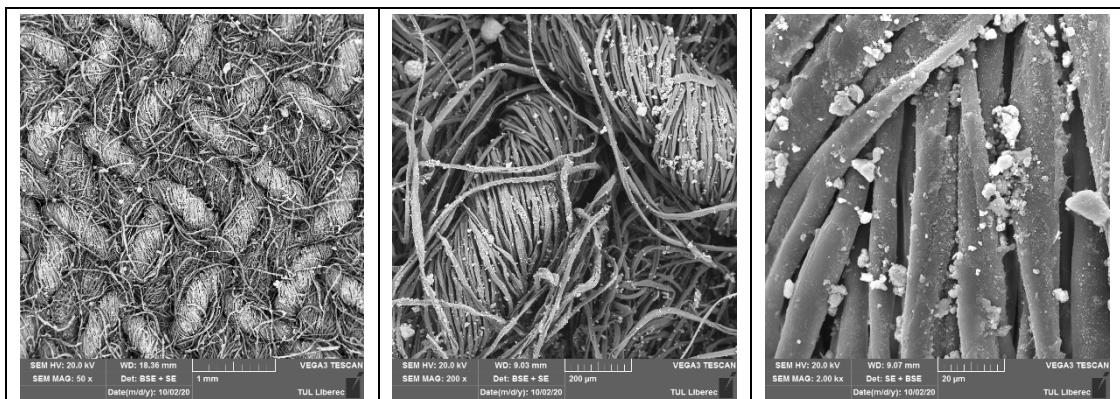


Figure 5.35. SEM of the treated cotton WCB with 2% zinc oxide nanoparticles

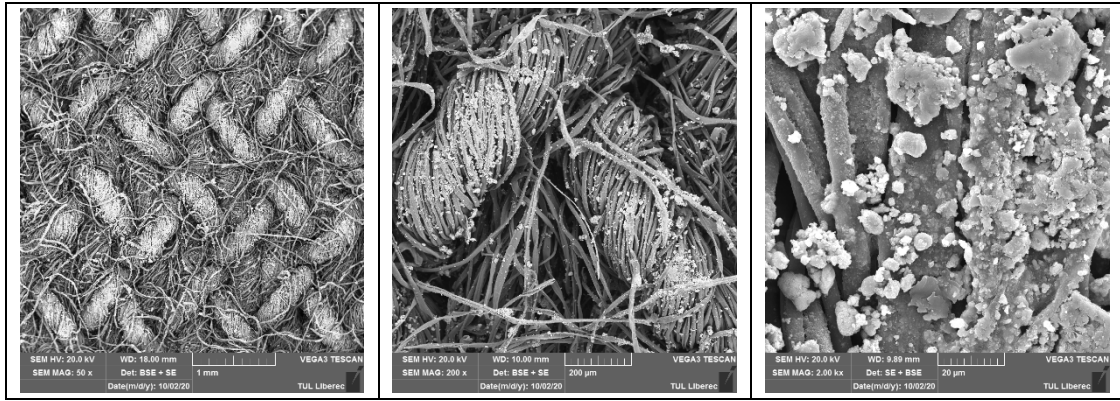


Figure 5.36. SEM of the treated cotton WCB with 3% zinc oxide nanoparticles

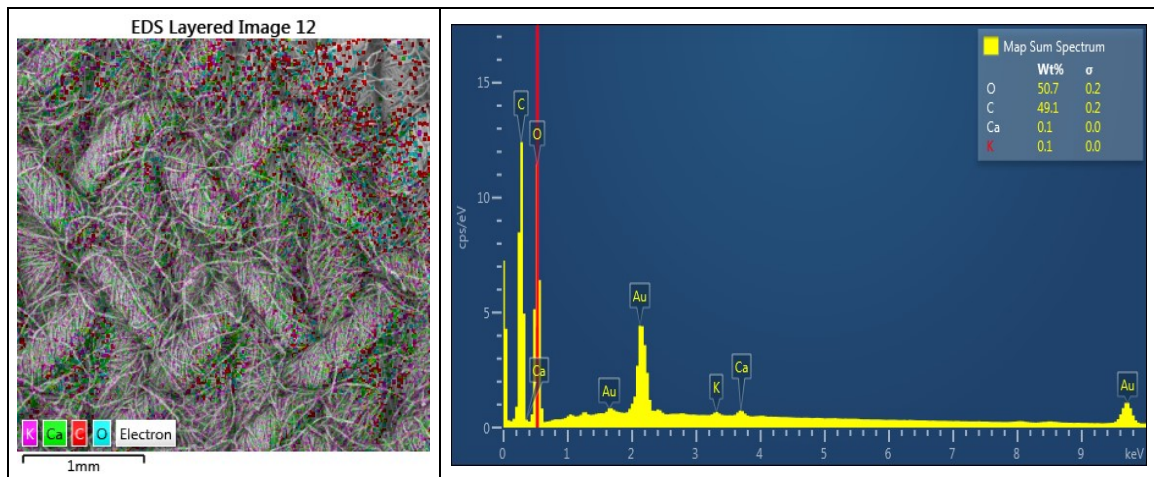


Figure 5.37. Energy dispersive X-ray map of the un-treated cotton WCB

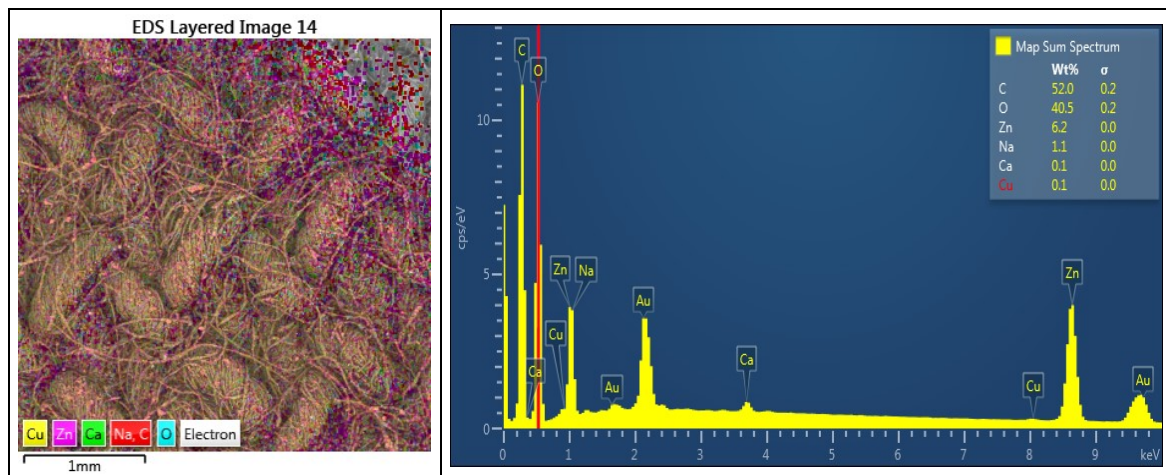


Figure 5.38. EDX map of the treated cotton WCB with 1% zinc oxide nanoparticles

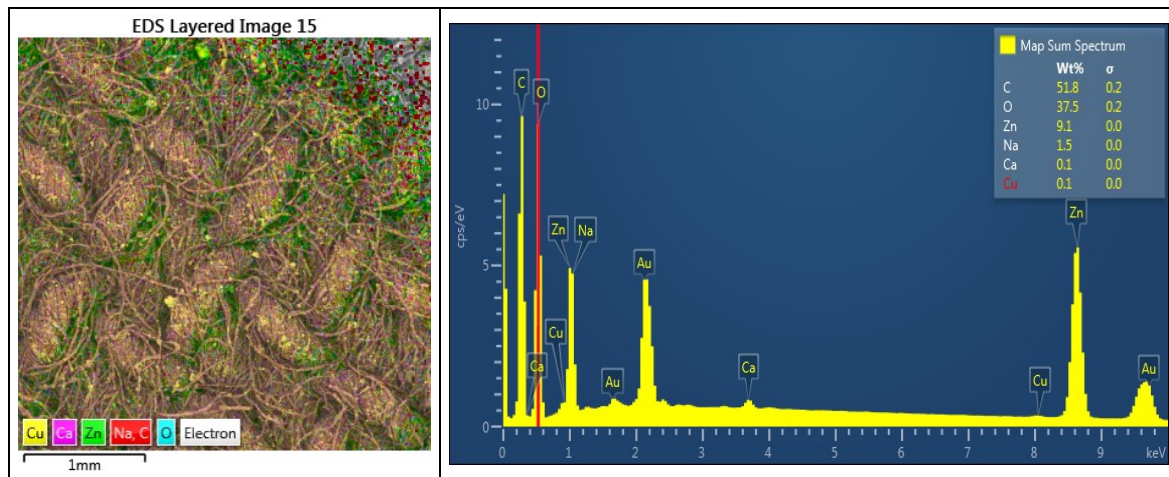


Figure 5.39. EDX map of the treated cotton WCB with 2% zinc oxide nanoparticles

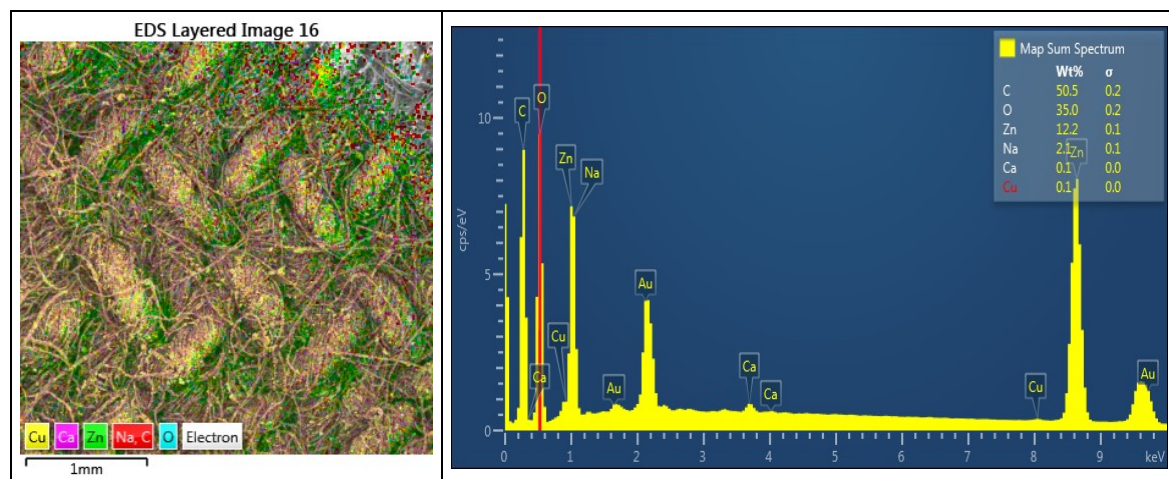


Figure 5.40. EDX map of the treated cotton WCB with 3% zinc oxide nanoparticles

5.2.6 Factors affecting the thermal properties testing

The measurement of clothing insulation with thermal manikin is a dynamically balance adjustment process. It means that continuous adjustment of heat flux makes the manikin skin temperature approach a constant temperature gradually under the heat diffusion. The final state is that the manikin skin temperature is steady in a narrow range and very close to the constant temperature [107]. At the same time, the central temperature of the thermal manikin is getting closer to the set skin temperature. With all such essential conditions achieved, the system gets into the balance stage. After a while, we can calculate testing results according to all the balance parameters and print them out, see Figure 5.41 [107].

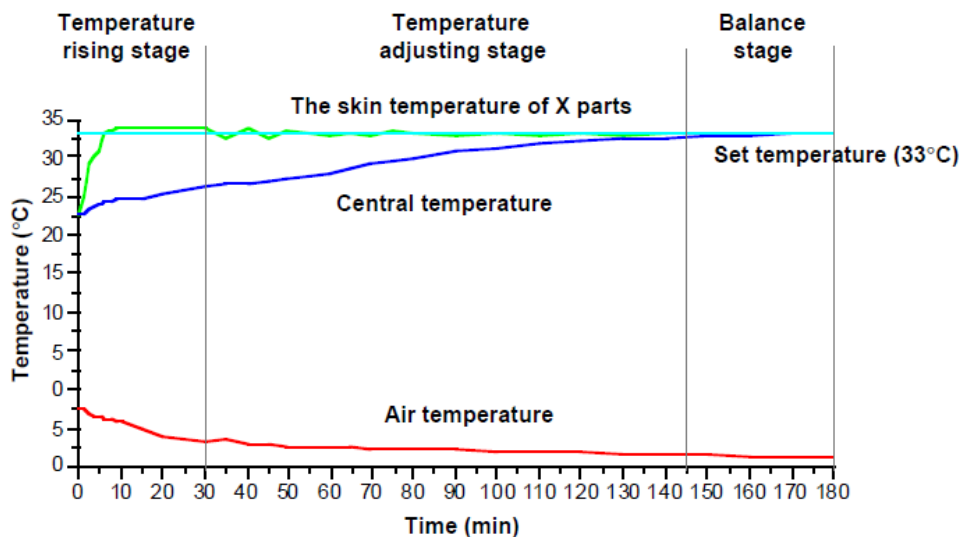


Figure 5.41. The skin temperature adjusting and control process of X parts of thermal manikin [107]

Most of the researches on the thermal comfort properties performed either on knitted fabrics or nonwoven [126-130]. Many researchers have studied the effect of raw materials and knitted fabric construction parameters on the comfort behaviour of fabrics. Investigations revealed that the type of fibres, fibre blends, yarn structure and its fineness, fabric structure, and different process parameters affect various comfort properties such as air permeability, moisture management, thermal conductivity, and thermal absorptivity [131-135]. So that, it is necessary to test and analyse the thermal comfort properties of WCBs, dealing with different yarns material, fabric structures, thickness, porosity, weight per unit area, and number of bandage layers as a function of the applied compression during testing on thermal foot manikin, PERMETEST, and ALAMBETA testing devices.

5.2.6.1 *Effect of bandage extension and number of layers on thermal resistance*

For comparison, all bandage types were wrapped on TFM one by one at the same extension levels (10 to 80%) using both two and three layers bandaging. Figures 5.42 & 5.43 illustrate that R_{ct} values are significantly decreasing when bandage extension increasing from 10 to 40 % due to the decrease of total thickness of layers. Then R_{ct} slightly increases by increasing extension from 40 to 60% that may be due to the higher porosity of bandages (0.364, 0.306, 0.471, and 0,325 for Cotton, CO-PA-PU, VI-PA, and VI-PU bandages respectively). After that R_{ct} values are decreasing for all samples, especially at 80% extension. The most significant factors for this decrease are the lower bandage thickness and higher compression values. Moreover it is illustrated that Cotton bandage has the lowest R_{ct} values due to yarns material and structure. This may be due to higher moisture regain of Cotton (8.5%) and Viscose

(11 - 12%) compared to Polyamide (4 - 4.5%) and Polyurethane (0.3 - 1.2%), which decreases the thermal resistance of Cotton and Viscose bandages [136-138].

As there are many factors can affect the thermal resistance measurements, it was necessary to measure R_{ct0} before each measurement using clothed TFM. There is R_{ct0} for each R_{ct} measurement to get the precise R_{ct} values of CB and simultaneously to monitor deviations of R_{ct0} values. The actual values of R_{ct} can be calculated directly by the device software inserting the measured R_{ct0} as a reference value. Moreover the obtained R_{ct} values could enable for accurate comparison between different bandage samples as illustrated by equation (5.14).

$$R_{ct(F)} = R_{ct(all)} - R_{ct0} \quad (5.14)$$

Where: $R_{ct(F)}$ is the net thermal resistance of the bandage sample (two or three layers), $R_{ct(all)}$ is the total thermal resistance of the (bandage sample + one layer of mercerized socks as clothed TFM), R_{ct0} is the initial thermal resistance of the clothed TFM covered with mercerized socks only.

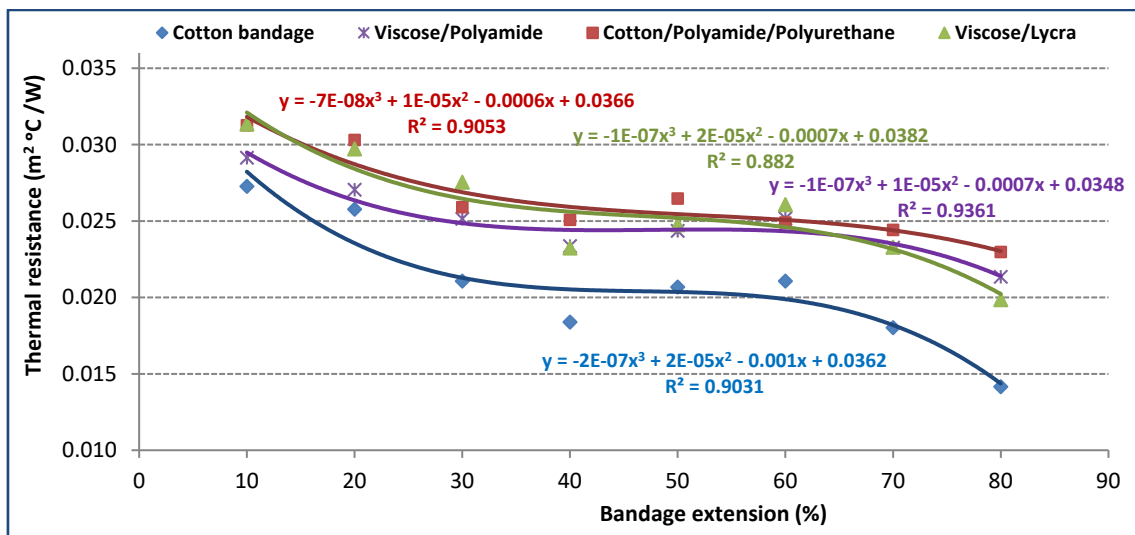


Figure 5.42. Effect of bandage extension on thermal resistance of two layers CB

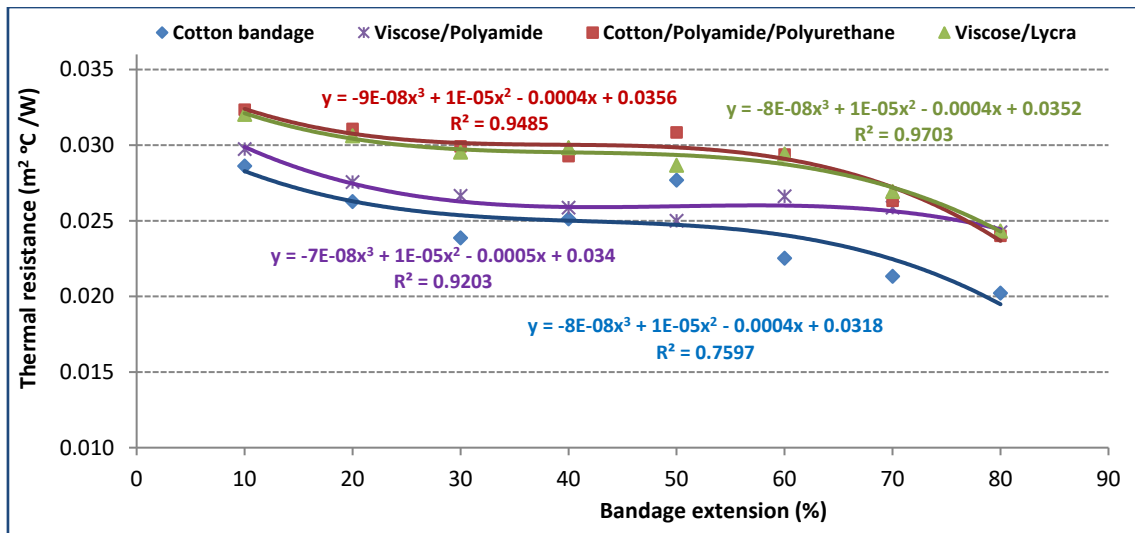


Figure 5.43. Effect of bandage extension on thermal resistance of three layers CB

5.2.6.2 Relationship between applied tension and thermal resistance

While increasing the applied bandage tension from 0.5 to 4N, the thermal resistance is decreasing. These results declare the effect of increasing the bandage compression and decreasing fabric thickness at higher values of extension. Moreover the bandage porosity is increasing based on the increase of bandage tension. So that R_{ct} is slightly increasing from 4 to 6N then R_{ct} is decreasing at higher tension 10N, as shown in Figure 5.44. The same behaviour for three layers, but the additional effect of third layer is lower than the first and second layers. This is attributed to the fact that the thermal resistance of the multilayer fabrics decreases under higher load values or due to the compression between layers.

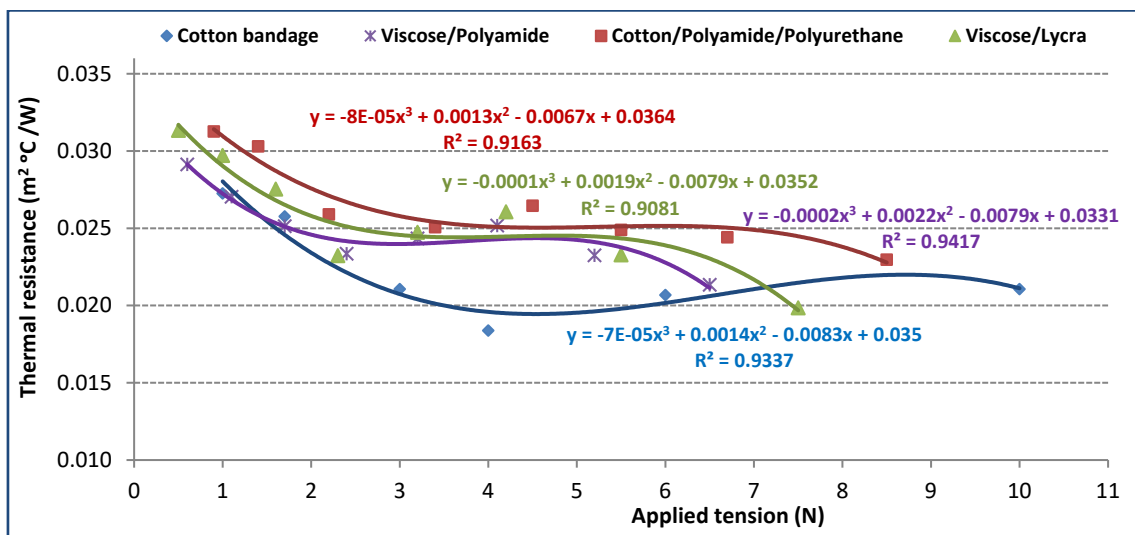


Figure 5.44. Effect of applied tension on thermal resistance of two layers WCB

5.2.6.3 Effect of total thickness of bandage layers on thermal resistance

While the bandages are wrapped on TFM at extension level ranges 10 to 80% using both 50% and 66% overlap. The total thickness of bandage layers at 10% extension is 2.04, 2.15, 1.53, and 2.07 mm. These values are decreasing at 80% to be 1.04, 1.11, 0.76, and 1.08 mm for Cotton, CO-PA-PU, VI-PA, and VI-PU bandages respectively. So that thermal resistance is decreasing by the decrease of total bandage thickness for both two and three layers bandaging, as shown in Figures 5.45 & 5.46 respectively. The reduction percent of R_{ct} results due to extension 10 to 80 % are 48.09, 26.63, 26.73, and 36.66% for Cotton, CO-PA-PU, VI-PA, and VI-PU bandages respectively using two layers while the reduction effect was lower for three layers as 29.37, 25.77, 18.52, and 24.08% respectively.

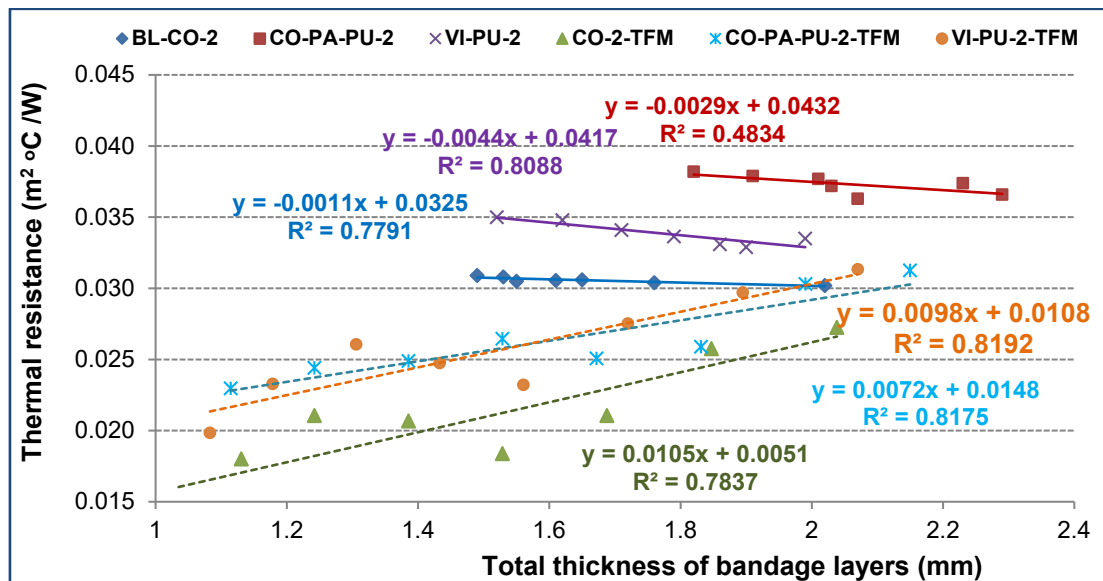


Figure 5.45. Effect of total thickness of layers on thermal resistance of two layers WCBs, on ALAMBETA and thermal foot manikin testing devices

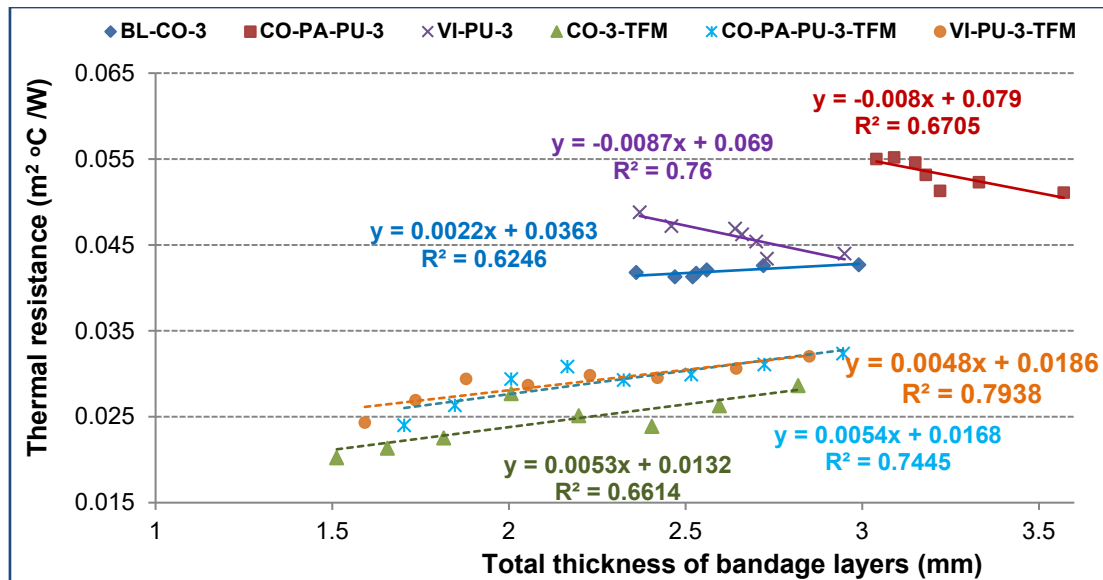


Figure 5.46. Effect of total thickness of layers on thermal resistance of three layers WCBs, on ALAMBETA and thermal foot manikin testing devices

5.2.6.4 Effect of bandage extension on thermal conductivity and resistance

ALAMBETA testing device was used to test thermal conductivity and resistance for all bandage samples at initial porosity (0% extension) and (20 – 100% extension) using two layers during testing. Figure 5.47 concludes the thermal conductivity values for Cotton, CO-PA-PU, VI-PA, and VI-PU bandages as 0.0624, 0.0627, 0.0379, and 0.0595 [W/(m.K)] at 0% extension whereas the conductivity decreases at 100% to 0.0489, 0.0506, 0.0336, and 0.0434 respectively. This reduction may be due to the decrease in bandage thickness and higher porosity values when increasing bandage extension to 100%.

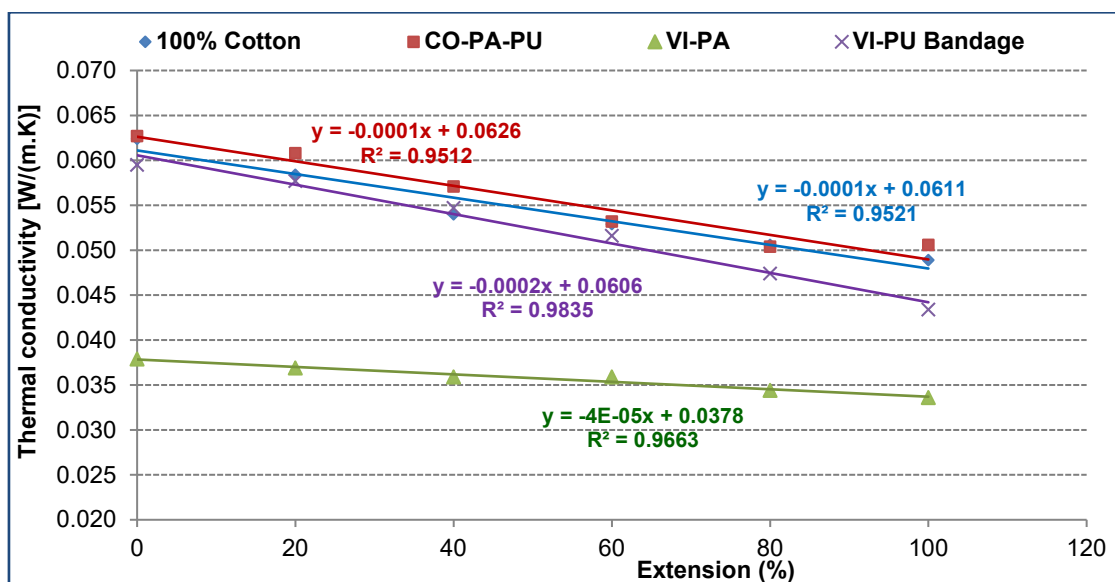


Figure 5.47. Effect of bandage extension on thermal conductivity coefficient, two layers

As for the thermal resistance, Figure 5.48 illustrates that R_{ct} is proportionally increasing with bandage extension. The R_{ct} values at 0% extension are 0.0302, 0.0366, and 0.0335 ($K.m^2/W$) whereas at 100% extension R_{ct} increases to 0.0309, 0.0382, and 0.035 for Cotton, CO-PA-PU and VI-PU bandages respectively. Only VI-PA bandage has an opposite trend, this may be due to its highest porosity and lowest areal density (gsm). There is a bit deviation between ALAMBETA and TFM testing results of CBs, because the compression effect is more significant when using the TFM model. Moreover ALAMBETA testing is performed on planner fabric which is not simulating the real bandage wrapping. So that according to TFM, the R_{ct} values are decreasing as the bandage extension increases from 10 to 80% due to the significant increase in bandage tension. While using ALAMBETA, the R_{ct} values are slightly increasing as the bandage extension increases from 0 to 100% due to the increase in total bandage porosity which increases the trapped air for each fabric layer. Both TFM and ALAMBETA testing results concluded that the 100% Cotton bandage has the lowest R_{ct} and the CO-PA-PU bandage has the highest R_{ct} values. These results confirmed that the yarns material and structure have significant effects on R_{ct} as well as the bandage tension and thickness of layers.

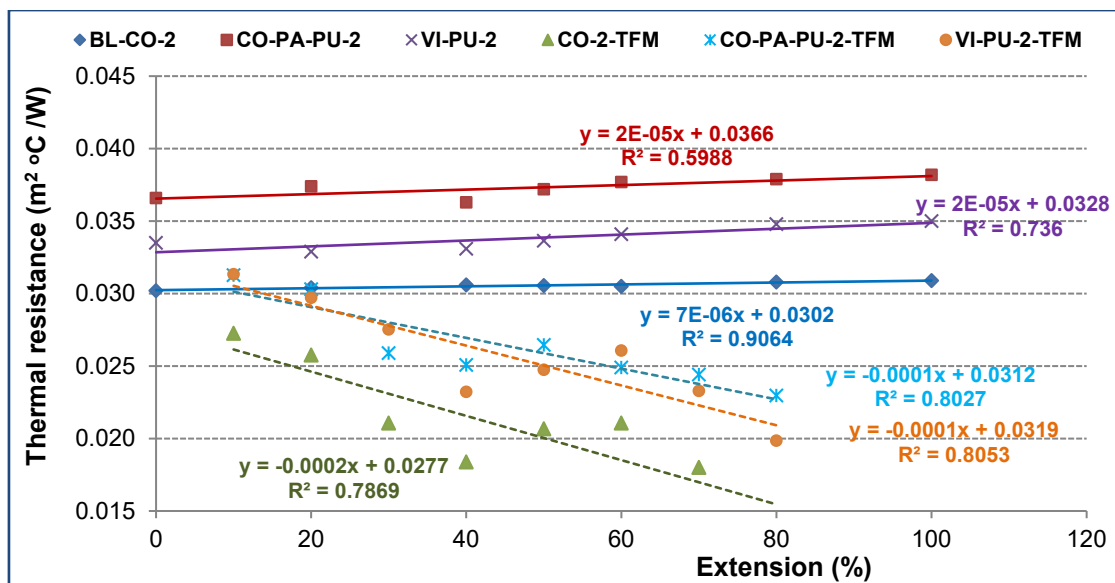


Figure 5.48. Effect of bandage extension on thermal resistance of two layers WCBs, on ALAMBETA and thermal foot manikin testing devices

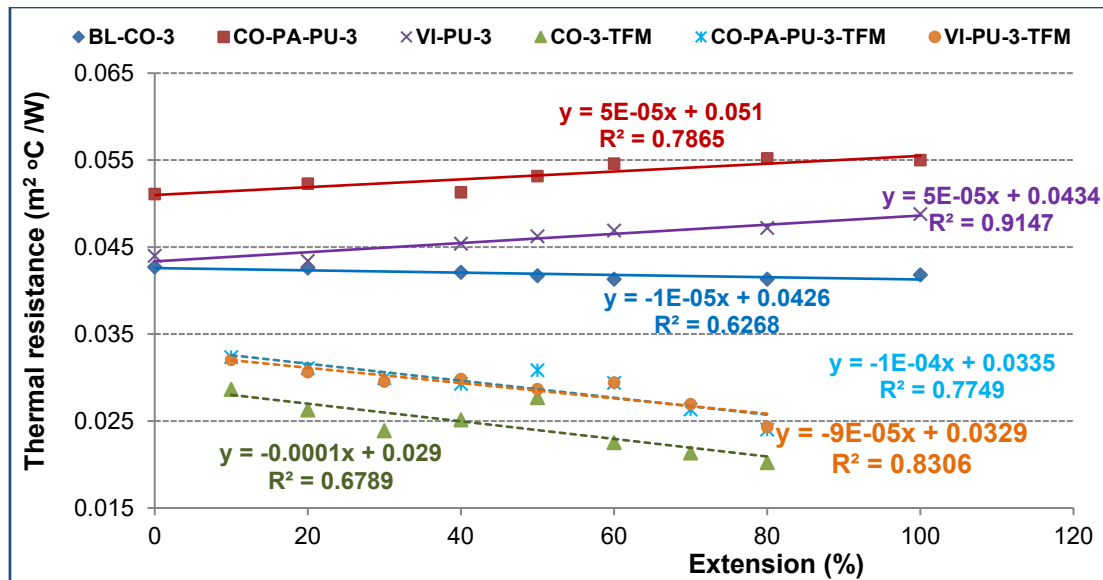


Figure 5.49. Effect of bandage extension on thermal resistance of three layers WCBs, on ALAMBETA and thermal foot manikin testing devices

5.2.6.5 Thermal resistance models and their applications

Thermal resistance of the fabrics can be calculated by means of experimental, analytical and numerical methods [139], [140]. There are many models to be found within the textile engineering and heat transfer fields for the thermal resistance prediction. The preference of selection depends on the requisite precision and nature of the solution. Conductive heat transfer is the simplest way to illustrate mathematically and is often the key way of heat transfer [141].

Numerical solutions deal with materials of irregular shapes and properties, different type of heat transfer and boundary conditions etc. Numerical methods also have the capability to achieve the maximum precision [142]. There are many commercially available soft wares that allow the users to solve their problems through numerical solutions. But these methods are inherently more difficult and complicated, and in some conditions, simple methods proven to be more accurate for much less effort [143]. Thermal resistance is also predicted by using ANN (artificial neural networks) and statistical models. Some researchers have predicted the thermal resistance of fabrics with mathematical approaches.

Schuhmeister suggested a relationship for the thermal conductivity prediction of fabrics by assuming one-third of fibres are parallel and two-third are in series with a homogeneous distribution in all directions [144]. Afterwards, many researchers used Schuhmeister's model by assuming different ratios of series and parallel components [145-147]. Presently, Mansoor et al. have modified Schuhmeister and Militky models by combining the water and fibre filling

coefficient for the prediction of thermal resistance of wet socks [148], [149].

Das et al. [150] have calculated the heat transfer through the fabric assemblies with the electric resistance and Fricke's law analogy by assuming them as cuboids packed with randomly oriented infinite fibres. Wie et al. have suggested a model for fabric thermal resistance prediction by assuming that heat is passing through the fabric as a combination of fibre & air in series plus the air in parallel [151].

Most of studies on R_{ct} of textiles were performed either on knitted fabrics or nonwoven, only a few research on woven fabrics [152-156]. So that it was necessary to evaluate and distinguish the R_{ct} of WCB, dealing with different yarns' material, fabric structures, and number of bandage layers as a function of the applied extension and packing density during testing. Then the experimental results of R_{ct} were validated using the three theoretical models.

a) Maxwell–Eucken2 (ME-2)'s Model

Maxwell–Eucken (ME) model, Equation (2), can be used to describe the effective thermal conductivity of a two-component material with simple physical structures. In Equation (2), λ_a , $\lambda_{polymer}$, F_a , and $F_{polymer}$ are the thermal conductivities and volume fractions, respectively, and subscripts representing the two components of the system. The effective thermal conductivity of the two-component material is λ_{fab} [157]. An emulsion is a dispersion of one liquid in another immiscible liquid. The phase that is present in form of droplets is the dispersed phase and the phase in which droplets are suspended is called the continuous phase. A number of effective thermal conductivity models require the naming of a continuous and a dispersed phase. The materials with exterior porosity, individual solid particles are surrounded by a gaseous matrix, and hence the gaseous component forms the continuous phase and the solid component forms the dispersed phase. For external porosity λ_a and $\lambda_{polymer}$ are considered as continuous & dispersed phase respectively [158], [159].

$$\lambda_{fab} = \frac{\lambda_a F_a + \lambda_{polymer} F_{polymer} \frac{3\lambda_a}{2\lambda_a + \lambda_{polymer}}}{F_a + F_{polymer} \frac{3\lambda_a}{2\lambda_a + \lambda_{polymer}}} \quad (2)$$

$F_{polymer}$ and $\lambda_{polymer}$ is calculated as per Equations (7) and (8).

b) Schuhmeister's Model

Schuhmeister summarized the relationship between the thermal conductivity of a fabric

and the fabric structural parameters by following Equation (3);

$$\lambda_{fab} = 0.67 \times \lambda_s + 0.33 \times \lambda_p \quad (3)$$

$$\lambda_s = \frac{\lambda_{polymer} \times \lambda_a}{\lambda_{polymer} F_a + \lambda_a F_{polymer}} \quad (4)$$

$$\lambda_p = F_{polymer} \lambda_{polymer} + F_a \lambda_a \quad (5)$$

Where λ_{fab} is the thermal conductivity of a fabric, $\lambda_{polymer}$ is the conductivity of fibres, λ_a is the conductivity of air, $F_{polymer}$ is the filling coefficient of the solid fibre, F_a is the filling coefficient of air in the insulation [160].

c) *Militky's Model*

Militky summarized the relationship between the thermal conductivity of a fabric and the fabric structural parameters by an empirical Equation (6) and the same steps for calculating λ_s and λ_p using Equations (4) and (5) respectively [146], [161];

$$\lambda_{fab} = \left(\frac{\lambda_s + \lambda_p}{2} \right) \quad (6)$$

5.2.6.6 *Average Thermal Conductivity & Filling Coefficient Calculations*

By assuming that fabric density is changing with wetting, which causes to change the filling coefficient, porosity, and thermal conductivity of the fabrics. On the basis of these assumptions following three equations are developed that will be used to find the fabric density, filling coefficient and thermal conductivity for different moisture levels. Average thermal conductivity for different fibres (within socks) at different moisture levels will be calculated as per Equation (7).

$$\text{Average Thermal Conductivity } (\lambda_{Polymer}) = \left(\frac{F_{fib1} \cdot \lambda_{fib1} + F_{fib2} \cdot \lambda_{fib2} + F_{fib3} \cdot \lambda_{fib3}}{F_{fib1} + F_{fib2} + F_{fib3}} \right) \quad (7)$$

F_{fib1} = First fibre filling coefficient, F_{fib2} = Second fibre filling coefficient ,

F_{fib3} = Third fibre filling coefficient, λ_{fib1} = First fibre thermal conductivity,

λ_{fib2} = Second fibre thermal conductivity , λ_{fib3} = Third fibre thermal conductivity

Filling coefficients for fibre and air are calculated as listed in Table 5.13 according to the following steps;

Table 5.13. Calculation of fibre filling coefficients

Measurement	$F_{\text{fib}} = \text{Fibre filling coefficient}$
Content	[%]
Weight	[g]
Area	[m ²]
Areal Density	[g.m ⁻¹]
Volumetric Density	$\frac{\text{Fabric Areal Density}}{\text{Fabric Thickness}}$ [Kg.m ⁻³]
Filling coefficient	$\frac{\text{Volumetric Density}}{\text{Fibre Density}}$

Air filling coefficient (F_a) is calculated as per below Equation (8);

$$\text{Air filling coefficient } (F_a) = 1 - F_{\text{fib}} \quad (8)$$

The output of Equations (7) & (8) are used as input for all above models. Thermal conductivity of water and air are taken as 0.6 and 0.026 (W.m⁻¹.K⁻¹) while density of water is 1000 (Kg/m³). The values of the different input parameters are used in this study are listed below in Table 5.14 [162].

Table 5.14. Properties of different fibres

Fibre Name	Density (Kg/m ³)	Thermal Conductivity [W/(m.K)]
Cotton	1540	0.05
Viscose	1530	0.05
Polyester	1360	0.04
Nylon 66	1140	0.03
Polypropylene	900	0.02
Wool	1310	0.05
Acrylic	1150	0.03

5.2.6.7 Validation of the experimental R_{ct} results on TFM and ALAMBETA with three theoretical models

The experimental results of R_{ct} matches with the three mathematical models that the increase in total fabric (WCB layers) thickness is associated with an enhancement in the R_{ct} values, as displayed in Figure 5.50. The ALAMBETA enables fast measurement of both steady-state and transient-state thermal properties, as shown in Figure 5.51. This diagram clearly demonstrated the maximum q_{max} , dynamic (transient) q_{dyn} and steady state q_{steady} heat flow [163]. Moreover there are significant similarities between the ALAMBETA results and both

Schuhmeister and Militky models, approximately 92 and 93% respectively, see Figure 5.52. Whereas the correspondence values for the TFM are approximately 82 and 83% respectively, as shown in Figure 5.53. This might be because the ALABETA testing is corresponded well to the use of socks inside a shoe (boundary conditions of first order).

The transient heat flow has been shown by equation (10), whereas the steady state heat flow has been shown by equation (11).

$$q_{dyn} = \frac{b \cdot (T_1 - T_2)}{\sqrt{\pi\tau}} \quad (10)$$

$$q_{steady} = \frac{T_1 - T_2}{R_{ct}} \quad (11)$$

Where b is the thermal absorptivity [$\text{W s}^{0.5} \text{m}^{-2} \text{K}^{-1}$], the temperature difference between the two convection surfaces ($\Delta T = T_1 - T_2$), and τ is the tortuosity [-] [164].

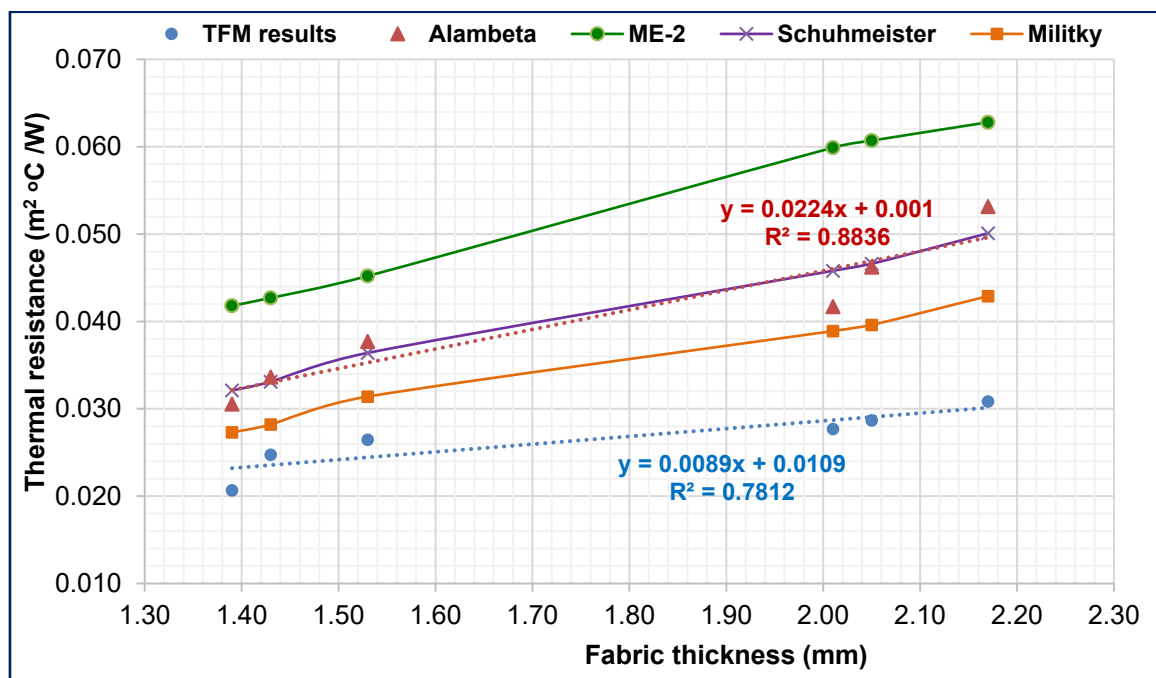


Figure 5.50. Experimental thermal resistance results for bandages by thermal foot manikin and ALAMBETA versus theoretical calculations by Maxwell-Eucken2, Schuhmeister and Militky models

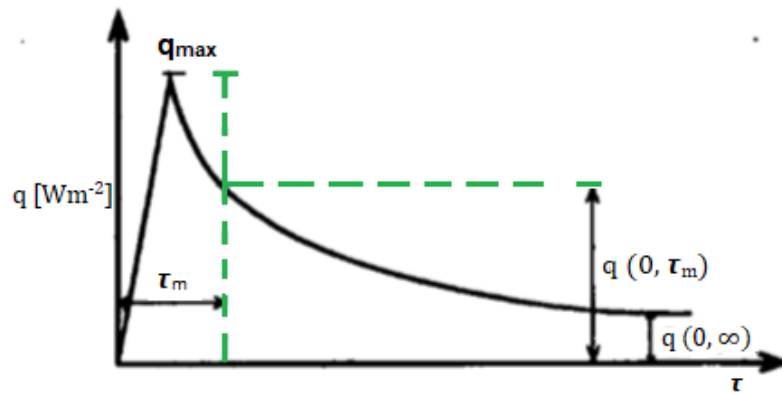


Figure 5.51. Time dependence heat flow after contact [163]

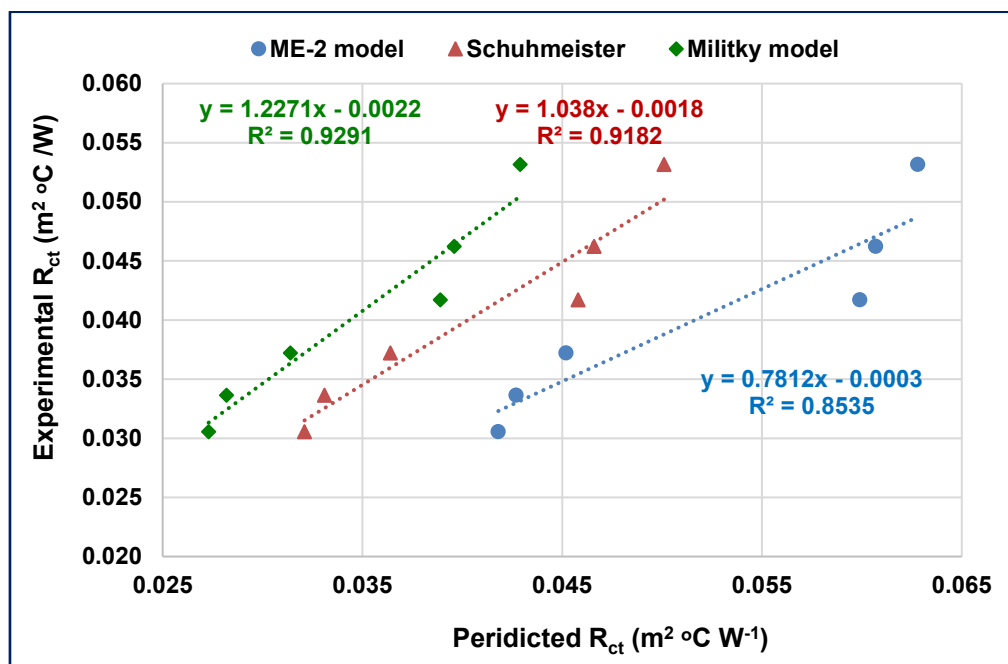


Figure 5.52. Experimental thermal resistance for bandages by ALAMBETA versus theoretical calculations by Maxwell-Eucken2, Schuhmeister and Militky models

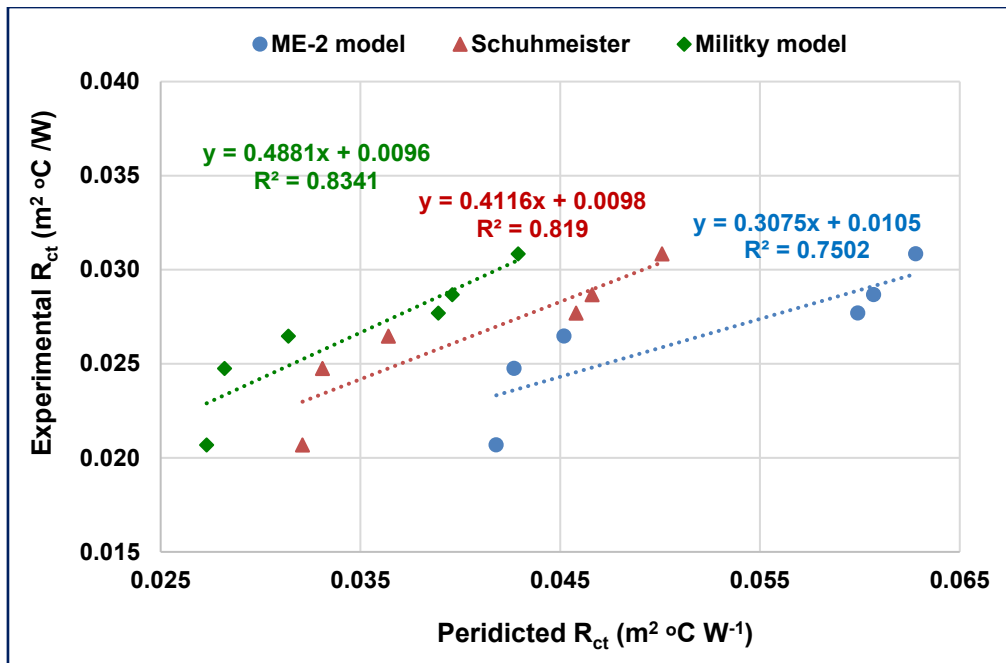


Figure 5.53. Experimental thermal resistance for bandages by thermal foot manikin versus theoretical calculations by Maxwell-Eucken2, Schuhmeister and Militky models

5.2.6.8 *Effect of bandage extension on water vapour resistance*

Water vapour permeability is the ability to transmit vapour out of the body, it can be calculated theoretically by equation (7). If the moisture resistance is too high to transmit heat, by the transport of mass and at the same time the thermal resistance of the textile layers considered by us is high, the stored heat in the body cannot be dissipated and causes an uncomfortable sensation [165]. Water vapour resistance was measured for all bandages using PERMETEST device at 0% extension, and 10 to 80% extension for two layers bandaging. Obtained results confirm that the R_{et} is decreasing when the bandage extension is increasing to 20% then it is improving till 60%, then it is significantly decreasing at 80% extension, as illustrated in Figure 5.54. However the testing on PERMETEST is fast, easy, and non-destructive test, but it is not exactly simulating the required testing method of R_{et} for CBs as compared to TFM in which case the compression influence and air layer between each two adjacent bandage layers are more significant factors.

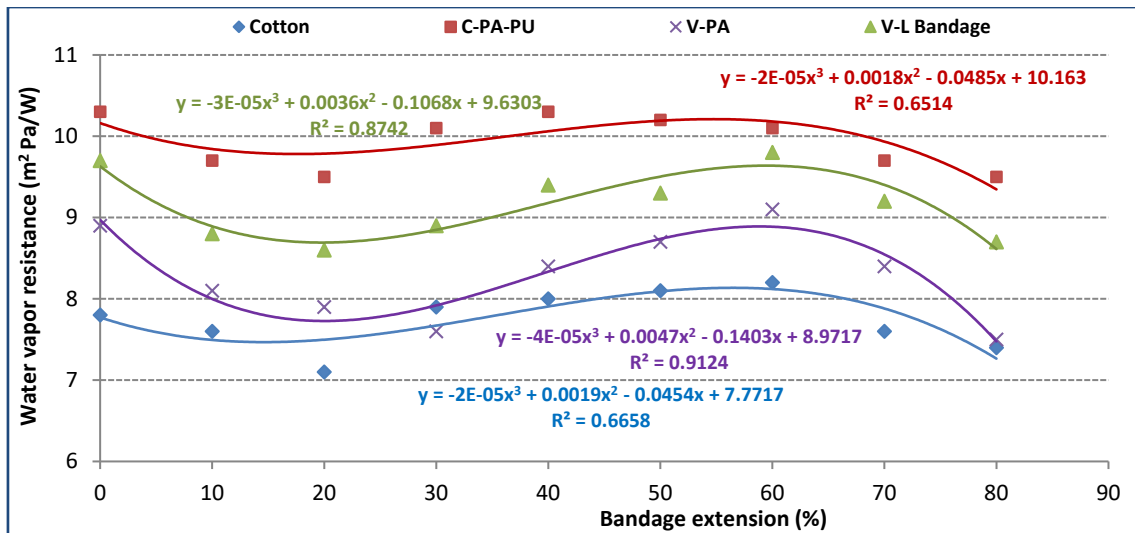


Figure 5.54. Effect of bandage extension on water vapour resistance

5.2.6.9 Effect of bandage extension on air permeability

Air permeability test was performed for all bandage samples at initial porosity of 0% extension and 10 up to 100% extension using two layers for testing. The obtained results confirmed that the air permeability values of all CBs are significantly improves when increasing the bandage extension at range 0% to 100%. Figures 5.55 emphasizes that VI-PA bandage has the highest air permeability due to higher porosity and lower areal density (83.34 g/m²) compared to other bandages, as previously illustrated in Figure 5.1.

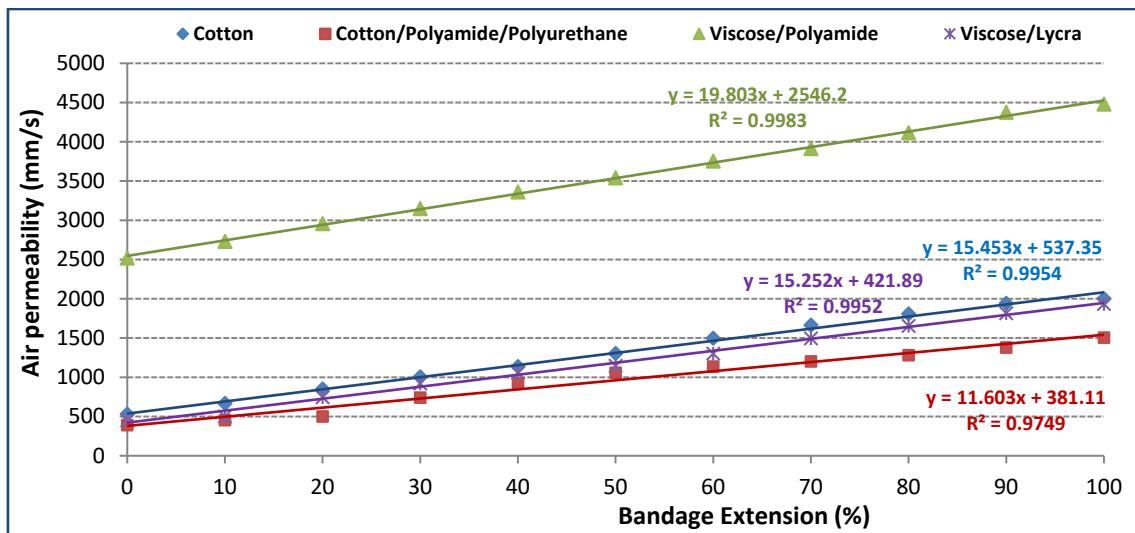


Figure 5.55. Effect of bandage extension on air permeability, two layers

5.2.7 Effect of compression bandages on the muscles' activation

5.2.7.1 Electromyography (EMG) test for Flexor Carpi (FC) muscle

Figure 5.56 illustrates the FC muscle voltage with and without wearing the VI-PA compression bandage during the standardized action (flexion-extension). The average muscle voltage with VI-PA WCB was 85.11 μV whereas without bandage 93.33 μV respectively. This concludes that wearing WCB decreases muscle activation by 8.81 %, as listed in Table 5.15.

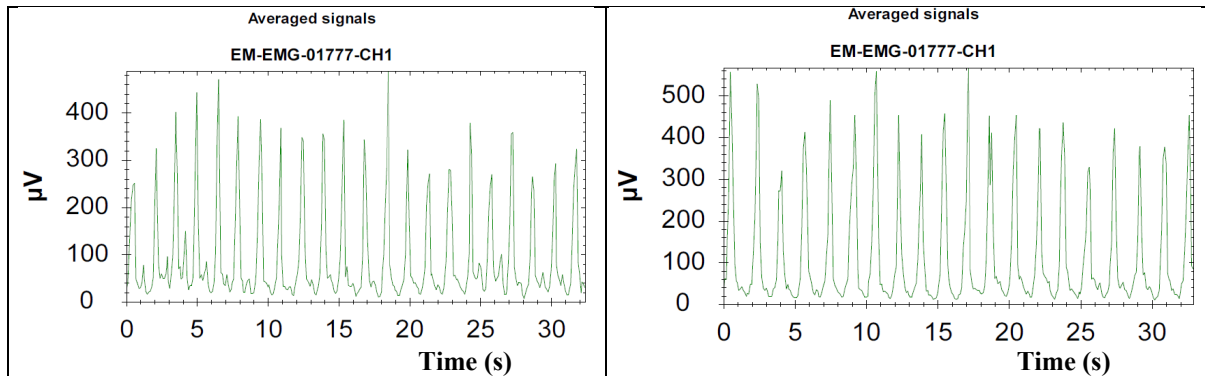


Figure 5.56. Flexor Carpi muscle voltage with and without WCB, (flexion-extension) action, 40 BPM.

Figure 5.57 shows the FC muscle voltage with and without wearing the VI-PA WCB during the action (squeezing a soft roll), the average EMG measured signal was 90.67 and 97.44 μV respectively (i.e. wearing WCB enables lower muscle activation by a percent 6.96 %), as illustrated in Table 5.16. The obtained results in Figures 5.56 & 5.57 confirm that wearing WCB enhances the FC Radialis muscle performance while performing the standardized protocol activities. The frequency of flexion and extension are similar and therefore, the effect of WCB focuses on a reduced muscle oscillation and improves muscle function and efficiency.

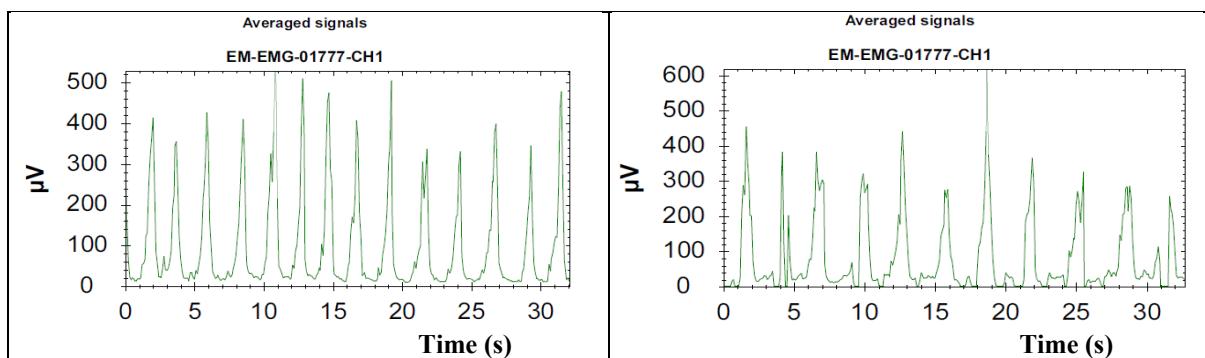


Figure 5.57. Flexor Carpi muscle voltage with and without VI-PA WCB, (squeezing a soft roll) action, 30 BPM.

5.2.7.2 EMG test of Medial Gastrocnemius (MG) muscle

Surface EMG signals were obtained from the MG and SO muscles by pre-amplified bipolar surface electrodes [166]. Figures 5.58 & 5.59 show MG muscle's performance with and without wearing the CO-PA-PU bandage during the standardized action (flexion-extension) and using the bleached Cotton bandage for walking action. Wearing WCB enables a significant decrease in MG muscle activity during flexion-extension action by 25.56% and 4.65% while walking, see Tables 5.17 and 5.18 respectively. This decrease may be due to the increase in the mean muscle fascicle length and the reduction in the mean muscle thickness and mean pennation angle [167]. Researchers have also claimed that the muscle force being exerted for a limb's motion and stability may be wasted on muscle flexion-extension, while compression garment may prevent muscle vibrations during sports activities which can enhance the athletic performance [97].

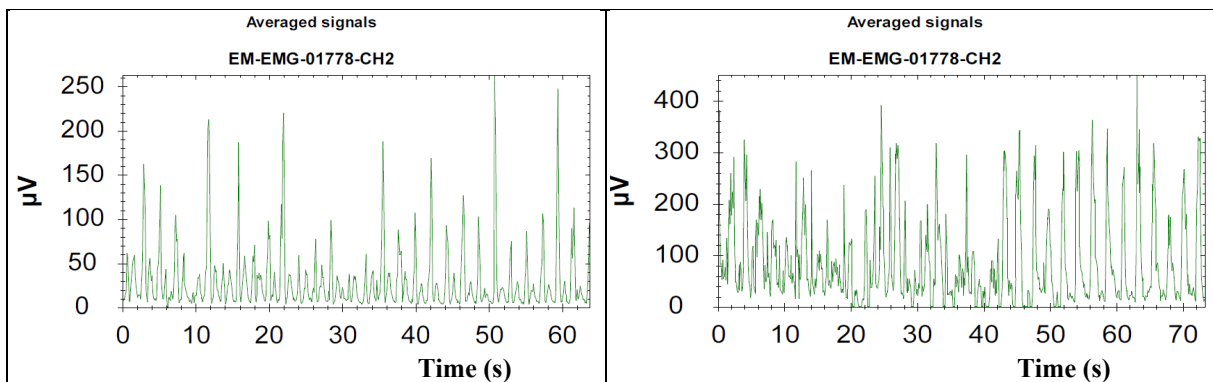


Figure 5.58. Medial Gastrocnemius muscle voltage with and without wearing CO-PA-PU bandage during (flexion-extension) action, 30 BPM.

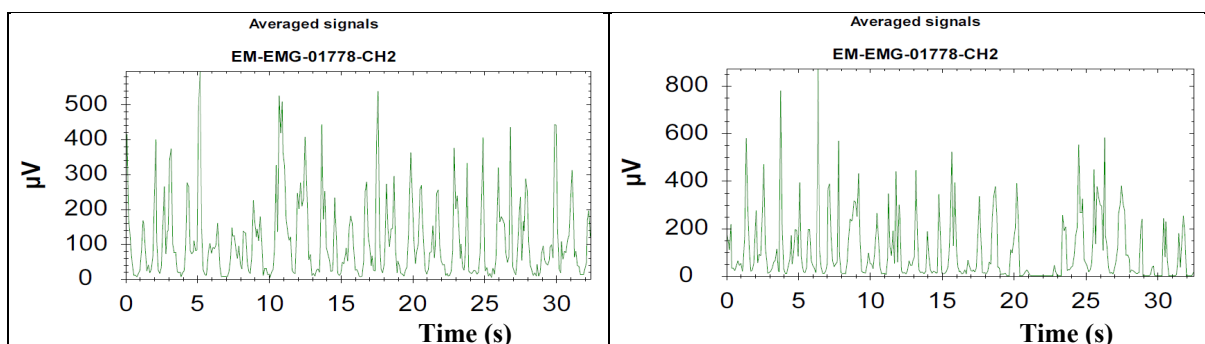


Figure 5.59. Medial Gastrocnemius muscle voltage with and without wearing bleached Cotton bandage while walking action, 40 BPM.

5.2.7.3 EMG test of Soleus (SO) muscle

Figures 5.60 & 5.61 show the SO muscle's behaviour with and without wearing the CO-PA-PU and bleached Cotton WCBs during the activities, flexion-extension and walking

respectively, at same speed (using metronome beats 20, 30, and 40 beats/min). Wearing WCB decreases SO muscle activity during flexion-extension action by a percent 22.68% and 33.86% while walking as summarized in Tables 5.17 & 5.16 respectively. These significant reductions in SO muscle activation clarify the enhancement of ankle muscle behaviour wearing WCB, because SO muscle is the main factor of controlling the walking performance while MG muscle is more effective for flexion-extension action.

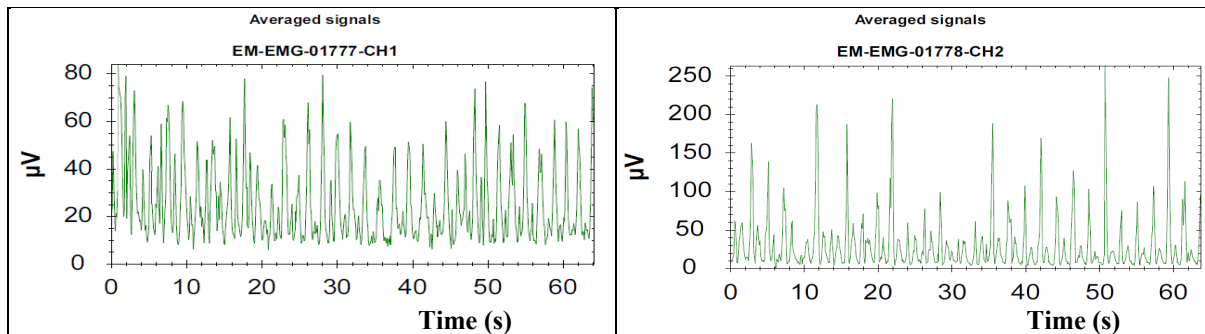


Figure 5.60. Soleus muscle voltage with and without wearing CO-PA-PU bandage during (flexion-extension) action, 30 BPM.

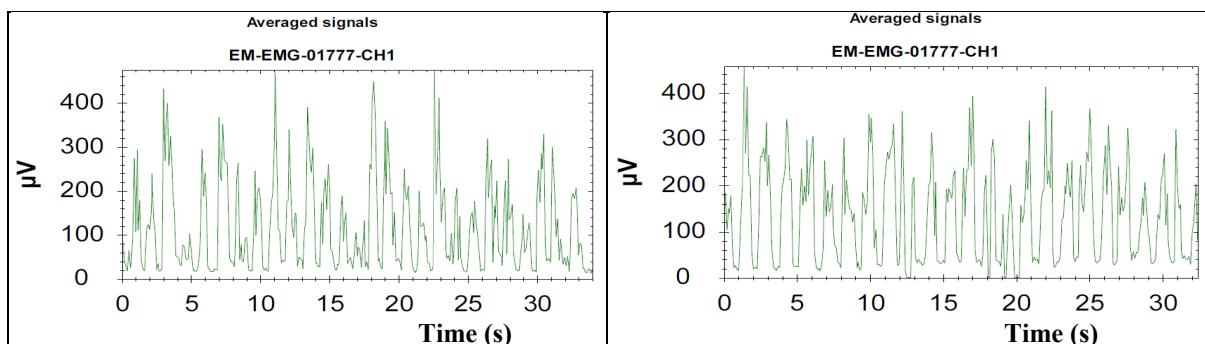


Figure 5.61. Soleus muscle voltage with and without wearing Cotton bandage while walking action, 40 BPM.

5.2.7.4 EMG mean voltage for FC, MG, and SO muscles

Emotion EMG system and Mega-win analysis were used to investigate the relationship between three types of WCBs and muscles activation. EMG mean voltage for FC muscle during standardized activities (squeezing a soft roll and flexion-extension) are illustrated as shown in Table 5.15. Average FC muscle voltages with and without wearing the VI-PA compression bandage were 90.67 and 97.44 μV respectively (i.e. wearing WCB decreases muscle activation by 6.96% during squeezing a soft roll action). Moreover using WCB decreases muscle voltage 8.81% during flexion-extension action.

Table 5.15. EMG mean voltage of the flexor carpi muscle's signals

Tested action	Metronome beats (BPM)	Mean voltage (μV)			Average 1 (μV)	Std. (μV)	
Squeezing a soft roll action	With bandage	20	77	72	76	75.00	2.16
		30	81	85	78	81.33	2.87
		40	110	116	121	115.67	4.50
		Average (Average 1)				90.67	3.17
	Without bandage	20	76	79	72	75.67	2.87
		30	93	97	104	98.00	4.55
		40	125	119	112	118.67	5.31
		Average (Average 1)				97.44	4.24
Flexion-extension action	With bandage	20	74	83	78	78.33	3.68
		30	85	80	87	84.00	2.94
		40	93	88	98	93.00	4.08
		Average (Average 1)				85.11	3.57
	Without bandage	20	81	85	77	81.00	3.27
		30	90	86	78	84.67	4.99
		40	115	106	122	114.33	6.55
		Average (Average 1)				93.33	4.93

EMG mean voltage for MG and SO muscles using the CO-PA-PU and bleached Cotton WCBs during the standardized activities (flexion-extension and walking) at the same speed (using metronome beats 20, 30, and 40 beats/min) can be summarized and compared as listed below in [Tables 5.16 and 5.17](#). Wearing bleached Cotton WCB while walking was associated with a decrease in average MG and SO muscles activation by a percent 10.66 and 18.24% respectively, see [Table 5.16](#). Whereas using CO-PA-PU WCB decreases MG and SO muscles activation by a percent 4.65 and 33.86% respectively. While wearing CO-PA-PU bandage during flexion-extension action decreases MG and SO muscles activation by a percent 25.56 and 22.68% respectively, see [Table 5.17](#).

Table 5.16. EMG mean voltage for leg muscles while walking (bleached Cotton bandage)

Case	Metronome beats (BPM)	Medial Gastrocnemius		Soleus Muscle	
		Mean voltage (μV)	Standard deviation	Mean voltage (μV)	Standard deviation
With bandage	20	75.33	2.87	74.00	2.94
	30	76.00	4.32	88.00	3.74
	40	103.00	6.98	117.33	4.99
	Average	84.78	4.59	93.11	3.97
Without bandage	20	80.33	3.30	96.00	5.35
	30	94.00	4.55	111.33	5.44
	40	110.33	7.04	134.33	7.04
	Average	94.89	4.96	113.89	5.94

Table 5.17. EMG mean voltage for leg muscles using CO-PA-PU WCB

Activity	Case	Medial Gastrocnemius		Soleus Muscle	
		Mean voltage (μV)	Standard deviation	Mean voltage (μV)	Standard deviation
Flexion – extension	with bandage	22.33	2.49	25.00	2.94
	without	30.00	3.74	32.33	4.92
	Reduction %	25.56	33.33	22.68	40.18
While walking	with bandage	82.00	4.55	83.33	4.11
	without	86.00	5.35	126.00	6.98
	Reduction %	4.65	15.09	33.86	41.09

5.2.7.5 Data analysis using Matlab software

The RMS value for each muscle's activation is calculated using Matlab software to clarify and compare the differences between different standardized actions for hand and leg muscles as shown in Tables 5.18 to 5.21. RMS values of the FC muscle using the Viscose-Polyamide bandage are illustrated in Table 5.18. Wearing VI-PA bandage was associated with lower muscle activation by a percent of 8.42 % for FC muscle during the standardized activity (squeezing a soft roll) and 14.82% during (flexion-extension action).

Table 5.18. RMS values for Flexor Carpi muscle signals

Tested action	Metronome beats (BPM)	RMS value			Average 1	Std.	
Squeezing a soft roll action	With bandage	20	136.98	139.8	133.7	136.83	2.49
		30	161.78	155	165.9	160.89	4.49
		40	185.7	180.43	173.78	179.97	4.88
	Average (Average 1)					159.23	3.95
	Without bandage	20	135.8	132.1	128.8	132.23	2.86
		30	179.7	189.11	198.4	189.07	7.63
		40	210.9	200.4	189.7	200.33	8.65
Average (Average 1)					173.88	6.38	
Flexion-extension action	With bandage	20	123.68	127.86	131.57	127.70	3.22
		30	132.36	125.68	138.87	132.30	5.38
		40	164.72	155.97	173.74	164.81	7.25
		Average (Average 1)					141.61
	Without bandage	20	152.45	147.7	143.21	147.79	3.77
		30	164.15	155.44	146.87	155.49	7.05
		40	195.46	184.27	206.67	195.47	9.14
Average (Average 1)					166.25	6.66	

Table 5.19. ANOVA for Tables 5.15 & 5.18 (Flexor carpi muscle signals)

Standardized Action	Dependent Variable	Sig.* (with or without bandage)	Sig.* (Metronome beats)
Squeezing a soft roll	Mean voltage	0.048	0.000
	RMS values	0.019	0.000
Flexion-extension	Mean voltage	0.045	0.000
	RMS values	0.000	0.000

* Significance at confidence interval 95 %

Table 5.20 concludes the RMS values for the human leg muscles' signals using the bleached Cotton bandage while walking. Wearing WCB was associated with a reduction of muscle activation as assured by lower RMS values for MG and SO muscles as average value of the obtained results at metronome beats 20, 30, and 40 beats/min.

Wearing CO-PA-PU CB decreases muscle activation -as confirmed by lower RMS values- by percentages of 19.86 and 14.36% for MG and SO muscles respectively during flexion-extension action, and a percent reduction of RMS values as 5.72 and 22.48 % for MG and SO muscles while walking action. The enhancement of muscles' performance wearing WCB may be due to a small increase in intramuscular pressure and in conjunction with the proposed reduction in muscle vibration [168].

Table 5.20. RMS values for MG and SO muscles' signals while walking (Cotton bandage)

Case	Metronome beats (BPM)	Medial Gastrocnemius		Soleus Muscle	
		RMS value	Standard deviation	RMS value	Standard deviation
With bandage	20	137.68	6.09	151.66	4.83
	30	147.46	6.19	145.98	6.79
	40	183.30	7.23	191.58	11.09
	Average	156.15	6.50	178.03	6.75
Without bandage	20	165.56	5.03	165.92	6.98
	30	181.48	9.21	205.65	9.50
	40	191.11	11.13	236.46	8.63
	Average	166.11	7.34	202.68	8.37

Table 5.21. ANOVA for Tables 5.16 & 5.20 (EMG mean voltage for leg muscles while walking)

Tested muscle	Dependent Variable	Sig.* (with or without bandage)	Sig.* (Metronome beats)
Medial Gastrocnemius	Mean voltage	0.011	0.000
	RMS values	0.000	0.000
Soleus	Mean voltage	0.000	0.000
	RMS values	0.000	0.000

* Significance at confidence interval 95 %

6. Chapter 6: Evaluation of Results and New Findings

The evaluation of the used plied warp yarns in the market for producing the WCB concluded that the warp yarn tenacity should be greater than 15.5 cN/Tex and its extension should be at least 12% to produce the highly stretched 100% Cotton WCB. The optimum twist of warp yarns was ranged 1800 - 2200 tpm for producing high extension Cotton WCBs.

Silver NPs coated yarn samples D₁ and D₂ showed a comparable antibacterial activity on both tested bacteria strains (E.C. and S.A.) using both quantitative and qualitative test methods. The NPs size and its distribution using SEM and EDX confirmed the antibacterial activity of the treated single and plied yarn samples. Moreover the new produced WCB structure were treated with Zinc Oxide NPs in powder form in addition to 15 g/L binder and had positive results of antibacterial activity for both gram-positive and gram-negative bacteria strains according to AATCC 147-2012 and AATCC 100-2019.

Candidate work introduced some modifications on the WCB structure. The bandage includes an integrated tension sensor, which causes a change in the spacing of coloured threads during its deformation. The solution is sensors in the bandage in the form of a different colour pick from the other structure of the bandage. Different colour picks with regular distance become visible due to deformation / stress in the bandage. These coloured weft threads are giving blue marks (rectangles of 2x1 cm² could be changed to squares of 2x2 cm² at 100% extension). Then presented a new method to predict the bandage tension as a function of bandage porosity; that enables the patient to use the bandage himself more easily and accurate. Long-stretch CO-PA-PU required 110% extension while short-stretch cotton WCB required only 60% extension to achieve the required mean bandage tension 10N; these values are achieving the required bandage pressure (4000 Pa or 30 mmHg) according to Laplace's law equation.

Picopress results confirmed that 100% Cotton bandages achieved the highest compression ranges (18-33, 27-43, and 36-61 mmHg) for ankle position and (8-16, 18-27, and 35-51 mmHg) for mid-calf position. Cotton SSB can be applied for severe leg ulcers and oedema cases that need high pressure ranges 50 to 70 mmHg depending on bandage extension and number of layers.

The experimental compression results were compared with theoretical pressure calculated by Laplace's equation. There is a significant deviation when applying Laplace's

equation for two and three layers bandaging ranging ± 0.68 to $\pm 15.64\%$ whereas Jawad Al Khaburi developed that equation to include the thickness and limb circumference due to multilayer bandaging; this modified equation decreased the deviation ranges to be ± 0.07 to $\pm 12.55\%$ at ankle position.

CO-PA-PU and 100% Cotton WCBs were selected to compare between long and short-stretch WCBs in resting and working actions. The SSB enabled higher working pressure on the ankle and calf muscles due to the interaction between lower leg and WCB during walking action or any activity. On the contrary LSB had a higher resting pressure because of the elastane filaments, as a result the patient should wear-off the LSB every day before sleep. Cyclic loading-unloading test confirmed that short-stretch WCB lost approximately 28.6% of its activity whereas LSB lost only 10.05% after 5 days of application.

Four types of WCBs were used for evaluating the R_{ct} and R_{et} on the TFM, ALAMBETA, and PERMETEST devices respectively using two and three layers bandaging techniques. According to TFM, R_{ct} values significantly decreased when the bandage extension increased from 10 to 40 % due to the decrease of fabric thickness, then R_{ct} slightly increased from 40 to 60% extension that might be caused by the higher porosity of WCBs (0.364, 0.306, 0.471, and 0.325 for 100% Cotton, CO-PA-PU, VI-PA, and VI-PU WCBs respectively). After that R_{ct} values decreased, especially at 80% extension due to the lower bandage thickness and higher applied tension. The PERMETEST results concluded that the R_{et} values decreased the extension increased to 20% then it was slightly increasing at 20 to 60%, after that decreased, especially at 80% extension due to the lower total bandage thickness and the little amount of trapped air between fabric layers.

The experimental results of R_{ct} by TFM and ALAMBETA were validated using Maxwell-Eucken2, Schuhmeister and Militky models. There were strong correlation between the Schuhmeister and Militky models with the ALAMBETA results. Obtained results of R_{ct} confirmed that clothed TFM was more accurate for measuring R_{ct0} and corresponding values of R_{ct} that might be due to the steady state condition and less effect of air convection. There were significant deviations between experimental results by the ALAMBETA and TFM because the high levels of applied tension during the bandage application were more effective on the TFM results.

The application of VI-PA WCB on hand muscles reduced the average FC muscle activation by a percent 7.17 and 8.92% during the standardized actions (squeezing a soft roll

and flexion-extension) respectively. Wearing bleached Cotton WCB enabled lower muscle activation and higher median frequency for MG and SO muscles by a percent of 4.65 and 34.13% during walking action. Using CO-PA-PU CB was associated with significantly reduction of MG and SO muscles activation by 26.67 and 21.88% during flexion-extension action. The obtained RMS values using Matlab software confirmed that wearing WCB improved the performance of FC, MG, and SO muscles and could enhance muscles' fatigue.

7. Chapter 7: References

- [1] Partsch, H., Clark, M., Mosti, G., Steinlechner, E., Schuren, J. A. N., Abel, M., ... & Hutchinson, J. (2008). Classification of compression bandages: practical aspects. *Dermatologic surgery*, **34(5)**, 600-609.
- [2] Franks, P. J., Barker, J., Collier, M., Gethin, G., Haesler, E., Jawien, A., ... & Weller, C. (2016). Management of patients with venous leg ulcers: challenges and current best practice. *Journal of wound care*, **25(Sup6)**, S1-S67.
- [3] Shubhangi, V. A. (2013). Review Article, Chronic Leg Ulcers: Epidemiology, Aetiopathogenesis, and Management. *Hindawi Publishing Corporation*, 2013 Ulcers, Article ID 413604. <http://dx.doi.org/10.1155/2013/413604>
- [4] Fletcher, J., Moffatt, C., Partsch, H., Vowden, K., & Vowden, P. (2013). Principles of compression in venous disease: a practitioner's guide to treatment and prevention of venous leg ulcers. *Wounds International*. Available: www.woundsinternational.com
- [5] Lohmann & Rauscher USA. 19 March 2019. Available: <https://www.lohmann-rauscher.com/us-en/products/compression-therapy/bandages/short-stretch-bandages/rosidal-tcs/>
- [6] Kumar, B., Das, A., & Alagirusamy, R. (2012). Analysis of sub-bandage pressure of compression bandages during exercise. *Journal of tissue viability*, **21(4)**, 115-124.
- [7] Halfaoui, R., & Chemani, B. (2016). New approach to predict pressure produced by elastic textile in the therapeutic treatment of venous leg. *Journal of Fundamental and Applied Sciences*, **8(2)**, 297-312.
- [8] Al Khaburi, J., Dehghani-Sanij, A. A., Nelson, E. A., & Hutchinson, J. (2012). Effect of bandage thickness on interface pressure applied by compression bandages. *Medical engineering & physics*, **34(3)**, 378-385.
- [9] Schuren, J., & Mohr, K. (2008). The efficacy of Laplace's equation in calculating bandage pressure in venous leg ulcers. *Wounds Uk*, **4(2)**, 38.
- [10] Rimaud, D., Convert, R., & Calmels, P. (2014). In vivo measurement of compression bandage interface pressures: the first study. *Annals of physical and rehabilitation medicine*, **57(6-7)**, 394-408.
- [11] Tubular bandage. February 14, 2019. Available: <https://katymedsolutions.com/products/lohmann-rauscher-tg-tubular-bandage-3-2-7x22-yds-size-9-beige-each.html>
- [12] Comprilan Stretch Bandage. February 14, 2019. Available: <https://airfreshener.club/quotes/comprilan-stretch-bandage.html>
- [13] Wang, P., Li, L., Yan, M. D., & Ru, F. (2014). Effects of compression garments on lower limb muscle activation via electromyography analysis during running. *Journal of Donghua University*, **32(1)**, 48-52.

- [14] Miyamoto, N., Hirata, K., Mitsukawa, N., Yanai, T., & Kawakami, Y. (2011). Effect of pressure intensity of graduated elastic compression stocking on muscle fatigue following calf-raise exercise. *Journal of Electromyography and Kinesiology*, **21(2)**, 249-254.
- [15] Goto, K., Mizuno, S., & Mori, A. (2017). Efficacy of wearing compression garments during post-exercise period after two repeated bouts of strenuous exercise: a randomized crossover design in healthy, active males. *Sports medicine-open*, **3(1)**, 1-10.
- [16] Martorelli, S. S., Martorelli, A. S., Pereira, M. C., Rocha-Junior, V. A., Tan, J. G., Alvarenga, J. G., ... & Bottaro, M. (2015). Graduated compression sleeves: effects on metabolic removal and neuromuscular performance. *The Journal of Strength & Conditioning Research*, **29(5)**, 1273-1278.
- [17] Al Khaburi, J., Dehghani-Sani, A. A., Nelson, E. A., & Hutchinson, J. (2011). The effect of multi-layer bandage on the interface pressure applied by compression bandages. *World Academy of Science, Engineering and Technology, International Journal of Mechanical, Aerospace, Industrial, Mechatronic and Manufacturing Engineering*, **5**, 1169-1174.
- [18] Erickson, C. A., et al. (1995). Healing of venous ulcers in an ambulatory care program: the roles of chronic venous insufficiency and patient compliance. *Journal of vascular surgery*, **22(5)**, 629-636.
- [19] February 15, 2020. <https://images.app.goo.gl/4gpoSykvAwcZepbF9>. Modulyss® Compression Support Open toe Ankle Length Socks for Workout and injuries Protection.
- [20] February 15, 2020. <https://bodyofhealthandlife.com/lymphedema-wrapping/>
- [21] British Standard. The elastic properties of flat, non-adhesive, extensible fabric bandages. BS 705 1995. London: BSI-British Standards Institution; 1995.
- [22] Aboalasaad, A. R. R., & Sirková, B. K. (2019). Analysis and prediction of woven compression bandages properties. *The Journal of The Textile Institute*, **110(7)**, 1085-1091.
- [23] Kaur, B. (2018). Bandages: Short-Stretch vs Long-Stretch. [Online]. JUNE 25, 2018.
- [24] De Carvalho, M. R., & de Oliveira, B. G. (2017). Compression therapy for venous leg ulcers: a systematic review of the literature. *Enfermería Global*, **16(1)**, 574-593.
- [25] Nair, B. (2014). Compression therapy for venous leg ulcers. *Indian dermatology online journal*, **5(3)**, 378-382.
- [26] Caprini, J. A., Partsch, H., & Simman, R. (2012). Venous Ulcers. *Journal of the American College of Clinical Wound Specialists*, **4(3)**, 54-60.
- [27] O'donnell, T. F., et al. (2014). Management of venous leg ulcers: Clinical practice guidelines of the Society for Vascular Surgery® and the American Venous Forum. . *Journal of vascular surgery*, **60(2)**, 3S-59S.
- [28] Aboalasaad, A. R. R., & Sirková, B. K. (2017). Analysis and prediction of compression bandages tension. Ph. D. Students Day, 6. Liberec, Czech Republic.
- [29] Sikka, M. P., Ghosh, S., & Mukhopadhyay, A. (2014). The structural configuration and stretch property relationship of high stretch bandage fabric. *Fibres and Polymers*, **15(8)**, 1779-1785.

- [30] Smith, B., & Waters, B. (1985). Extending applicable ranges of regression equations for yarn strength forecasting. *Textile Research Journal*, **55(12)**, 713-717.
- [31] Malik, Z. A. (2011). *Relationship Between Tensile Strength Of Yarn And Woven Fabric* (Doctoral dissertation, Mehran University of Engineering & Technology Jamshoro).
- [32] Essam, J. M. (1928). 4—THE PHYSICAL PROPERTIES OF FABRICS: THE EFFECTS OF YARN AND WEAVING STRUCTURE. PART I. *Journal of the Textile Institute Transactions*, **19(2)**, T37-T58.
- [33] Chattopadhyay, R. (2008). Design of Apparel Fabrics: Role of fibre, yarn and fabric parameters on its functional attributes. *Journal of Textile Engineering*, **54(6)**, 179-190.
- [34] Taylor, H. M. (1959). 9—Tensile and tearing strength of cotton cloths. *Journal of the Textile Institute Transactions*, **50(1)**, T161-T188.
- [35] Seo, M. H., Realf, M. L., Pan, N., Boyce, M., Schwartz, P., & Backer, S. (1993). Mechanical properties of fabric woven from yarns produced by different spinning technologies: Yarn failure in woven fabric. *Textile research journal*, **63(3)**, 123-134.
- [36] Kumar, B., Das, A., & Alagirusamy, R. (2013). Study on interface pressure generated by a bandage using in vitro pressure measurement system. *The Journal of the Textile Institute*, **104(12)**, 1374-1383.
- [37] Ruckley C. V, Evans C. J, Allan P. L, et al. Chronic venous insufficiency, Clinical and duplex correlations. The Edinburgh Vein Study of venous disorders in the general population. *Journal of Vascular Surgery*, 2002, **36(3)**, 520-525.
- [38] Mozes G, Gloviczki P. Venous embryology and anatomy. In J.J. Bergan, editor, *The Vein Book*, 2007 Elsevier Academic Press, San Diego, CA, pages 15-25.
- [39] Blair, STD., Wright, D. D., Backhouse, C. M., Riddle, E., & McCollum, C. N. (1988). Sustained compression and healing of chronic venous ulcers. *British Medical Journal*, **297(6657)**, 1159-1161.
- [40] Valencia, I. C., Falabella, A., Kirsner, R. S., & Eaglstein, W. H. (2001). Chronic venous insufficiency and venous leg ulceration. *Journal of the American Academy of Dermatology*, **44(3)**, 401-424.
- [41] Dolibog, P., Franek, A., Taradaj, J., Dolibog, P., Blaszcak, E., Polak, A., ... & Kolanko, M. (2014). A comparative clinical study on five types of compression therapy in patients with venous leg ulcers. *International journal of medical sciences*, **11(1)**, 34.
- [42] Huang, J. (2016). Review of heat and water vapour transfer through multilayer fabrics. *Textile Research Journal*, **86(3)**, 325-336
- [43] Ghosh, A., Mal, P., Majumdar, A., & Banerjee, D. (2017). An investigation on air and thermal transmission through knitted fabric structures using the Taguchi method. *Autex Research Journal*, **17(2)**, 152-163. DOI: 10.1515/aut-2016-0009
- [44] Qian, X., Fan, J. (2009). A quasi-physical model for predicting the thermal insulation and moisture vapour resistance of clothing. *Applied ergonomics*, **40(4)**, 577-590.

- [45] SALOPEK, C. I., Skenderi, Z. (2010). Approach to the Prediction of Thermophysiological Comfort, Chapter 09 in DAAAM International Scientific Book 2010, pp. 081-088, B. Katalinic (Ed.). DOI: 10.2507/daaam.scibook.2010.09
- [46] O'Callaghan, P. W., & Probert, STD. (1977). Thermal resistance behaviour of single and multiple layers of clothing fabrics under mechanical load. *Applied Energy*, **3(1)**, 3-12.
- [47] Karunamoorthy, S., & Das, A. (2014). Study on thermal resistance of multilayered fabrics under different compressional loads. *The Journal of The Textile Institute*, **105(5)**, 538-546.
- [48] Abdel-Rehim, Z. S., Saad, M. M., El-Shakankery, M., & Hanafy, I. (2006). Textile fabrics as thermal insulators. *AUTEX Research Journal*, **6(3)**, 148-161.
- [49] Hsu, W. C., Tseng, L. W., Chen, F. C., Wang, L. C., Yang, W. W., Lin, Y. J., & Liu, C. (2017). Effects of compression garments on surface EMG and physiological responses during and after distance running. *Journal of Sport and Health Science*.
- [50] Massó, N., Rey, F., Romero, D., Gual, G., Costa, L., & Germán, A. (2010). Surface electromyography applications in the sport. *Apunts Med Esport*, **45(165)**, 121-130.
- [51] Neckář, B. (1990). Yarn – Forming, structure and properties. SNTL Prague (Prague).
- [52] Hearle, J. W. S., Grosberg, P. and Backer, S. (1969). Structural Mechanics of Fibres, Yarns and Fabrics. Wiley-Inter science (New York).
- [53] Neckar, B. (2014). Weaves Structure and Properties. Lectures. Retrieved June, 25, 2016. Web site: <http://www.ktt.tul.cz/>.
- [54] Mertová, I., Moučková, E., Neckář, B., & Vyšanská, M. (2018). Influence of Twist on Selected Properties of Multifilament Yarn. *Autex Research Journal*, **18(2)**, 110-120.
- [55] Goswami, B. C., Martindale, J. G., & Scardino, F. L. (1977). Textile yarns; Technology, structure, and applications. *John Wiley & Sons*, New York, 1977, p. 183.
- [56] Pan, N. (1992). Development of a constitutive theory for short fibre yarns: Mechanics of staple yarn without slippage effect. *Textile research journal*, **62(12)**, 749-765.
- [57] Moučková, E., Mertová, I., Hajsá, Š., & Vyšanská, M. 2018. Behavior of Two and Three-Fold Twisted Multifilament Yarns. *Fibres and Textiles (4)*, 51-60.
- [58] Abbasi, S. A., Peerzada, M. H., & Jhatial, R. A. (2012). Characterization of low twist yarn: Effect of twist on physical and mechanical properties. *Mehran University Research Journal of Engineering & Technology*, **31(3)**, 553-558.
- [59] Sreenivasan, K., & Shankaranarayana, K. S. (1961). Twist and tension as factors in yarn characteristics. *Textile research journal*, **31(8)**, 746-753.
- [60] Kotb, N. A. (2012). Predicting yarn quality performance based on fibres types and yarn structure. *Life Science Journal*, **9(3)**, 1009-1015.
- [61] Altas, S., & Kadoğlu, H. (2012). Comparison of conventional ring, mechanical compact and pneumatic compact yarn spinning systems. *Journal of Engineered Fibres and Fabrics*, **7(1)**, 155892501200700110.

- [62] Żurek, W. (1975). The structure of yarn. *Foreign Scientific Publications Department of the National Center for Scientific*, **73(54014)**, Technical and Economic Information. Warsaw, Poland, 1975.
- [63] Carnaby, G. A., Postle, R., & de Jong, S. (1988). *Mechanics of Wool Structures*. John Willy & Sons, New York, 1988.
- [64] Langenhove, L. V. (1997). Simulating the Mechanical Properties of a Yarn Based on the Properties and Arrangement of its Fibres, Part I: The Finite Element Model. *Textile Research Journal*, **67**,263-268.
- [65] Gegauff, M. C. (1907). Strength and elasticity of cotton threads. *Bull. Soc. Ind. Mulhouse*, **77**, 153-176.
- [66] Gurney, H. P. (1925). The distribution of stresses in cotton products. *Journal of the Textile Institute Transactions*, **16(9)**, T269-T289.
- [67] Ghosh, A., Ishtiaque, S., Rengasamy, S., Mal, P., & Patnaik, A. (2005). Predictive models for strength of spun yarns: An overview. *AUTEX Research journal*, **5(1)**, 20-29.
- [68] Neckář, B., & Das, D. (2017). Tensile behavior of staple fibre yarns part I: theoretical models. *The Journal of The Textile Institute*, **108(6)**, 922-930.
- [69] Johannsen, O. (1930). *Handbook of cotton spinning, weaving and factory equipment (Vol. 1)*. Leipzig: Verlag von B. F. Voigt (in German).
- [70] Platt, M. M. (1950). Mechanics of Elastic Performance of Textile Materials: Part IV: Some Aspects of Stress Analysis of Textile Structures—Staple—Fibre Yarns. *Textile Research Journal*, **20(8)**, 519-538.
- [71] Hearle, J. W. S. (1965). Theoretical analysis of the mechanics of twisted staple fibre yarns. *Textile Research Journal*, **35(12)**, 1060-1071.
- [72] M. Zubair. [Thesis] 2017. Tensile Behavior of Staple Spun Yarn. Technical University of Liberec. Liberec, Czech Republic.
- [73] Mehmood, N., Hariz, A., Templeton, S., & Voelcker, N. H. (2014). An improved flexible telemetry system to autonomously monitor sub-bandage pressure and wound moisture. *Sensors*, **14(11)**, 21770-21790.
- [74] Maqsood, M., Hussain, T., Malik, M. H., & Nawab, Y. (2016). Modelling the effect of elastane linear density, fabric thread density, and weave float on the stretch, recovery, and compression properties of bi-stretch woven fabrics for compression garments. *The Journal of The Textile Institute*, **107(3)**, 307-315.
- [75] ASTM 2256 Standard Test Method for Tensile Properties of Yarns by the Single-Strand Method, 2002.
- [76] Samadi, N., Hosseini, S. V., Fazeli, A., & Fazeli, M. R. (2010). Synthesis and antimicrobial effects of silver nanoparticles produced by chemical reduction method. *DARU Journal of Pharmaceutical Sciences*, **18(3)**, 168.

- [77] AATCC Test Method 147. Antibacterial activity assessment of textile materials: parallel streak method. In: AATCC technical manual, American Association of Textile Chemists and Colorists, Durham, North Carolina, USA, 2011.
- [78] AATCC Test Method 100-2004. (2005). Antibacterial finishes on textile materials: Assessment of. *AATCC Technical Manual, American Association of Textile Chemists and Colorists*, Research Triangle Park, NC.
- [79] Emam, H. E., Mowafi, S., Mashaly, H. M., & Rehan, M. (2014). Production of antibacterial colored viscose fibres using in situ prepared spherical Ag nanoparticles. *Carbohydrate polymers*, **110**, 148-155.
- [80] Emam, H. E., Manian, A. P., Široká, B., Duelli, H., Redl, B., Pipal, A., & Bechtold, T. (2013). Treatments to impart antimicrobial activity to clothing and household cellulosic-textiles—why “Nano”-silver?. *Journal of Cleaner Production*, **39**, 17-23.
- [81] Hebeish A. A., El-Rafie M. H., Abdel-Mohdy F. A., et al. (2010). Carboxymethyl cellulose for green synthesis and stabilization of silver nanoparticles. *Carbohydrate Polymers*, **82**, 933–941.
- [82] El-Rafie M. H., Ahmed H. B., Zahran M. K. (2014). Characterization of nanosilver coated Cotton fabrics and evaluation of its antibacterial efficacy. *Carbohydrate polymers*, **107**, 174-181.
- [83] Zahran M. K., Ahmed H. B., El-Rafie M. H. (2014a). Surface modification of Cotton fabrics for antibacterial application by coating with AgNPs-Alginate composite. *Carbohydrate polymers*, **108**, 145-152.
- [84] Zahran M. K., Ahmed H. B., El-Rafie, M. H. (2014c). Facile size regulated synthesis of silver nanoparticles using pectin. *Carbohydrate polymers*, **111**, 971–978.
- [85] Mallik K., Witcomb M. J., Scurell M. S. (2005). Redox catalytic property of gold nanoclusters: Evidence of an electron-relay effect. *Applied Physics A*, **80**, **4**, 797–801.
- [86] Kamat P. V. (2002). Photophysical, photochemical and photocatalytical aspects of metal nanoparticles. *Journal of Physical Chemistry B*, **106**, 7729–7744.
- [87] Liz-Marzan L. (2006). Tailoring surface plasmons through the morphology and assembly of metal nanoparticles. *Langmuir*, **22**, 32–41.
- [88] Cao Y. C., Jin R., Nam J., et al. (2003). Raman-dye-labeled nanoparticle probes for proteins. *Journal of American Chemical Society*, **125**, 14676–14677.
- [89] Shipway A. N., Lahav M., Willner I. (2000). Nanostructured gold colloid electrodes. *Advanced Materials*, **12**, **13**, 993–998.
- [90] M. H. El-Rafie, H. B. Ahmed, M. K. Zahran. (2014). Facile precursor for synthesis of silver nanoparticles using alkali treated maize starch. *International Scholarly Research Notices*, **Volume 2014**, Article ID 702396, 12 pages.
- [91] Hossam E. Emam, Avinash P. Manian, Barbora Široká, et al. (2014). Copper (I) oxide surface modified cellulose fibres— Synthesis, characterization and antimicrobial properties", *Surface and Coatings Technology*, **254**, 344–351.
- [92] Hossam E. Emam, Manal K. El-Bisi. (2014). Merely Ag nanoparticles using different cellulose fibres as removable reductant. *Cellulose*, **21**, 4219–4230.

- [93] ISO 13934-1:1999(E): Textiles -Tensile properties of fabrics- Part 1: Determination of maximum force and elongation at maximum force using the strip method.
- [94] Nareerut, J., Blažena, M., Jelka, G., & Shamsunder, B. S. (2017). THE INFLUENCE OF STRETCH FABRIC MECHANICAL PROPERTIES ON CLOTHING PRESSURE. *Vlákna a textil (Fibres and Textiles)*, Vol.24, Issue 2, 2017, ISSN 1335-0617, pp. 43-48.
- [95] Gvs14. (Sep. 2012). Anterior Forearm Muscles [Online]. Available: <https://anatomystudybuddy.wordpress.com/2012/09/20/flexor-carpi-radialis/>
- [96] Luqman. (May 02, 2017). Pearson Benjamin Cummings [Online]. Available: <https://humananatomyly.com/gastrocnemius-muscle/>
- [97] P. Wang, J. McLaren, K. F. Leong, et al. A Pilot study: evaluations of compression garment performance via muscle activation test. *Procedia Engineering* 2013, **60**, pp. 361-366.
- [98] Cram, J. R. (2011). Cram's introduction to surface electromyography. Jones & Bartlett Learning.
- [99] C. Gatti, D. L. Case, J. Langenderfer. (2008 February). Evaluation of three methods for determining EMG-muscle force parameter estimates for the shoulder muscles. *Clin Biomech (Bristol, Avon)*. **23(2)**, pp. 166–174.
- [100] Mekjavic I, Lenart B, Vrhovec M, et al. (2005). Static and Dynamic Evaluation of Biophysical Properties of Footwear: The Jozef Stefan Institute Sweating Thermal Foot Manikin System. In Prevention of Cold Injuries (pp. 6-1 – 6-8). Meeting Proceedings RTO-MP-HFM-126, Paper 6, 2005.
- [101] SENSORA INSTRUMENTS & CONSULTING, REG. No. 183 306 81, VAT No. CZ440128092 Na Výbežku 312, 460 15 LIBEREC, Czech Republic. <http://www.sensora.eu/PermetestManual09.pdf>
- [102] Bogusławska-Bączek, M., & Hes, L. (2013). Effective water vapour permeability of wet wool fabric and blended fabrics. *Fibres & Textiles in Eastern Europe*.
- [103] Hes, L. (2008). Non-destructive determination of comfort parameters during marketing of functional garments and clothing. *Indian Journal of Fibre and Textile Research*.
- [104] Hes L. Catalogues of the ALAMBETA and PERMETEST instruments, SENSORA Co., Czech Republic.
- [105] Havlová, M. (2014). Model of vertical porosity occurring in woven fabrics and its effect on air permeability. *Fibres & Textiles in Eastern Europe*, 22, **4(106)**: 58-63.
- [106] Air Permeability ASTM D737-96 Standard Test Method for Air Permeability of Textile Fabrics. www.astm.org.
- [107] Nilsson, H., & Holmér, I. (2000). Proceedings of the Third International Meeting on Thermal Manikin Testing, *3IMM, at the National Institute for Working Life, October 12-13, 1999*. www.niwl.se/ah/nr2000:4
- [108] SALOPEK, C. I., Skenderi, Z. (2010). Approach to the Prediction of Thermophysiological Comfort, Chapter 09 in DAAAM International Scientific Book 2010, pp. 081-088, B. Katalinic (Ed.). DOI: 10.2507/daaam.scibook.2010.09

- [109] Elnashar, E. A. (2005). Volume porosity and permeability in double-layer woven fabrics. *AUTEX Research Journal*, **5(4)**, 207-217.
- [110] Cay, A., Atrav, R., & Duran, K. (2007). Effects of warp-weft density variation and fabric porosity of the Cotton fabrics on their colour in reactive dyeing. *Fibres & Textiles in Eastern Europe*, **1(60)**, 91-94.
- [111] Rashid, A., & Hani, A. (2013). Analysis of woven natural fibre fabrics prepared using self-designed handloom. *International Journal of Automotive and Mechanical Engineering*. DOI: 10.15282/ijame.8.2013.10.0098
- [112] Gooijer, H. (1998). *Flow resistance of textile materials*, 1998.
- [113] Szosland, J., Babska, A., & Gasiorowska, E. (1999). Air-penetrability of woven multi-layer composite textiles. *Fibres & Textiles in Eastern Europe*, **7(1)**, 34-37.
- [114] Gee, N. C. (1953). Cloth setting and setting theories. *Textile Manu*, **80**, 381-384.
- [115] Peirce, F. T., & Womersley, J. R. (1978). *Cloth Geometry*. Textile Institute, Manchester, England.
- [116] Love, L. (1954). Graphical relationships in cloth geometry for plain, twill, and sateen weaves. *Textile Research Journal*, **24(12)**, 1073-1083.
- [117] Kemp A. (1958). An Extension of Pierce's Cloth Geometry to the Treatment of Non-circular Threads. *J Text. Inst.*, **vol. (49)**, 44-49.
- [118] Hamilton J.B. (1964). A General System of Woven-Fabric Geometry. *J Text. Inst.*, **vol. 55**, 66-82.
- [119] Neckář B. *Theory of Structure and Mechanics of Fibrous Assemblies* (1st Edition). Woodhead Publishing: India, 2012.
- [120] Seyam, A., & El-Shiekh, A. (1993). Mechanics of woven fabrics: Part III: Critical review of weavability limit studies. *Textile research journal*, **63(7)**, 371-378.
- [121] Hsieh, Y. L. (1995). Liquid transport in fabric structures. *Textile Research Journal*, **65(5)**, 299-307.
- [122] Partsch, H., Mortimer, P. Compression for leg wounds. *British Journal of Dermatology* 2015, **173(2)**, 359–369. <https://doi.org/10.1111/bjd.13851>
- [123] Chemani, B., Halfaoui, R. (2014). Influence of pressure from compression textile bands: Their uses in the treatment of venous human leg ulcers. *International Journal of Physical Sciences*, **9(7)**, 146–153. <https://doi.org/10.5897/IJPS2014.4117>
- [124] Rimaud, D., Convert, R., & Calmels, P. (2014). In vivo measurement of compression bandage interface pressures: the first study. *Annals of physical and rehabilitation medicine*, **57(6-7)**, 394-408. Doi: 10.1016/j.rehab.2014.06.005
- [125] Chassagne, F., et al. (2018). Numerical Model Reduction for the Prediction of Interface Pressure Applied by Compression Bandages on the Lower Leg. *IEEE Transactions on Biomedical Engineering*, **65(2)**, 449-457.

- [126] Skenderi, Z., Cubric, I. S., Srdjak, M., (2009). Water Vapour Resistance of Knitted Fabrics under Different Environmental Conditions. *Fibres & Textiles in Eastern Europe*, **17**, 72-75.
- [127] Kotb, N. A., Salman, A. A., Ghazy, H. M., Abu El-Anain, E. H., (2011). Quality of Summer Knitted Fabrics Produced from Microfibre / Cotton Yarns. *Journal of Basic and Applied Scientific Research*, **1(12)**, 3416-3423.
- [128] Ramachandran, T., Manomani, G., Vigneswaran, C., (2010). Thermal behaviour of ring – and compact – spun yarn single jersey, rib and interlock knitted fabrics. *Indian Journal of Fibre & Textile Research*, **35**, 250-257.
- [129] Oglakcioglu, N., Marmarali, A., (2007). Thermal Comfort Properties of Some Knitted Structure. *Fibres & Textiles in Eastern Europe*, **15**, 94-96.
- [130] Hes, L., (1987). Thermal properties of nonwovens. Proceedings of Congress Index 87, Geneva
- [131] Chidambaram, P., Govind, R., Venkataraman, K. C., (2011). The Effect of Loop Length and Yarn Linear Density on the Thermal Properties of Bamboo Knitted Fabric. *Autex Research Journal*, **11(4)**, 102-105.
- [132] Ogulata, R. T., Mavruz, S., (2010). Investigation of Porosity and Air Permeability Values of Plain Knitted Fabrics. *Fibres and Textiles in Eastern Europe*, **18**, 71-75.
- [133] Onofrei, E., Rocha, A. M., Catarino, A., (2011). The Influence of Knitted Fabrics' Structure on the Thermal and Moisture Management Properties. *Journal of Engineered Fibres and Fabrics*, **6(4)**, 10-22.
- [134] Ramakrishnan, G., Dhurai, B., Mukhopadhyay, S., (2009). An Investigation into the Properties of Knitted Fabrics made from Viscose Microfibres. *Journal of Textile and Apparel, Technology and Management*, **6(1)**, 1-9.
- [135] Cubric, I. S., Skenderi, Z., Bogdanic, A. M., Andrassy, M., (2012). Experimental study of thermal resistance of knitted fabrics. *Experimental Thermal and Fluid Science*, **38**, 223-228.
- [136] Gokarneshan N (2018). Some Significant Developments in Bandage Fabrics. *J Nurse Patient Health Care* **1(1)**: 105
- [137] Kumar, B., Das, A., & Alagirusamy, R. (2014). Effect of material and structure of compression bandage on interface pressure variation over time. *Phlebology*, **29(6)**, 376-385.
- [138] Ding, D., Tang, T., Song, G., & McDonald, A. (2011). Characterizing the performance of a single-layer fabric system through a heat and mass transfer model-Part II: Thermal and evaporative resistances. *Textile Research Journal*, **81(9)**, 945-958.
- [139] Khalil, A., Fouda, A., Těšinová, P., & Eldeeb, A. S. (2020). Comprehensive Assessment of the Properties of Cotton Single Jersey Knitted Fabrics Produced From Different Lycra States. *Autex Research Journal*, 1(ahead-of-print).
- [140] Bhattacharjee, D., & Kothari, V. K. (2009). Heat transfer through woven textiles. *International Journal of Heat and Mass Transfer*, **52(7-8)**, 2155-2160.
- [141] Jaeger, J. C., & Carslaw, H. S. (1959). Conduction of heat in solids. Clarendon P.
- [142] Cleland, A. C. (1990). Food refrigeration processes. *Elsevier Applied Science*.

- [143] Cleland, A. C., & Earle, R. L. (1977). A comparison of analytical and numerical methods of predicting the freezing times of foods. *Journal of Food Science*, **42(5)**, 1390-1395.
- [144] Schuhmeister, J. (1877). Ber. K. Akad. Wien (Math-Naturw. Klasse), **76**, 283.
- [145] Baxter, S. T. (1946). The thermal conductivity of textiles. *Proceedings of the Physical Society*, **58(1)**, 105.
- [146] Militky, J. (2011). Cut resistance of textile fabrics, selected topics of textile and material science. TUL FT Liberec.
- [147] Bogaty, H., Hollies, N. R., & Harris, M. (1957). Some thermal properties of fabrics: part I: The effect of fiber arrangement. *Textile Research Journal*, **27(6)**, 445-449.
- [148] Mansoor, T., Hes, L., Bajzik, V., & Noman, M. T. (2020). Novel method on thermal resistance prediction and thermo-physiological comfort of socks in a wet state. *Textile Research Journal*, 0040517520902540.
- [149] Mansoor, T., Hes, L., & Bajzik, V. (2020). A New Approach for Thermal Resistance Prediction of Different Composition Plain Socks in Wet State (Part 2). *Autex Research Journal*, 1(ahead-of-print).
- [150] Das, A., Alagirusamy, R., & Kumar, P. (2011). Study of heat transfer through multilayer clothing assemblies: a theoretical prediction. *AUTEX Research Journal*, **11(2)**, 54-60.
- [151] Wei, J., Xu, S., Liu, H., Zheng, L., & Qian, Y. (2015). Simplified model for predicting fabric thermal resistance according to its microstructural parameters. *Fibres & Textiles in Eastern Europe*.
- [152] Srdjak, M., Skenderi, Z., Cubric, I. S. (2009). Water Vapor Resistance of Knitted Fabrics under Different Environmental Conditions. *Fibres & Textiles in Eastern Europe*, **17(2)**, 72-75.
- [153] Oğlakcioğlu, N., Marmarali, A. (2007). Thermal comfort properties of some knitted structures. *Fibres & Textiles in Eastern Europe*, **15(5-6)**, 64-65.
- [154] Mangat, M. M., Hes, L., & Bajzik, V. (2015). Thermal resistance models of selected fabrics in wet state and their experimental verification. *Textile Research Journal*, **85(2)**, 200-210.
- [155] Mansoor, T., Hes, L., Skenderi, Z., Siddique, H. F., Hussain, S., & Javed, A. (2019). Effect of preheat setting process on heat, mass and air transfer in plain socks. *The journal of the Textile Institute*, **110(2)**, 159-170.
- [156] Hes, L., & de Araujo, M. (2010). Simulation of the effect of air gaps between the skin and a wet fabric on resulting cooling flow. *Textile Research Journal*, **80(14)**, 1488-1497.
- [157] Eucken, A. (1940). General laws for the thermal conductivity of various types of material and states of matter. *Research in the field of engineering A*, **11 (1)**, 6-20.
- [158] Kumar, P., & Topin, F. (2014). Simultaneous determination of intrinsic solid phase conductivity and effective thermal conductivity of Kelvin like foams. *Applied Thermal Engineering*, **71(1)**, 536-547.
- [159] Carson, J. K. (2017). Use of simple thermal conductivity models to assess the reliability of measured thermal conductivity data. *International Journal of Refrigeration*, **74**, 458-464.

- [160] Mao, N., & Russell, S. J. (2007). The thermal insulation properties of spacer fabrics with a mechanically integrated wool fiber surface. *Textile Research Journal*, **77**(12), 914-922.
- [161] Militky J. 2006. Prediction of textile fabrics thermal conductivity. In: Fan J (ed.) Thermal manikins and modelling, Hong Kong Polytechnic University, pp 131-138.
- [162] F. Ullmann, Ullmann's fibers, vol. 1. Weinheim: Wiley-VCH Verlag, 2008
- [163] Hes, L., & Dolezal, I. (1989). New method and equipment for measuring thermal properties of textiles. *Sen'i Kikai Gakkaishi (Journal of the Textile Machinery Society of Japan)*, **42**(8), T124-T128.
- [164] Neves, S. F., Campos, J. B. L. M., & Mayor, T. S. (2015). On the determination of parameters required for numerical studies of heat and mass transfer through textiles—Methodologies and experimental procedures. *International Journal of Heat and Mass Transfer*, **81**, 272-282.
- [165] Oğlakcioğlu, N., Marmarali, A. (2007). Thermal Comfort Properties of Some Knitted Structures. *FIBRES & TEXTILES in Eastern Europe*, **15**(5 – 6), 64 – 65.
- [166] Sell K., Ghigiarelli J., Kitsos J., et al. (2011). Electromyographic analysis of abdominal and lower back muscle activation during abdominal exercises using an objective biofeedback device. *JEP online*, **14**(5), pp. 54-65.
- [167] James M. W., Meghan J. and Ana I. N. (2013). The Effect of external compression on the mechanics of muscle contraction. *Journal of Applied Biomechanics*, **29**, pp. 360-364
- [168] Duffield R., Cannon J., King M. (2010). The effects of compression garments on recovery of muscle performance following high-intensity sprint and plyometric exercise. *Journal of Science and Medicine in Sport*, pp. 136-140.

8. List of papers published by the author

- Accepted and published articles:

- 1) Aboalasaad, A. R. R., Sirkova, B. K., El-Hossini, A. L. M., & HEBEISH, A. (2017). **Effect of mercerization followed by cross-linking on cotton fabric properties.** *TEKSTİL VE KONFEKSİYON*, 27(3), 251-258.
- 2) Aboalasaad, A.R., Kolčavová, B.S., & Berk, G.G. (2018, December). **Effect of Compression Bandages on Muscle's Behaviour.** In *IOP Conference Series: Materials Science and Engineering*, (Vol. 460, No. 1, p. 012034). IOP Publishing.
- 3) Aboalasaad, A. R. R., & Sirková, B. K. (2019). **Analysis and prediction of woven compression bandages properties.** *The Journal of The Textile Institute*, 110(7), 1085-1091.
- 4) Aboalasaad, A. R., Skenderi, Z., Kolčavová, S. B., & Khalil, A. A. (2020). **Analysis of Factors Affecting Thermal Comfort Properties of Woven Compression Bandages.** *Autex Research Journal*, 20(2), 178-185.
- 5) Aboalasaad, A. R., Sirková, B. K., & Ahmad, Z. (2020). **Influence of tensile stress on woven compression bandage structure and porosity.** *Autex Research Journal*, 20(3), 263-273.
- 6) Aboalasaad, A. R., Sirková, B. K., Tešinová, P., & Khalil, A. (2020). **Guidelines for measuring thermal resistance on thermal Foot Manikin.** *Materials Today: Proceedings*, 31, S232-S235.
- 7) Amany Khalil, Pavla Těšinová, Abdelhamid Aboalasaad. **Thermal Comfort Properties of Cotton/Spandex Single Jersey Knitted Fabric**, *Industria Textila*. (Manuscript ID: 1760). Accepted for publishing on 23.01.2020 in issue 3/2021
- 8) Abdelhamid R. R. Aboalasaad, Brigita Kolčavová Sirková, Pavlína Bílá, Amany A. S. Khalil. **Comparative study of long and short-stretch woven compression bandages.** *Autex Research Journal*. DOI: <https://doi.org/10.2478/aut-2020-0035>, Published online: 24 Oct 2020.
- 9) Aboalasaad, A.R.R., Hassan, M. **The relation between viscose fibers' characteristics and their yarn properties.** *Vlakna a Textil*, 27(5), pp. 4-9
- 10) A. R. Aboalasaad, B. K. Sirková, T. Mansoor, Z. Skenderi, A. S. Khalil. **Theoretical and Experimental Evaluation of Thermal Resistance for Compression Bandages.** *Autex Research Journal*. Published online: 20 Nov 2020. DOI: <https://doi.org/10.2478/aut-2020-0052>
- 11) Abdelhamid R.R. Aboalasaad, Brigita K. Sirková, and Gözde G. Berk. **Enhancement of Muscle's Activity by Woven Compression Bandages.** Submitted on January 21, 2020. *Industria Textila Magazine*, ID: 1789. Accepted on October 09, 2020 for publishing in issue

4/2021

- **Submitted articles for publishing (under review):**

- 12) **Abdelhamid R.R. Aboalasaad, Brigita K. Sirková, and Moaaz A.S. Eldeeb. Influence of Woven Bandage Composition on Its Elasticity and Durability.** Submitted on December 11, 2020. Journal of the Textile Institute, ID: JOTI.6077.

- **List of conferences and workshops:**

- 1) **A.R.R. Aboalasaad, B. Kolčavová S. “Analysis and Prediction of Compression Bandages Tension”,** International conference (CEC), PhD student day, September 14th, 2017.
- 2) **A. R. R. Aboalasaad, Brigita S. Kolčavová, and Gözde G. Berk. “Effect of compression bandages on muscle's behaviour”.** Autex 2018 - 18th World Textile Conference, June 20-22, 2018 (Award for best student poster presentation).
- 3) **Ahmad Z., Sirková B., and Aboalasaad A.R.R. “Yarn deformation in multifilament single layer woven structures using Fourier series”,** Autex, Istanbul, Turkey 2018, ISBN 978-961-6900-17-1.
- 4) **A.R.R. Aboalasaad, Z. Skenderi, B. K. Sirková, Tariq Mansoor. “Measurement of Thermal Resistance on Thermal foot manikin Compared to ALAMBETA”,** PhD students day, 03.12.2018, Liberec.
- 5) **A.R.R. Aboalasaad, B.K. Sirková, P. Tešinová, A. Khalil. “Optimum Conditions for Measuring Thermal Resistance on Thermal foot manikin”.** 4th International conference on natural fibres, Porto, Portugal, 1-3 July 2019. Accepted as oral presentation.
- 6) **Khalil, A., Tešinová, P., & Aboalasaad, A. R. “Thermal comfort properties of single jersey knitted fabric produced at different Lycra states”.** Poster presentation in ICNF 2019, Porto, Portugal. pp. 422-423
- 7) **Abdelhamid R. R. Aboalasaad, Brigita Kolčavová Sirková. “Effect of twist level of warp yarns on woven bandage properties”.** Workshop for PhD students, 12.11.2019, Liberec, Czech Republic.
- 8) **Khalil, Amany; Tešinová, Pavla; Aboalasaad, Abdelhamid. “Geometrical and Thermal Properties of Stretched Single Jersey Knitted Fabric”.** Workshop for PhD students, 12.11.2019, Liberec, Czech Republic.
- 9) **Abdelhamid R.R. Aboalasaad, Mohamed Eldessoki, and Ebraheem Shady. “Correlation between Viscose Fibers’ Characteristics and Their Yarn Properties”.** NART Conference, 18-20 September 2019, Liberec, Czech Republic. Poster presentation.

Please you can find the full list of publication on the following website:

<https://scholar.google.cz/citations?user=xrKgg2IAAAAJ&hl=en>

9. Curriculum Vitae

9.1 Personal Data

Name: Abdelhameid Rajab Ramadan Aboalasaad.

Nationality: Egyptian, Sex: Male.

Date of birth: 10.01.1981, Dakahliya, Egypt.

Permanent Address: 6 Amr Ibn Elaas Street, Mansoura, Egypt.

Army service: Exempted, Marital status: Married, has three kids.

Email: cabdo6@gmail.com & abd.elhameidrajabramadan.abo.el.asaad@tul.cz

Mobile number: +420776690508.

9.2 Education

- M.Sc. degree in textile engineering "**Effect of High Concentrations of Alkaline Mediums in Wet Processing on Cotton Fabrics**", 2010.
- Bachelor science in textile engineering, Mansoura University, June 2003, "**Very good with honour degree**", **Ranked 1st of class**.
- Undergraduate project: "**Computer Application for Simulation and Prediction of Sewing Stitches Properties**", with grade "**Excellent**".

9.3 Employment Experience

- 1) **PhD scholar** in Technical University of Liberec, Department of Technologies and Structures, (26.3.2015) till now.
- 2) **Lecturer assistant**, from (11-2010) to (3-2015), Faculty of Engineering, Textile Department, Mansoura University, Egypt.
- 3) **Demonstrator**, from (5-2007) until (11-2010), Faculty of Engineering, Textile Department, Mansoura University, Egypt.
- 4) **AutoCAD & 3D Studio Max Designer and Trainer**, from (4-2004) till (5-2007), El-Aseil office, Mansoura, Egypt.

9.4 Internship

- 1) Internship no I in Egypt (23.05.2016 to 21.07.2016)
- 2) Internship no II in Egypt (12.11.2016 to 11.12.2016)
- 3) Internship III in Istanbul, Turkey (02.09.2017 to 30.12.2017)
- 4) Internship IV in Zagreb, Croatia (11.07.2018 to 30.09.2018).

9.5 Training

- 1- Training in "Mansoura-Espania Company for Spinning and Weaving", Egypt. From (8:10-2003).
- 2- Training in "Masr Company for Spinning and Weaving", Mahala El Kobra, Egypt. From (6:9-2002).
- 3- Training in "Dakahlia (DTEX) Company for Spinning and Dying" in Mansoura, Egypt. (6:9-2001).

9.6 Personal Skills

▪ Computer:

Software:

- 3D Studio Max.
- AutoCAD, Auto Lisp.
- Mat lap, C++.
- Adobe Photoshop.
- Windows operation system (Win XP, win 7, win 8, win 10).
- Internet (Browsing, Searching...).

Hardware:

- Aware of common hardware problems.

▪ Languages:

- First language : Arabic (Native)
- Second language: English (Very good)
- Third language : French (Little listening and speaking).